



National Library of Canada

Cataloguing Branch
Canadian Theses Division

Ottawa, Canada
K1A 0N4

Bibliothèque nationale du Canada

Direction du catalogage
Division des thèses canadiennes

NOTICE

The quality of this microfiche has been dependent upon the quality of the original thesis submitted for microfilming. Every effort has been made to ensure the highest quality of reproduction possible.

If a paper microfilm is sent to the university which granted the degree.

Some pages may have indistinct print especially if the original pages were typed with a poor typewriter ribbon or if the original source is a poor photocopy.

Previously copyrighted materials (journals, articles, published text, etc.) are so marked.

Reproduction in any part of this film is governed by the Canadian Copyright Act (R.S.C. 1970, c. C-30). Please read the authorization forms which accompany microfiche.

THIS DISSERTATION
HAS BEEN MICROFILMED
EXACTLY AS RECEIVED

AVIS

La qualité de cette microfiche dépend grandement de la qualité de la thèse soumise au microfilmage. Nous avons tout fait pour assurer une qualité supérieure de reproduction.

Si un microfilm est renvoyé à l'université qui a décerné le diplôme.

La qualité d'impression de certaines pages peut laisser à désirer, surtout si les pages originales ont été dactylographiées avec de mauvais rubans ou si l'université nous a fait parvenir une photocopie de mauvaise qualité.

Les documents qui font déjà l'objet d'un droit d'auteur (articles de revue, examens publiés, etc.) ne sont pas microfilmés.

La reproduction, même partielle, de ce microfilm est soumise à la Loi canadienne sur le droit d'auteur (S.C. 1970, c. C-30). Veuillez prendre connaissance des formulaires d'autorisation qui accompagnent cette thèse.

LA THESE A ÉTÉ
MICROFILMÉE TELLE QUE
NOUS L'AVONS REÇUE

THE UNIVERSITY OF ALBERTA

DEPOLYMERIZATION OF MONOMER ALL-DIME-ACRYLATE

by

(C)

PAVEL SLAVOMIR NEUDOREL

A THESIS

SUBMITTED TO THE FACULTY OF GRADUATE STUDIES AND RESEARCH
IN PARTIAL FULFILLMENT OF THE REQUIREMENTS FOR THE DEGREE
OF DOCTOR OF PHILOSOPHY

DEPARTMENT OF CHEMISTRY

EDMONTON, ALBERTA

SPRING, 1977

THE UNIVERSITY OF ALBERTA
FACULTY OF GRADUATE STUDIES AND RESEARCH

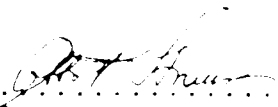
The undersigned certify that they have read,
and recommend to the Faculty of Graduate Studies and
Research, for acceptance, a thesis entitled


PYROLYSIS OF MONOMER AND DIMETHYLSILANE

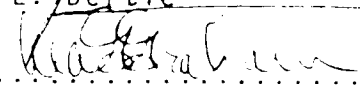
submitted by

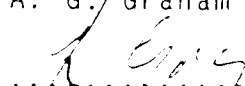
PAVEL SLAVOMIR NEUDOREL

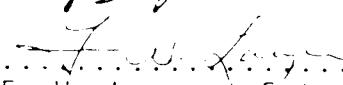
in partial fulfilment of the requirements for the degree
of Doctor of Philosophy.


.....
O. P. Strausz - Supervisor


.....
J. E. Bertie


.....
W. A. G. Graham


.....
J. Gray - Physics


.....
F. W. Lampe - External
Examiner

Date 3/17/77 1977

ABSTRACT

The initial stages of the pyrolysis of monomethylsilane have been investigated between 340 and 440°C in the pressure range 40 - 400 torr. The major products are hydrogen and 1,2-dimethyldisilane (DMDS) and the minor products are dimethylsilane (DMS) and polymer. The rate of decomposition is strongly dependent on the nature of the reactor surface. In the presence of ca. 10% ethylene the yields of H₂ and DMDS are greatly reduced and DMS is not formed. Under these conditions the only observable reaction is homogeneous unimolecular elimination of H₂ to form silylene, $\text{CH}_3\text{SiH}_3 \xrightarrow{1} \text{CH}_3\text{SiH}_2 + \text{H}_2$, followed by insertion of silylene into the substrate to form DMDS. The rate parameters for reaction (1) are $\log k_1 (\text{s}^{-1}) = (14.95 \pm 0.11) - (63,200 \pm 330) / 2.3RT$ from which $\Delta H_f^\ddagger(\text{CH}_3\text{SiH}_2) = 53 \text{ kcal/mol}$ and $D(\text{CH}_3\text{SiH-H}) = 69 \text{ kcal/mol}$. The preexponential factor is consistent with a three-centered transition state. In parallel and in competition with the molecular reaction (1), heterogeneous Si-H cleavage also takes place, $\text{CH}_3\text{SiH}_3 \xrightarrow{2} \text{CH}_3\text{SiH}_2^\cdot + \text{H}^\cdot$, followed by a chain mechanism propagated by H[•] and $\text{CH}_3\text{SiH}_2^\cdot$ and terminated by $\text{CH}_3\text{SiH}_2^\cdot$ radicals. The average chain length is about 10⁶.

The pyrolysis of dimethylsilane was also briefly investigated between 440 and 500°C and 41 - 395 torr. The yields of the major products, H₂ and 1,1,2,2-tetramethyldisilane (TMDS), and particularly those of the minor products, monomethyl- and trimethylsilane (MMS, TMS) are surface-dependent. Ethylene has no apparent effect on the rates of formation of H₂ and TMDS but suppresses those of MMS and TMS. A reaction mechanism similar to that proposed for the pyrolysis of monomethylsilane is assumed to take place, involving molecular, $(\text{CH}_3)_2\text{SiH}_2 \xrightarrow{01} (\text{CH}_3)_2\text{Si:} + \text{H}_2$ and radical, $(\text{CH}_3)_2\text{SiH}_2 \xrightarrow{02} (\text{CH}_3)_2\text{SiH}\cdot + \text{H}\cdot$ primary steps. The rate parameters for the molecular reaction are $\log k_{01}(\text{s}^{-1}) = (14.3 \pm 0.3) - (68,000 \pm 1,000)/(2.3 \text{ RT})$ from which $D((\text{CH}_3)_2\text{Si-H}) \sim 74 \text{ kcal/mol}$ and $\Delta H_f^0((\text{CH}_3)_2\text{Si:}) \sim 44 \text{ kcal/mol}$. The detailed processes occurring in the chain propagation and termination reactions could not be fully elucidated but it appears that reaction (02) is also heterogeneous.

The implications and ramifications of these results with regard to the thermal decomposition of other silicon-containing compounds are discussed.

ACKNOWLEDGEMENTS

The author wishes to express his sincere gratitude to Professor O. P. Strausz for his assistance, friendly guidance, constant encouragement and support throughout the course of this work.

Special thanks are due to Drs. T. Yokota and I. Safarik for invaluable help in the interpretation of kinetic and thermochemical data, and to Mr. A. Jodhan for experimental assistance.

The author is indebted to Drs. A. J. Vanderwielen and J. I. Matthews for stimulating discussions and to Dr. R. S. McDaniel and Professor F. W. Birss for the use of their computer programs.

The helpful assistance of the technical staff of the department is acknowledged.

The author would also like to thank Dr. E.M. Lown for her careful, critical reading of the manuscript and for her assistance and helpful suggestions during its preparation.

The conscientious efforts of Mrs. L. Cech in the typing of this thesis are much appreciated.

The author also wishes to express his deep gratitude to his wife, Marie, whose understanding and constant encouragement did much to make this work possible.

A bursary and three scholarships from the National Research Council of Canada, and Teaching Assistantships from the University of Alberta are gratefully acknowledged.

TABLE OF CONTENTS

	Page
ABSTRACT.....	iv
ACKNOWLEDGEMENTS.....	v
LIST OF TABLES.....	xiv
LIST OF FIGURES.....	xx
CHAPTER I INTRODUCTION.....	1
A. Silicon Chemistry.....	1
1. Comparison Between Silicon and Carbon.....	2
2. Thermochemistry.....	4
3. Silyl Radicals.....	7
4. Silylenes.....	13
5. Homogeneous Decomposition of Some Silicon Compounds.....	19
i. Mercury (3P_1) Photo- sensitized Decomposi- tion.....	19
ii. Vacuum U.V. Photolysis.	20
iii. Chemical Activation....	22
6. Pyrolysis.....	26
i. Disilanes.....	27
ii. Monosilane and Methylsilanes.....	30

TABLE OF CONTENTS (cont'd)

	Page
B. Bimolecular Reactions.....	37
C. Present Investigation.....	42
CHAPTER II EXPERIMENTAL.....	45
A. Vacuum Systems.....	45
B. Pyrolytic Furnace Assembly.....	49
C. Analytical Methods.....	52
1. Gas Chromatography.....	52
i. Thermal Conductivity	
G.C.	52
ii. Flame Ionization G.C. ...	54
2. Mass Spectral Analysis.....	56
D. Experimental Procedure.....	56
1. Pyrolysis.....	56
2. Product Analysis.....	5
3. Substrate Purification.....	59
i. Monomethylsilane.....	59
ii. Dimethylsilane.....	60
E. Materials.....	61

TABLE OF CONTENTS (cont'd)

	Page
CHAPTER III PYROLYSIS OF MONOMETHYLSILANE.....	63
A. Results.....	64
1. The Reaction Products and Their Distribution.....	64
i. Gaseous Products.....	65
ii. Polymer	68
2. Reaction Order of Hydrogen Formation.....	74
3. Surface Effects and Influence of the Polymer on Surface Activity.....	75
i. Effect of Variation of the Surface/Volume Ratio.....	83
ii. Effect of the Nature of the Surface.....	92
4. Effect of Added Ethylene....	97
5. Arrhenius Parameters for the Molecular Process.....	102
i. Order of Formation of Hydrogen and DMDS.....	105
ii. Rate Constants and Arrhenius Parameters for Hydrogen and DMDS Formation.....	105
Isotopic Labelling Experiments.....	110

TABLE OF CONTENTS (continued)

	Page
B. Discussion.....	111
1. The Primary Reaction Steps.....	113
2. Possible Reaction Mechanism.....	115
3. Effect of Added Ethylene on the Molecular and Radical Processes.....	118
i. Molecular Process, Reactions (1), (3) and (4).....	119
ii. Radical Reactions.....	123
iii. Arrhenius Parameters for H ₂ and DMDS Formation in the Presence of Ethylene.....	130
4. Pyrolysis in the Absence of Ethylene: the Radical Process.....	132
i. Reaction Orders for the Products of the Radical Process.....	132
ii. Chain Propagation.....	143
iii. Chain Termination.....	145
iv. Formation of Dimethyl- silane.....	146
v. Rate Constants and Arrhenius Parameters for the Radical Process.....	150
vi. Chain Initiation Step: Homogeneous or Heterogeneous?.....	161
vii. Length of the Radical Chain.....	163

TABLE OF CONTENTS (continued)

	Page
5. Some Thermochemical implications of the Arrhenius Parameters for the Molecular Weight.....	168
i. The Activation Energy.....	169
ii. The Preexponential Factor.....	172
CHAPTER IV. PYROLYSIS OF DIMETHYLSILANE.....	182
A. Results.....	182
1. The Reaction Products.....	182
2. Time Study.....	183
3. Effect of the Nature of the Surface.....	183
4. Determination of the Reaction Orders, and the Effect of Ethylene on the Reaction Rates.....	186
B. Discussion.....	191
1. Comparison of the Pyrolysis of DMS and MMS: Similari- ties and Differences.....	191
i. Different Thermal Stability.....	196
ii. Effect of Added Ethylene.....	197
iii. The Reaction Orders.....	198

TABLE OF CONTENTS (cont'd)

	Page
2. Reaction Scheme for the Pyrolysis of Dimethylsilane.....	199
3. Determination of the Rate Constants for the Molecular and Radical Processes in the Pyrolysis of DMS.....	202
4. Arrhenius Parameters for the Molecular and Radical Processes in the Pyrolysis of Dimethylsilane.....	209
5. Some Thermochemical Implications of the Arrhenius Parameters for the Molecular Process.....	216
i. Activation Energy.....	217
ii. Preexponential Factor... ..	219
 CHAPTER V SUMMARY AND CONCLUSIONS.....	 223
 BIBLIOGRAPHY.....	 231
 APPENDIX I I. SPECTRUM OF $(CH_3)(C_2H_5)SiH_2$	 239
II SPECTRUM OF $(CH_3)_2(C_2H_5)SiH$	240
III CORRECTION PROCEDURE FOR THE DECOMPOSITION OF POLYMER.....	241

LIST OF TABLES

Number		Page
I-1	Selected Bond Dissociation Energies of Silicon Compounds.....	6
I-2	Values of E_d^0/kT_0 for Various Silyl and Methylated Silyl Radicals.....	10
I-3	Arrhenius Parameters for Hydrogen Abstraction by Methyl Radical from Silanes.....	14
I-4	Primary Quantum Yields in the 147.0 and 125.6 nm Photolysis of Monomethylsilane.....	21
I-5	Primary Mechanism for the 147.0 nm Photolysis of Dimethylsilane- d_2	23
I-6	Reaction Paths and Rate Constants for the Decomposition of Chemically Activated Diethylsilane.....	25
I-7	Arrhenius Parameters for the Elimination of Silylenes from Disilanes.....	29
II-1	Thermal Conductivity S.C. Operating Conditions.....	53
II-2	Materials Used.....	62
III-1	Variation of the Product Yields with Time in the Pyrolysis of MeSiH ₃ at 422°C.....	56
III-2	Product Yields in the Pyrolysis of MeSiH ₃ at High Conversion.....	60
III-3	The Yield of Gases from Polymer Decomposition at 360°C as a Function of Time.....	72

LIST OF TABLES (cont'd)

Number		Page
III-4	Variation of the Hydrogen Yield with Monomethylsilane Pressure at Different Temperatures.....	76
III-5	Variation of the Hydrogen Yield with Monomethylsilane Pressure at 421°C.....	77
III-6	Variation of the Hydrogen Yield with Monomethylsilane Pressure at 400°C.....	78
III-7	Variation of the Hydrogen Yield with Monomethylsilane Pressure at Different Temperatures.....	9
III-8	Reaction Order of Hydrogen Formation in the Pyrolysis of Monomethylsilane at Different Temperatures.....	82
III-9	The Products of MeSiH ₃ Pyrolysis as a Function of Reaction Time at 416°C.....	85
III-10	The Products of MeSiH ₃ Pyrolysis as a Function of Reaction Time at 415°C.....	86
III-11	Product Yields as a Function of Pressure of MeSiH ₃ at 415°C in a Packed Vessel.....	87
III-12	Product Yields as a Function of Pressure of MeSiH ₃ at 415°C in the Unpacked Vessel.....	88
III-13	Effect of Polymer Deposition on the Product Yields in Successive Pyrolysis of MeSiH ₃ at 415°C.....	95
III-14	Effect of Polymer Treatment in a "Seasoned" Vessel on the Rate of Pyrolysis of Monomethylsilane at 415°C.....	98
III-15	Effect of Added Ethylene on the Product Yields in the Pyrolysis of MeSiH ₃	100

LIST OF TABLES (cont'd)

Number		Page
III-16	The Monomethylsilane-Ethylene System: The Yield of H ₂ and DMDS as Function of MeSiH ₃ Pressure and Time at Different Temperatures, and the Calculated First Order Rate Constants for H ₂ and DMDS Formation.....	103
III-17	Monomethyl-Ethylene System: Orders of Formation of Hydrogen and DMDS.....	107
III-18	Arrhenius Parameters for H ₂ and DMDS Formation in the Monomethylsilane-Ethylene System.....	110
III-19	Isotopic Distribution of Hydrogen from the Pyrolysis of Monomethylsilane-d ₃	112
III-20	Reaction Scheme for the Pyrolysis of MeSiH ₃	116
III-21	Yields of Hydrogen from the Molecular and Radical Processes in the Pyrolysis of Monomethylsilane at 441°C and 429°C.....	133
III-22	Yields of Hydrogen by the Molecular and Radical Processes in the Pyrolysis of Monomethylsilane at 421°C.....	134
III-23	Yields of Hydrogen by the Molecular and Radical Processes in the Pyrolysis of Monomethylsilane at 400°C.....	135
III-24	Yields of Hydrogen by the Molecular and Radical Processes in the Pyrolysis of Monomethylsilane at 380°C.....	136
III-25	Yields of Hydrogen by the Molecular and Radical Processes in the Pyrolysis of Monomethylsilane at 361°C and 341°C.....	137

LIST OF TABLES (cont'd)

Number		Page
III-26	Product Yields by the Molecular and Radical Processes in the Pyrolysis of Monomethylsilane at 415°C in the Unpacked Vessel.....	138
III-27	Yields of Products by the Molecular and Radical Processes in the Pyrolysis of Monomethylsilane at 415°C in the Packed Vessel.....	139
III-28	Reaction Orders for H_2, Rad in the Pyrolysis of $MeSiH_3$ at Different Temperatures.....	141
III-29	Reaction Orders for $H_2, Rad, DMDS, Rad$ and DMS in the Pyrolysis of $MeSiH_3$ at 415°C.....	142
III-30	Pyrolysis of $MeSiH_3$: First Order Rate Constants for H_2 Formation as a Function of Temperature.....	157
III-31	Arrhenius Parameters for Hydrogen Formation in the Pyrolysis of Monomethylsilane.....	158
III-32	Apparent Rate Constants for H_2, Rad as a Function of Temperature for Linear and Quadratic Termination of the Chain.....	160
III-33	Apparent Arrhenius Parameters for H_2, Rad in the Pyrolysis of $MeSiH_3$ for Two Extreme Cases of Chain Termination.....	163
III-34	Estimated Contributions from Some Fundamental Vibrations of CH_3SiH_3 to the Entropy of Activation at 670°K.....	179

LIST OF TABLES (cont'd)

Number		Page
III-35	Contributions to the Entropy of Activation ΔS^\ddagger at 670°K.....	180
IV-1	Product Yields as a Function of Time in the Pyrolysis of Me_2SiH_2 at 490°C.....	184
IV-2	The Effect of Polymer Deposition on the Product Yields in the Pyrolysis of Me_2SiH_2 at 490°C.....	187
IV-3	Product Yields and Rates of Formation as a Function of Dimethylsilane Pressure at 500°C and 480°C; Effect of Added Ethylene.....	188
IV-4	Product Yields and Rates of Formation as a Function of Dimethylsilane Pressure at 490°C; Effect of Added Ethylene.....	189
IV-5	Product Yields and Rates of Formation as a Function of Dimethylsilane Pressure at 460 and 440°C; Effect of Added Ethylene.....	190
IV-6	Reaction Order for Product Formation in the Pyrolysis of Dimethylsilane and Different Temperatures.....	195
IV-7	First Order Rate Constants for H_2 and TMDS Formation in the Pyrolysis of DMS.....	204
IV-8	Rate Constant Ratios $k_{06}^2/k_{02}/k_{08}$ for H_2 and TMDS Formation by the Radical Process in the Pyrolysis of DMS at Different Temperatures.....	205
IV-9	Rate Constant Ratios k_{06}/k_{09-1} for H_2 and TMDS Formation by the Radical Process in the Pyrolysis of DMS at Different Temperatures.....	208

LIST OF TABLES (cont'd)

<u>Number</u>		<u>Page</u>
IV-10	Arrhenius Parameters for the Rate Constant Ratios of the Radical Process in the Pyrolysis of DMS.....	214
IV-11	Estimated Contributions of the Si-H Vibrational Modes in Me_2SiH_2 to the Entropy of Activation at 730°K.....	221

LIST OF FIGURES

<u>Number</u>		<u>Page</u>
II-1	High Vacuum System.....	46
II-2	Auxiliary Vacuum System for Photolysis and Purification of Methylsilane and Dimethylsilane.....	48
II-3	Sectional View of the Pyrolytic Furnace.....	50
III-1	Product Yields as a Function of Time in the Pyrolysis of MeSiH ₃ at 422°C.....	67
III-2	H ₂ +CH ₄ Yields from Polymer Decomposi- tion at 360°C as a Function of Time....	73
III-3	Order Plots for H ₂ Formation in the Pyrolysis of MeSiH ₃ at 381, 400, 421 and 441°C.....	80
III-4	Order Plots for H ₂ Formation in the Pyrolysis of MeSiH ₃ at 341 and 361°C...	81
III-5	Rate of H ₂ Formation as a Function of MeSiH ₃ Pressure at 415°C in Reaction Vessels of Different S/V Ratios.....	89
III-6	Rate of DMDS Formation as Function of MeSiH ₃ Pressure at 415°C in Reaction Vessels of Different S/V Ratios.....	90
III-7	Rate of DMS Formation as Function of MeSiH ₃ Pressure at 415°C in Reaction Vessels of Different S/V Ratios.....	91
III-8	Effect of Increased Polymer Deposition on the Product Yields in Successive Pyrolyses of MeSiH ₃ at 415°C.....	96

LIST OF FIGURES (cont'd)

Number		Page
III-9	Effect of Added Ethylene on the Rates of Product formation in the Pyrolysis of ~ 405 torr MeSiH_3 at 415°C	101
III-10	Order Plots for H_2 and DMDS at Different Temperatures in the Presence of $\sim 10\%$ Ethylene.....	106
III-11	Arrhenius Plots for H_2 and DMDS Formation from the Pyrolysis of MeSiH_3 in the Presence of $\sim 10\%$ Ethylene.....	109
III-12	Correlation Between the Products of the Radical Process in the Pyrolysis of MeSiH_3 at 415°C : Rate $(\text{H}_2)_{\text{Rad}}$ and Rate $(\text{DMDS})_{\text{Rad}}$ versus Rate (DMS)	148
III-13	Rate $(\text{H}_2)_{\text{Total}}/[\text{MMS}]$ versus $[\text{MMS}]^{1/2}$ and $[\text{MMS}]$ at 421°C	154
III-14	Arrhenius Plots for the First Order Rate Constants $(k_1+k_2)^{\text{lin}}$ and $(k_1+k_2)^{\text{quad}}$ Based on Hydrogen Formation.....	157
III-15	Arrhenius Plots for the Rate Constants $\{k_6 2k_2/k_4\}^{\text{lin}}$ and $\{k_5(k_2/k_7)^{1/2}\}^{\text{quad}}$ Based on hydrogen Formation.....	162
IV-1	Product Yields as a Function of Time in the Pyrolysis of ~ 125 torr Me_2SiH_2 at 490°C	185
IV-2	Order Plots for H_2 and TMDS Formation in the Pyrolysis of Me_2SiH_2 at Different Temperatures.....	192

LIST OF FIGURES (cont'd)

Number		Page
IV-3	Order Plots for IM ₂ and MM ₂ Formation in the Pyrolysis of Me ₃ SiH ₂ in the absence of Ethylene at 440, 450 and 460 C.....	193
IV-4	Order Plots for IM ₂ and MM ₂ Formation in the Pyrolysis of Me ₃ SiH ₂ in the Absence of Ethylene at 460 and 490 C.....	194
IV-5	The Plots of Equations (14) and (15) at Different Temperatures.....	203
IV-6	The Plots of Equations (17) and (18) at Different Temperatures.....	207
IV-7	Arrhenius Plot for the First Order Rate Constant k_{01}	211
IV-8	Arrhenius Plots for the Rate Constant Ratio $k_{06}(2k_{02}/k_{08})$, based on H ₂ and TMDS Formation in the Pyrolysis of DMS.....	212
IV-9	Arrhenius Plots for the Rate Constant Ratio k_{06}/k_{09-1} , based on H ₂ and TMDS Formation in the Pyrolysis of DMS.....	213
AIII-1	Correction of the Observed H ₂ Yields for Decomposition of the Polymer.....	242

CHAPTER I

INTRODUCTION

A. Silicon Chemistry

Silicon is the second most abundant element on earth and its great technical importance (e.g. silicone oils, rubbers, semiconductors, etc.) has undoubtedly contributed to the rapid growth of silicon chemistry, particularly in the last decade. In particular, significant progress has been achieved with regard to the kinetic-mechanistic aspects of gas phase reactions of silicon-containing compounds where silyl radicals, R_3Si^\cdot , and silylenes, $R_2Si:$, are often important intermediates. It has also become increasingly apparent that there are considerable differences in the chemical properties and reactivities of silicon and carbon analogs.

In this chapter some salient characteristics of the silicon atom and the chemistry of silyl radicals and silylenes will be briefly reviewed. The mechanisms of the thermal decompositions of silicon hydrides and methylated silanes will be discussed in some detail and the theory of unimolecular reactions will be outlined.

1. Similarities between silicon and carbon

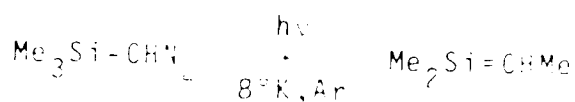
Silicon belongs to the group III element of the periodic table and lies immediately below carbon, therefore both silicon and carbon have similar ground state electronic configurations, $ns^2 np^2$, where $n = 2$ for carbon and 3 for silicon. Since the main mode of bonding is by sp^3 hybridization, similar types of compounds such as hydrides, halides, ethers, etc., exist for both elements.

In spite of apparent similarities, there are however some important differences in the physical and chemical properties of analogous carbon and silicon compounds. For example, because the silicon atom is larger than carbon and is less electronegative, it forms weaker bonds with hydrogen and stronger bonds with more electronegative atoms such as Cl, O, N.

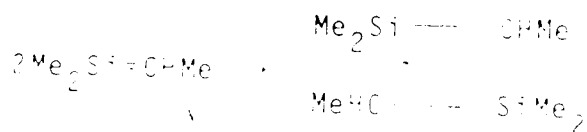
A more significant property of silicon is the availability of vacant 3d orbitals by which it can expand its coordination number to five or six to form sd or sp^3d hybrids, respectively^{1a,d}. The vacant 3d orbitals in silicon lie about 100 kcal/mole above the highest occupied orbitals, whereas in carbon the energy difference is about 200 kcal/mole^{1a}. In carbon, the 3d orbitals are not likely to mix satisfactorily with the 2s and 2p orbitals, not only because they are substantially higher in energy, but also because the radial maximum of the 3d

orbitals are not likely to compare that of the $2s$ and $2p$ orbitals.² Silicon d orbitals, on the other hand, are more readily available for the formation of additional bonds and stabilization of intermediates and transition states, and may also enter into d_p interactions with neighboring groups or atoms.^{2,3}

Another important difference between silicon and carbon compounds is the stability of p_p - p_p bonds. Although it was long believed that silicon does not form double bonds, convincing evidence has been obtained in the last few years for the transient existence of π -Si⁴, Si=C⁵, Si=C⁵, Si=N⁶ and Si=S⁷ bonded reaction intermediates; very recently, Me₂Si-CHMe has been identified⁸ as an intermediate in the irradiation of trimethylsilyl diazomethane in an argon matrix at 8 K.



The Si=C bond is highly reactive. Trimethylsilylaethylene undergoes dimerization above 45 K:



The first stable compound having a p_p - p_p silicon-carbon bond.

Significant progress has recently been made in the determination of bond dissociation energies $D(\text{Si-H})$, $D(\text{Si-Si})$ and $D(\text{Si-C})$ by kinetic^{15,16,17} and electron impact studies.¹⁸ Some selected bond dissociation energies of silicon compounds are given in table I-1; they seem to indicate, first, that the bond dissociation energies $D(\text{Si-H})$, $D(\text{Si-Si})$ and $D(\text{Si-C})$ are apparently independent of the number of methyl groups attached to silicon¹³ and secondly, that the second bond dissociation energy in SiH_2 is significantly lower than the first¹⁹. This is not observed in carbon compounds, e.g.

$D(\text{CH}_3\text{-H}) = 104 \pm 1$, $D(\text{CH}_2\text{-H}) = 104 \pm 6$, $D(\text{CH-H}) = 108 \pm 6$,
 $D(\text{C-H}) = 111 \text{ kcal/mol}$ ²². Similar large differences between the first and second BDEs were also observed for $D(\text{Si-Cl})$ in SiCl_4 ¹⁹ and for $D(\text{Si-C})$ in Me_4Si ²⁷.

It appears therefore that the stabilities of the divalent species, silylenes, are greater than those of the carbene analogs. Increasing stability of divalent radical species is a general pattern observed in group IVb elements, and thus silylenes are expected to play important roles in many gas phase reactions of silicon compounds.

TABLE I-1
Selected Bond Dissociation Energies of
Silicon Compounds

Compound	D(Bond) ^d	Reference
H ₃ Si-H	94±3	18
	88	13
H ₂ Si-H	59	19
HSi-H	84	19
Si-H	70	19
H ₅ Si ₂ -H	90	20
MeSiH ₂ -H	89±4	11
Me ₂ SiH-H	89±4	13
Me ₃ Si-H	89±4	13
	88	16
	89.9±2.6	15
Cl ₃ Si-H	91.3±1.4	19
H ₃ Si-SiH ₃	81±4	21
Me ₃ Si-SiMe ₃	81	22
	80.5±1.0	17
Me-SiH ₃	85±4	13
	86±4	18
Me-SiMe ₃	85	23
Me ₃ SiCH ₂ -H	97	24
Me ₅ Si ₂ CH ₂ -H	96	25

^a in kcal/mol.

3. Silyl Radicals

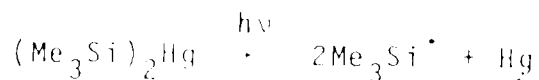
The structures of alkyl and silyl radicals are different. Whereas the methyl radical CH_3^\bullet is planar²⁹, the SiH_3^\bullet radical is pyramidal²⁹. The effects of substituents on the structure of silyl radicals have been reviewed recently³⁰.

Silyl radicals undergo elementary reactions similar in type to those encountered in the chemistry of alkyl radicals such as dissociation, combination, disproportionation, addition to multiple bonds, atom abstraction, etc.; however, they often proceed with different rates and/or yield different kinds of products.

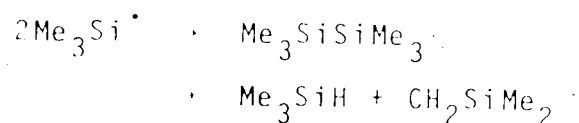
Information on the thermal stabilities of silyl radicals is still very limited, but in general they appear to be more stable than their carbon analogs: the trimethylsilyl radical, for example, has been found³¹ to be thermally more stable than its hydrocarbon analog the *t*-butyl radical, since decomposition was not observed up to 400°C. Similarly, dimethylsilyl³¹ and disilyl³² radicals are stable up to 200 and 220°C, respectively.

Relatively few elementary reactions of silyl radicals have been investigated kinetically, particularly in the gas phase, since not many "clean" radical sources are known.

Gammie et al.³³ used the photolysis of bis-trimethylsilyl mercury,



as a source of trimethylsilyl radicals. The disproportionation-combination rate constant ratio,



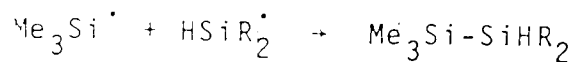
$k_d/k_c = 0.046$ is much smaller than that for t-butyl radicals, 3.6 ³⁴, due to the instability of the silicon-carbon σ - σ bond. Gammie et al.³³ also photolyzed the mercurial in the presence of silanes having readily abstractable hydrogen, and measured rate constants for H abstraction by trimethylsilyl radicals:



It was also possible to estimate the rate constant ratio of the cross-disproportionation

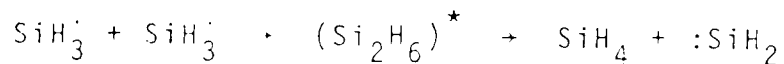


and combination reactions



between trimethylsilyl radicals and other silyl radicals, and the values of k_d/k_c are summarized in Table 1-2.

The mercury (3P_1) photosensitized decomposition of silicon hydrides^{32,35} and alkyl silanes^{31,36} is another relatively clean source of silyl radicals in the gas phase, and has been used to measure the rate of recombination of trimethylsilyl radicals³⁶ and k_d/k_c ratios for different silyl radicals. The results are also given in Table 1-2. The pressure dependence of the k_d/k_c ratio for disilyl radicals³² reflects the instability of the chemically activated tetrasilane molecule. The chemically activated product disilane formed by recombination of monosilyl radicals is unstable up to 1000 torr^{32,35}:

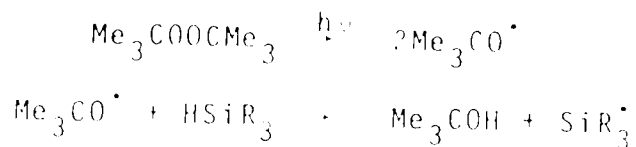


This is in marked contrast to the recombination of methyl radicals where the product, ethane, is stabilized above a few torr total pressure.

Photolytic decomposition of di-t-butylperoxide in the presence of silicon hydrides has been used for some kinetic studies of silyl radicals in the liquid phase. Silyl radicals are produced by H-abstraction by t-butoxy radicals, e.g.

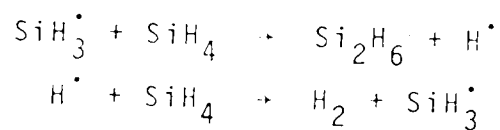
TABLE I-2
 Values of k_d/k_c for Various Silyl and
 Methylated Silyl Radicals

Radicals	k_d/k_c (25°C)	Reference
$\text{Me}_3\text{Si} + \text{Me}_3\text{Si}$	0.046 ± 0.011	33
$\text{Me}_3\text{Si} + \text{Me}_3\text{Si}$	0.03	31
$\text{Me}_3\text{Si} + \text{Me}_2\text{SiH}$	0.28	33
$\text{Me}_3\text{Si} + \text{MeSiH}_2$	0.50	33
$\text{Me}_2\text{SiH} + \text{Me}_2\text{SiH}$	0.14	31
$\text{MeSiH}_2 + \text{MeSiH}_2$	0.11	31
$\text{MeSiD}_2 + \text{MeSiD}_2$	0.04	31
$\text{Si}_2\text{H}_5 + \text{Si}_2\text{H}_5$	0.12 (400 torr)	32
$\text{SiH}_3 + \text{SiH}_3$	∞ (up to 1000 torr)	32,35



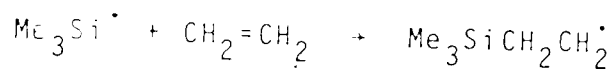
and their concentration can be monitored by electron spin resonance spectroscopy.

Thus Gaspar, Haizlip and Choo³⁷ used combined flash photolysis and electron spin resonance spectroscopic methods to study the reactions of SiH_3^\cdot and $\text{Me}_3\text{Si}^\cdot$ radicals with the parent silanes between -150° to -120°C and -82° to 20°C , respectively. Bimolecular self-reaction has been established as the dominant path for disappearance of the radicals, and no evidence was found for the propagation of the chain by reactions



which were postulated in the pyrolysis of SiH_4 ^{38,39}.

The same technique has also been used to study the rate of addition of SiH_3^\cdot and $\text{Me}_3\text{Si}^\cdot$ radicals to ethylene⁴⁰ which was concluded to be a very efficient scavenger of silyl radicals. The rate constant for the addition reaction



is $k(\text{M}^{-1}\text{s}^{-1}) = 10^{7.0} \exp(-2,500/RT)$; the fact that the activation energy is considerably lower than for methyl, ethyl and n-propyl radical addition to ethylene, 6.8⁴¹, 5.5⁴² and 7.4 kcal/mol⁴¹, respectively, is explained in terms of stabilization of the carbon-centered free radical by a β -silicon substituent. Monosilyl radicals, SiH_3^\cdot , react with ethylene even faster than $\text{Me}_3\text{Si}^\cdot$ ⁴⁰.

Similarly, Pollock et al.³² found that the rate of addition of disilyl radicals, $\text{Si}_2\text{H}_5^\cdot$, to ethylene is about three orders of magnitude faster than the corresponding rate for $\text{C}_2\text{H}_5^\cdot$ radicals; this was attributed to the greater physical size of the silicon 3p orbitals, greater polarizability and availability of the 3d orbitals on silicon, and the tetrahedral configuration of the silyl radical.

Both ethylene and nitric oxide have been found to be very efficient scavengers of silyl radicals and this fact has been used to help elucidate the decomposition mechanisms of a variety of silicon compounds^{31,32,43-50}.

Since $D(\text{Si-H})$ is lower than $D(\text{C-H})$, the rate of hydrogen abstraction from saturated compounds by silyl radicals is expected to be slower than that by the corresponding alkyl radicals, which abstract H atoms from Si-H bonds very efficiently. A large body of information has become available on the hydrogen abstraction reactions

by alkyl radicals from a variety of silanes^{51,52}. The A factors are similar to those for abstraction from alkanes but the activation energies are lower, in agreement with the trend in the bond dissociation energies. The Arrhenius parameters for H abstraction by methyl radicals from Si-H bonds of monosilane⁶⁰ and methylsilanes⁶¹ are listed in Table I-3, where it is seen that the activation energies for abstraction from all the methylsilanes are practically the same. This is also consistent with recent bond strength measurements (Table I-1). Silicon forms stronger bonds to halogens than does carbon, and abstraction of halogen atoms by silyl radicals from alkyl halides is an exothermic process.

The chemistry of silyl radicals and some Arrhenius parameters associated with these reactions have been recently reviewed^{30,51-53}.

4 Silylenes

Silylenes, the divalent radical silicon analogs of carbenes, play a very important role in silicon chemistry.

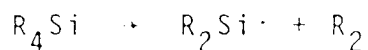
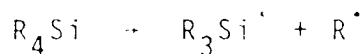
In contrast to carbene, $:CH_2$, in which the triplet ground state is nearly linear⁵⁴ (FCH angle = 140°); the $:SiH_2$ ground state appears to be a bent singlet^{54,55}.

TABLE I-3
Arrhenius Parameters for Hydrogen Abstraction by
Methyl Radicals from Silanes

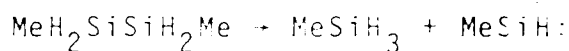
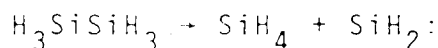
Reactant	$\log A, (M^{-1}s^{-1})$	$E_a, \text{ kcal/mol}$	Reference
SiH_4	9.26 ± 0.17	7.47 ± 0.29	60
CH_3SiH_3	9.28 ± 0.24	8.13 ± 0.39	61
$(\text{CH}_3)_2\text{SiH}_2$	9.04 ± 0.18	8.30 ± 0.31	61
$(\text{CH}_3)_3\text{SiH}$	8.69 ± 0.27	8.31 ± 0.47	61

(HSiH angle = 92°) and therefore little diradical character is expected.

Silylenes are formed in the decomposition of many silicon compounds brought about by the action of heat, radiation, electron impact, silent electric discharge, or by chemical activation; in most decompositions, however, silylene formation by the so-called "molecular" process is accompanied by single bond homolyses which lead to the formation of silyl radicals:



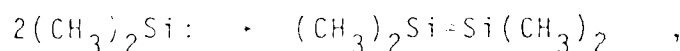
Although the formation of silylene requires the splitting of two bonds, this is partly compensated for by the formation of a new bond and thus the endothermicity of the molecular process might actually be lower than that for single bond fission. A fine balance has been found to exist between these two modes of decomposition⁵⁶ and this aspect will be considered later in more detail. It has been shown that pyrolysis of some disilanes, e.g.⁵⁷⁻⁵⁹



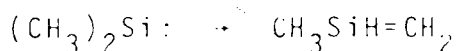
may be used as a clean and convenient source of silylenes.

Silylenes may either polymerize, react with the silane precursors or with a "trapping" reagent. Polymerization, insertion into single bonds, and addition to multiple bonds are three types of reactions which characterize most of the known chemistry of silylenes⁵⁹, of which several review articles are available^{51,52,54,56,62}.

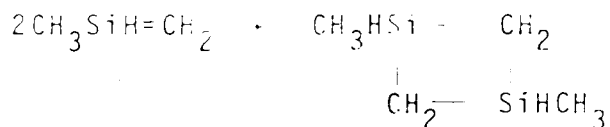
Very recently, evidence has been obtained⁶³ for dimerization of dimethylsilylene to tetramethyldisilane,



and a novel rearrangement to 1-methylsilaethylene



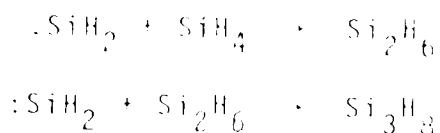
followed by dimerization to 1,3-dimethyl-1,3-disilacyclobutane



has been suggested⁶³.

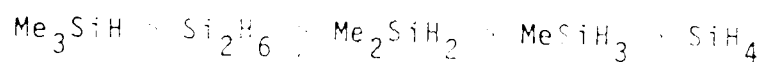
Silylenes are generally less reactive than carbenes⁶⁴; they insert rapidly into Si-H, Si-O and Si-halogen bonds, but not into Si-C, C-H or C-C bonds; insertion into the Si-Si bond has also been suggested⁶⁵.

The absolute rates and Arrhenius parameters for insertion into silane and disilane,

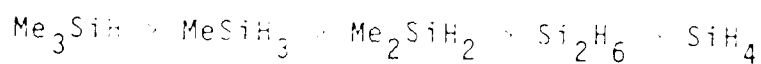


have been measured: $k_{\text{SiH}_4} = 10^{9.7} \exp(-1300+1100)/RT$ and $k_{\text{Si}_2\text{H}_6} = 10^{9.9} \exp(-400-1200)/RT (\text{M}^{-1}\text{s}^{-1})$, respectively.⁶⁶ The high preexponential factors and low activation energies indicate that insertion of $\cdot\text{SiH}_2$ into the Si-H bond is an extremely rapid process.

Relative rates of insertion of $\cdot\text{SiH}_2$ into the Si-H bond of silicon hydrides and methylsilanes have been measured by two groups who offered two alternative explanations for the observed trends. Ring et al.^{65,67} found the following order of reactivity (per Si-H bond),



and rationalized the results in terms of the electrophilic nature of $\cdot\text{SiH}_2$ and the hydridic character of Si-H bonds, i.e. the greater the negative charge on the hydrogen, the faster the rate of insertion. Cox and Purnell⁶⁸ however found a different order of reactivity,



and concluded that the difference in reactivity is not due to differences in the strength of the Si-C bond.⁶⁶ In view of the present reactivity values of 1.0×10^4 for ethylene, the calculation offered by Jenkins et al. appears to be more plausible.

Silylene also reacts with a variety of unsaturated organic compounds. Addition across the double bond has been shown^{59, 62, 63} to give organosilyl silacyclopentane derivatives, e.g.,



Silylene reacts very rapidly with 1,3-butadiene, and Jenkins et al.⁷¹ found that addition of SiH_2 to 1,3-butadiene can compete favorably with insertion into Si_2H_6 ; the reactivity of silylenes toward ethylene, however, is relatively low. For example, Atwell and Weyenberg⁵⁹ reported the following order of relative reactivities toward SiMe_2 :

saturated hydrocarbons < benzene < ethylene < dimethylacetylenetrihydrosilane < dienes and alkyne.

Since ethylene is an effective scavenger of silyl radicals on the one hand but is unreactive toward silylene on the other, this can be used to advantage in

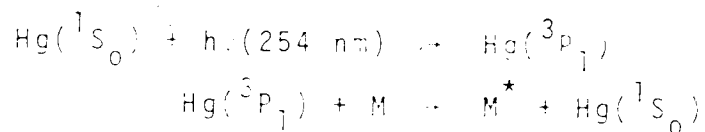
elucidation of the types of bond cleavage occurring in the decomposition of many silicon compounds.

5. Homogeneous Decomposition of Some Silicon Compounds

Significant advances have recently been made with regard to the kinetic and mechanistic aspects of the homogeneous gas phase decompositions of some silicon-containing compounds, particularly silicon hydrides and methylsilanes. The results, which will now be reviewed, can be classified according to the methods used, namely, mercury photosensitization, direct photolysis, chemical activation and pyrolysis.

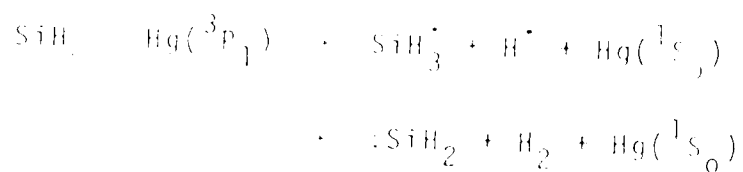
(i) Mercury (3P_1) Photosensitized Decomposition

Since most silicon hydrides and methylsilanes absorb only in the vacuum UV region, mercury photosensitization can be used to advantage:



The energy transferred to the substrate M is 112 kcal/mol, a quantity more than sufficient to induce rupture of Si-C, Si-H or Si-Si bonds.

The occurrence of radical and molecular primary steps in the $\text{Hg}(^3\text{P}_1)$ photosensitized decomposition of monosilane has been proposed^{2,44,31}



but the experiments conducted in the presence of nitric oxide⁴⁸ suggested that formation of silylene is not important.

Similarly, Nay et al.³¹ showed that the only major process of importance in the $\text{Hg}(^3\text{P}_1)$ photosensitized decomposition of methylsilanes is Si-H bond cleavage. A minor contribution from a molecular process leading to H_2 and silylenes was postulated in the cases of MeSiH_3 and Me_2SiH_2 in order to account for a significant mass imbalance between the major products.

(ii) Vacuum UV Photolysis

The gas phase photolysis of monomethylsilane has been investigated^{45,46} using the xenon and krypton resonance lines at 147.0 and 223.6 nm respectively (the absorption of methylsilane is continuous in this region⁷³). The primary quantum yields are summarized in Table I-4.

TABLE I-4
 Primary Quantum Yields in the 147.0^a and
 123.6 nm^b Photolysis of Monomethylsilane^c

	147.0 nm	123.6 nm
CH ₃ SiD ₃ + hν		
1 CH ₃ SiD + D ₂	0.32	0.16
2 CH ₃ SiD + 2D	0.05	0.09
3 CH ₂ SiD ₂ + HD	0.23	0.37 (0.14)
4 CHSiD ₃ + H ₂	0.07	0.11
5 CH ₃ D + SiD ₂	0.09	0.08
6 CH ₃ + D + SiD	0.26	0.25
7 CH ₃ + D + D ₂ + Si	0.00	0.17
8 CH ₃ + SiD ₃	0.01	0.00
	1.03	1.23 (1.00)

^a Photonic energy 195 kcal/mol.

^b Photonic energy 231 kcal/mol.

^c References 45 and 46.

where it is seen that the primary quantum yield for the elimination of molecular hydrogen and formation of methylsilylene, step (1), becomes more important as the photopic energy is decreased. This seems to indicate that molecular elimination is the lowest energy path for decomposition of methylsilane and might assume more significance as the energy content is decreased.

The gas phase photolysis of dimethylsilane at 147.0 nm has been investigated by Alexander⁴⁷ and the primary mechanism is shown in Table I-5. In view of the large amount of energy absorbed by the molecule, it is not surprising to find a very complex fragmentation pattern; molecular elimination of hydrogen from the silicon atom and formation of dimethylsilylene, step (6), is apparently unimportant.

(iii) Chemical Activation

A chemically activated molecule is formed either by radical recombination, insertion or addition of divalent species. The energy content of a newly formed vibrationally excited molecule can be calculated from thermochemical data.

The kinetics of decomposition of chemically activated dimethylsilane have been studied by Hase,

TABLE I-5
 Primary Mechanism for the 147.0 nm^a Photolysis of
 Dimethylsilane-d₂^b

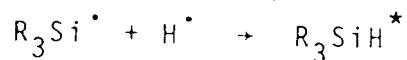
	ϕ
$(\text{CH}_3)_2\text{SiD}_2 + h\nu$ 1 $\text{CH}_3\text{SiD} + \text{CH}_3\text{D}$	0.15
2 $\text{CH}_3\text{SiD} + \text{CH}_3 + \text{D}$	0.20
3 $\text{SiD}_2 + 2\text{CH}_3$	0.08
4 $\text{CH}_2\text{SiD}_2 + \text{CH}_4$	0.05
5 $\text{CH}_3\text{SiD}_2\text{H} + \text{CH}_2$	0.04
6 $(\text{CH}_3)_2\text{Si} + \text{D}_2$	0.07
7 $\text{CHSiD}_2 + \text{CH}_3 + \text{H}_2$	0.04
8 $\text{CHCH}_3\text{Si} + \text{D}_2 + \text{H}_2$	0.07
9 $\text{CH}_2\text{CH}_3\text{Si} + \text{HD} + \text{D}$	0.09
10 $\text{CHCH}_3\text{SiD} + \text{HD} + \text{H}$	0.05
11 $\text{CH}_2\text{CH}_3\text{SiD}_2 + \text{H}$	0.05
12 $\text{CH}_2\text{CH}_3\text{SiD} + \text{HD}$	0.12
	<u>1.01</u>

^a Photonic energy 195 kcal/mol.

^b From reference 47.

Mazac and Simons⁷⁴. Vibrationally excited dimethylsilane, having an average energy content of ≈ 130 kcal/mol, was produced by insertion of singlet methylene into the Si-H bond of methylsilane. The decomposition paths and the rate constants are shown in Table I-6. Comparison of Tables I-5 and I-6 substantiates the previous suggestion that molecular elimination of hydrogen from simple silicon hydrides becomes more important as the energy available is lowered. This process might therefore be expected to be of major significance in thermal decompositions.

On the other hand, Cowfer et al.⁷⁵ studied the reactions of hydrogen atoms with SiH_4 , CH_3SiH_3 , $(\text{CH}_3)_2\text{SiH}_2$ and $(\text{CH}_3)_3\text{SiH}$, where chemically activated molecules are formed by radical combination reactions such as



(the minimum excitation energy is approximately $E^* \approx D(\text{Si-H}) \approx 90$ kcal/mol), and concluded that decomposition via molecular elimination channels is negligible since they require rigid transition states: this would markedly decrease the sum of states available to the transition state complex and therefore substantially lower the rate of molecular elimination compared to single bond cleavage. The authors also pointed out that

TABLE I-6
 Reaction Paths and Rate Constants for the
 Decomposition of Chemically Activated^a
 Dimethylsilane^b

Reaction.	$10^9 k, s^{-1}$
$(CH_3)_2SiH_2^* \rightarrow$ products	4.0
1 $CH_3 + CH_3SiH_2$	~ 0.90
2 $CH_4 + CH_3SiH$	0.85
3 $(CH_3)_2Si: + H_2$	1.90
4 $(CH_3)_2SiH + H$	~ 0.30

^a Average excitation energy 129 ± 4 kcal/mol.

^b From reference 74.

since the bond dissociation energy $D(\text{Si-CH}_3)$ is lower than $D(\text{Si-H})$, the main mode of decomposition of methylsilanes should be via Si-C bond cleavage.

6. Pyrolysis

In thermal activation the heat absorbed by the molecule is converted into vibrational energy which is assumed to be equipartitioned among the various internal degrees of freedom. Because of this energy equipartitioning the weakest bond in the molecule is the one which is eventually homolyzed. Although there are exceptions, most molecules decompose from the highest vibrational level of the ground, singlet state, and hence much of the kinetic and thermochemical data available today have been derived from pyrolysis experiments.

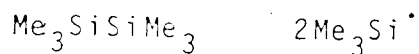
Quite frequently, however, the system may be complicated by the occurrence of heterogeneous processes, radical chain reactions and secondary thermal decomposition of the products. In many cases these difficulties can be overcome by studying the effects of surface, addition of radical scavengers, and by keeping the reaction conversion very low. Flow systems have been used to advantage in cases of high product instability.

Pyrolyses of simple alkanes proceed by the well-known Rice-Herzfeld mechanism⁷⁶ in which the initial slow dissociation of the parent molecule into radicals via homogeneous C-C bond cleavage is followed by fast radical chain reactions. Except for the case of methane, primary molecular elimination of hydrogen does not appear to be significant. In contrast, silicon-containing analogs apparently decompose by parallel and independent radical and molecular processes; the reactions are often partly heterogeneous and radical chain mechanisms are allegedly involved.

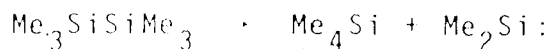
(i) Disilanes

The pyrolysis of disilanes has attracted a great deal of attention in recent years and the mechanism of the decompositions of Si_2H_6 and of all the methylated disilanes are now well understood.

With the exception of hexamethyldisilane^{16,17} where dissociation of the Si-Si bond and formation of $\text{Me}_3\text{Si}^\cdot$ radicals



occurs simultaneously with Me_2Si elimination,



all the other methyl-disilanes^{27,58,77} were found to decompose exclusively by unimolecular, homogeneous gas phase elimination of silylenes. The pyrolyses of Si_2H_6 ^{57,79,80} and Si_3H_8 ^{65,77,79} also proceed via elimination of silylene.

Some Arrhenius parameters for the elimination of silylenes from disilanes are shown in Table I-7. It is significant that all the activation energies, except that for Me_6Si_2 , reaction (3), lie within a narrow range, 48.0 ± 2.0 kcal/mol; these values correspond approximately to the reaction enthalpies since the activation energies for the reverse reactions, insertion of silylenes into Si-H bonds, are very small and close to zero⁶⁶. All the reactions (except (3)) involve a 1,2-hydrogen shift and since the bond dissociation energies $D(\text{Si-H})$ in the silane products, i.e. SiH_4 , MeSiH_3 , Me_2SiH_2 and Me_3SiH , are independent of the number of methyl groups attached to the silicon atom, (cf. Table I-1) it might therefore appear that $D(\text{Si-Si})$ and $D(\text{Si-H})$ in disilanes are also unaffected by increased methylation on the silicon atoms¹³. The relatively high activation energy for reaction (3), and the fact that to date there is no evidence of silylene insertion into Si-C bonds suggest that the activation

TABLE I-7
Arrhenius Parameters for the Elimination of Silylenes from Disilanes

Reaction		$\log A(s^{-1})$	$E_a, kcal/mol$
$Me_3SiSiMe_2H$	$Me_2Si: + Me_3SiH$ (1)	12.9 ± 0.31	47.4 ± 0.9 ^a
$HMe_2SiSiMeH_2$	$Me_2Si: + MeSiH_3$ (2)	12.56 ± 1.80	46.0 ± 5.3 ^a
$Me_3SiSiMe_3$	$Me_2Si: + Me_4Si$ (3)	13.70 ± 0.70	67.4 ± 0.8 ^b
$HMe_2SiSiMeH_2$	$MeSiH: + Me_2SiH_2$ (4)	13.66 ± 0.55	46.2 ± 1.4 ^a
MeH_2SiSiH	$MeSiH: + SiH_4$ (5)	14.14 ± 0.34	49.9 ± 0.4 ^c
$MeH_2SiSiMe_2$	$:SiH_2 + MeSiH_3$ (6)	15.28 ± 0.15	50.7 ± 0.4 ^c
H_3SiSiH_3	$:SiH_2 + SiH_4$ (7)	14.52 ± 0.36	49.2 ± 1.1 ^c

^a Reference 27; ^b Reference 17; ^c Reference 77; ^d Reference 57.

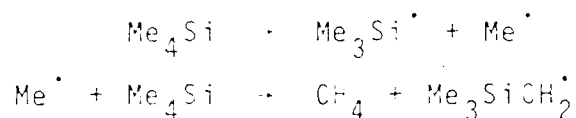
energy for the reverse reaction (-3) must be high. This is in agreement with Davidson's earlier qualitative prediction⁵⁶ that silylene elimination is only important if the precursor silane molecule contains Si-H bonds into which insertion is possible.

(ii) Monosilane and Methylsilanes

In comparison with disilanes, the pyrolyses of monosilane and methylsilanes appear to proceed by more complex reaction mechanisms which have not yet been fully clarified.

(a) Tetramethylsilane

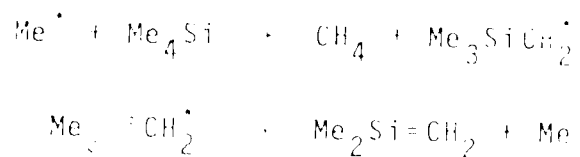
The pyrolysis of tetramethylsilane has been extensively used for the preparation of carbosilanes⁹¹, compounds with alternate silicon and carbon atoms in the molecular skeleton. The kinetics of the pyrolysis of Me_4Si have been investigated in a flow system⁸². Methane was one of the major reaction products, presumably formed by $\text{Me}_3\text{Si-Me}$ bond cleavage,



and the following first order rate constant was reported:

$$\log k(s^{-1}) = (14.3 \pm 0.23) - (6760 \pm 800)/(2.3RT)$$

The activation energy however is less than $D(\text{Me}_3\text{Si}-\text{Me})$ 85 kcal/mol^{13,23}, and this seems to indicate the presence of free radical chain reactions in the system, such as⁵¹



Some heterogeneous reactions must also participate in the decomposition of tetramethylsilane, since the rate of decomposition and the relative product yields were both affected by the nature of the reaction vessel surface⁸². Moreover, the low thermal stabilities of some of the products and radical intermediates preclude the assignment of a complete mechanism.

(b) methylsilane

Complications of a similar nature have also been encountered in the pyrolysis of trimethylsilane. This reaction was originally proposed⁸³ to be a radical non-chain process, in which hydrogen and methane are formed by Si-H and Si-C cleavage respectively. The following Arrhenius parameters were determined:

$$\log k_{\text{H}_2} (\text{s}^{-1}) = 15.1(0.7) - (10,300/RT) - 1.1(0.1)$$

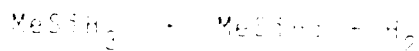
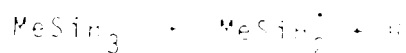
$$\log k_{\text{CH}_4} (\text{s}^{-1}) = 15.9(0.7) - (10,500/RT) - 1.1(0.1)$$

However $D(\text{Me}_3\text{Si-H}) = 89 \text{ kcal/mol}^{13,14,16}$ and $D(\text{Me-SiMe}_2\text{H}) = 81 \text{ kcal/mol}^{13}$ which suggests that the actual mechanism is not quite so simple as previously proposed¹³, moreover, recent experiments^{51,52} strongly indicate the presence of radical chain reactions.

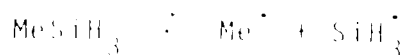
(c) Dimethylsilane and Monomethylsilane

The pyrolysis of dimethylsilane has not been reported in the literature and only qualitative results on the pyrolysis of monomethylsilane have been described^{39,55,56}.

The pyrolysis of monomethylsilane was claimed⁵⁵ to be "a remarkably clean" reaction, since the major products consisted only of hydrogen and 1,2-dimethyldisilane; dimethylsilane and a solid polymer were minor products⁵⁵. King et al.³⁹ suggested that both methylsilyl and methylsilylene radicals are formed in primary reactions:



and Davidson⁵⁶ claimed that Si-C cleavage



takes place as well.

(d) Monosilane

The nature of the primary steps in the pyrolysis of monosilane is probably one of the most controversial issues in the chemistry of silicon compounds and in spite of numerous studies carried out over the last 40 years there is still no agreement on the mechanism of this reaction. Because the experimental results on this reaction were of prime importance in the elucidation of our own work, the pyrolysis of SiH_4 will be discussed in more detail.

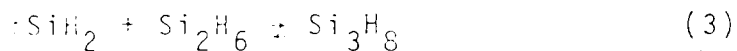
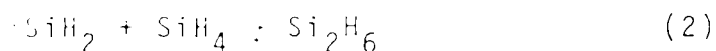
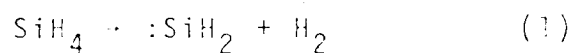
The first extensive analytical and kinetic investigation of the pyrolysis of SiH_4 was carried out by Furnell and Walsh³⁸. At low conversions the two major products were H_2 and Si_2H_6 in a ratio of 1.26; the minor products were Si_3H_8 and a polymeric solid. The orders of formation of H_2 and Si_2H_6 were 1.5 with respect to the substrate, and the rate of formation of the major products could be described by the relation

$$R(\text{H}_2) = \frac{1}{1.26} R(\text{Si}_2\text{H}_6) = 10^{15.2} \exp\left(\frac{-55,900}{RT}\right) [\text{SiH}_4]^{3/2} \text{ M}^{-1} \text{ s}^{-1}$$

Purnell and Walsh also observed that the reaction rates were fast and erratic in a fresh, nitric acid-washed vessel, but were lower and more reproducible once the surface became coated by silicon; in such silicon-coated vessels, the reaction rates were independent of the surface to volume ratio which suggests, but however does not prove, the absence of heterogeneous reactions. The addition of inert gases caused an acceleration of the reaction rates but the reaction orders were unaffected.

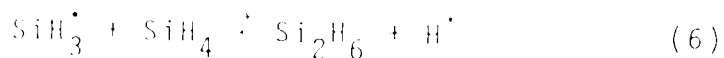
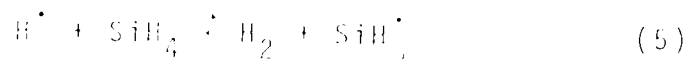
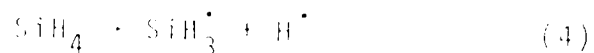
Purnell and Walsh suggested two mechanisms which would be consistent with their results: mechanism A, molecular hydrogen elimination followed by insertion of styrene into the substrate:

Mechanism A:



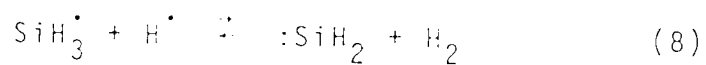
and mechanism B, homolytic silicon-hydrogen bond rupture followed by a free radical chain propagated by H atoms and SiH_3^\cdot radicals:

Mechanism B:

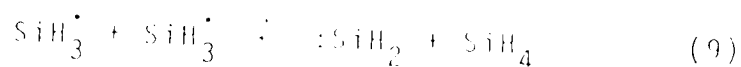


Thermochemical considerations led Purnell and Walsh to favour mechanism A. Moreover, the decomposition was carried out at relatively low pressures (35 - 230 torr) where the unimolecular first order rate constant for a light molecule such as SiH_4 may well be pressure-dependent; this would explain the experimental reaction order of 1.5 and the accelerating effect of inert gases on the rate of decomposition.

Further support in favour of mechanism A came from the work of John and Purnell⁸⁷ who obtained the data required to calculate the equilibrium constant between the products of the two possible modes of decomposition of SiH_4 ,



At 600°K, $K_8 = 10^{15.9}$ and thus SiH_4 should preferentially decompose via silylene elimination. John and Purnell⁸⁷ also calculated the analogous equilibrium constant for the case of Si_2H_6 ,



Similarly, at 600 K, $K_9 = 10^{11.3}$, again predicting that silylene formation predominates as was observed experimentally⁵⁷.

Other experimental data⁶⁶ on the insertion reactions of :SiH_2 into H_2 reaction⁵⁷ (-1), support the occurrence of Mechanism A.

Mechanism B, however, is favoured by Ring and coworkers^{39,88} who considered the kinetics of the radical mechanism and showed that the experimental activation energy is consistent with mechanism B; however, the experimentally observed A factor, $10^{15.2} \text{ s}^{-1}$, cannot be reconciled with mechanism B unless the rate of $\text{SiH}_3^\cdot + \text{SiH}_3^\cdot$ recombination reaction is unusually slow, having an A factor of approximately $10^6 \text{ M}^{-1} \text{ s}^{-1}$. Recent measurements of the rates of self-reactions of silyl radicals^{33,36,37,89,90} indicate, however, that the A factor for the combination of silyl radicals is approximately $10^{10} \text{ M}^{-1} \text{ s}^{-1}$.

The types of products formed in pyrolysis experiments conducted in the presence of other reagents provides more direct and compelling evidence for the occurrence of radical mechanism B. Thus H_2 and D_2 were formed in the pyrolysis of SiD_4 in the presence of H_2 ³⁹, and the products formed in the presence of acetylene⁸⁸ are

consistent with $\cdot\text{SiH}_3$ rather than $:\text{SiH}_2$ precursors.

Similarly, in the co-pyrolysis of SiH_4 and SiD_4 ³⁹, HD was formed in quantities comparable with those of H_2 and D_2 .

It has also been shown⁸⁸ that orbital symmetry correlations apparently favour single bond dissociation over molecular cleavage.

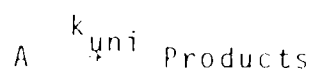
It appears therefore that the thermal decomposition of SiH_4 can proceed by two initial steps, in parallel and in competition, one yielding $:\text{SiH}_2 + \text{H}_2$ and the other, $\cdot\text{SiH}_3 + \text{H}$. At this point, it should be recalled that Purnell and Walsh³⁸ noted that heterogeneous processes might participate in the decomposition and if this is so, one would expect the radical processes to be the most affected. This aspect of the mechanism has been completely neglected in recent discussions and in the kinetic schemes of Ring et al.^{39,88}

B. Unimolecular Reactions

The understanding of most thermal decompositions is closely tied to the theory of unimolecular reactions, which will now be briefly outlined.

A gas phase unimolecular reaction is the simplest kind of elementary reaction since it involves the isomerization or decomposition of a single isolated

reactant molecule:

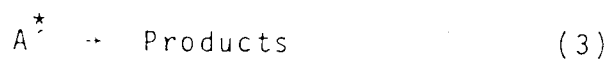


and

$$R_{uni} = k_{uni}[A]$$

However, detailed studies of several unimolecular reactions have shown that the first order rate coefficient k_{uni} is constant only at high pressures and declines at low pressures.

The original theory of unimolecular reactions, developed by Lindemann⁹¹, was based on the following concepts. A fraction of the reactant molecules becomes energized in bimolecular collisions and eventually the energy content becomes greater than the critical quantity E_0 required for decomposition. The energized molecules can either be de-energized by further collisions or undergo unimolecular reaction. The mechanism is expressed by the following reactions:



where A^* is a substrate molecule sufficiently energized that it can react, and M is any bath molecule. By

applying the steady state approximation to the concentration of A^* , the rate expression for the Lindemann scheme is

$$R_{\text{uni}} = k_3[A^*] = \frac{k_1 k_3 [M]}{k_2 [M] + k_3} [A] \quad (4)$$

Equation (4) qualitatively predicts the decline or "fall-off" in the first order rate constant at lower pressures; however, quantitative agreement between the experimental and calculated "fall-off" curves has been generally rather poor.

In the simple Lindemann theory all the rate constants were taken to be energy independent. Hinshelwood⁹² proposed that k_1 is energy dependent and included contributions from the vibrational degrees of freedom in statistical calculations on the probability that the energy content of A is greater than E_0 . Shortly after Hinshelwood's proposal, Rice and Ramsperger⁹³ and, independently, Kassel⁹⁴, suggested that the original Lindemann mechanism of collisional energization and de-energization is probably correct but that the rate of conversion of an energized molecule to the product, reaction (3), is a function of its energy content. The main achievement of the RRK theory was the derivation of an expression for the energy dependence of k_3 .

Kassel⁹⁴ treated the reactant molecule as a system of loosely coupled oscillators having identical

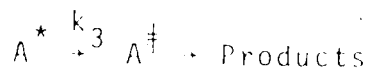
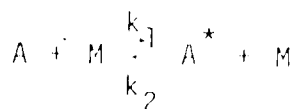
frequencies, allowing a free flow of energy between the normal modes. Assuming that the rate constant $k_3(E)$ is related to the probability that the critical energy E_0 is concentrated in a certain part of the molecule (in one oscillator), he derived the relationship⁹⁴

$$k_3(E) = \nu \left(\frac{E - E_0}{E} \right)^{s-1} \quad (5)$$

where E_0 is the critical energy, E is the total energy of the molecule, s is the number of oscillators, and ν is identified with the experimental high pressure A-factor⁹⁷

Reasonable agreement has been found between experimental and theoretical fall-off curves with the proper choice of the parameters; however, the fact that s , the number of oscillators, cannot be predicted by theory, makes this method somewhat empirical. It has been found, however, for a large number of reactions, that the required value of s is about half the total number of oscillators in the molecule.

Marcus⁹⁵ further refined the RRK treatment and the resulting RRKM method is the most widely used and successful model to date. The evaluation of the rate constants is based on the methods of quantum statistical mechanics and transition state theory is incorporated into the calculation. The following reaction scheme is used:



where A^* is an energized molecule of energy content $E^* > E_0$, but the energy distribution is unfavourable for reaction. A^\ddagger is the transition state complex, which corresponds to the top of an energy barrier between the reactant and products.

In the evaluation of the energy dependence of the rate constant k_3 , the vibrational energy of the molecule is assumed to undergo rapid statistical redistribution. The contributions from external and internal rotations are less significant.

The energy dependence of the rate constant k_3 is given by the following expression,

$$k_3(E^*) = \kappa \frac{Q^\ddagger}{Q^*} \frac{\Sigma P(E^\ddagger)}{h N(E^*)} \quad (6)$$

where κ is the degeneracy of the reaction path (i.e. the number of ways a certain reaction can occur), Q^* is the rotational partition function, $\Sigma P(E^\ddagger)$ is the total number of vibrational-rotational quantum states of A^\ddagger with energy $E^\ddagger = E^* - E_0$, and $N(E^*)$ is the density of quantum states of the substrate at an energy E^* . The RRKM expression for the

overall first order rate constant is

$$k_{\text{uni}} = \frac{\lambda Q^\ddagger}{h Q^* Q_A} \int_{L_0}^{\infty} \frac{P(E^*) \exp(-E^*/kT) dE^*}{1 + k_3(E^*)/k_2[M]} \quad (7)$$

The de-energization rate constant k_2 is usually considered to be independent of energy content and can be approximated by the collision number.

The RRKM model can in principle be applied to any unimolecular reaction taking place in a ground state molecule and its widespread use in pyrolytic, photolytic and chemically activated systems has been very successful for the elucidation of many elementary reactions. Moreover, the experimental fall-off regions of k_{uni} can be correctly predicted on the basis of this model.

C. The Present Investigation

Although the rate constant parameters for a variety of elementary reactions of organosilicon radicals are rapidly becoming available, the range of studies is still severely limited by the unavailability of suitable sources of silyl radicals.

Thermal decomposition of silicon compounds is one potential source of silicon radicals but surprisingly very few substrates have been investigated. Kinetic data

on the relative importance of molecular and radical processes are very sparse indeed and therefore the occurrence or non-occurrence of these processes cannot be elucidated on structural or thermochemical grounds. Thus some disilanes were found to pyrolyze via molecular elimination of silylenes and others predominantly via silyl radicals; the simplest member of the series, monosilane, to feature both radical and molecular modes of decomposition.

We were decided to initiate a systematic study of the pyrolyses of a number of silicon compounds. Monomethylsilane was chosen for the first investigation since it is a rather simple molecule and the kinetics of decomposition were expected to be relatively straightforward.

We were also cognizant of the possibility that monomethylsilane, like monosilane, may decompose via competing radical and molecular processes, and therefore decided to examine the reaction in the presence of a radical scavenger. Since ethylene scavenges silyl radicals very efficiently but is relatively unreactive towards silylenes, its effect can be used to advantage in the elucidation of the radical and molecular processes occurring. In spite of the high thermal stability of ethylene, its potential as a radical scavenger in the

thermal decomposition of silicon compounds had not yet been explored.

At the time this work was initiated preliminary results of the pyrolysis of monomethylsilane were published by Ring et al.^{39,85}. Their results are qualitatively in agreement with ours, but do not allow mechanistic or kinetic interpretation.

We also decided to investigate the pyrolysis of dimethylsilane in order to assess the possible effects of increasing methyl substitution on the silicon atom on the nature and rates of the elementary processes.

CHAPTER II

EXPERIMENTAL

A. Vacuum Systems

Two vacuum systems were utilized, the main one for pyrolysis and separation of products, and the auxiliary one for purification and pyrolysis of the substrates.

(1) The main apparatus was a conventional high vacuum static system (Figure II-1), constructed of Pyrex glass and evacuated to 10^{-6} torr by means of a two-stage mercury diffusion pump, backed by a Welch Duo-Seal Model 1405 oil rotary pump. Delmar mercury float valves, Hoke teflon-seated valves (numbers TY440 and 425106Y-316-SS) or glass stopcocks lubricated with high vacuum Apiezon N and L grease were used throughout. The valve leading to the reactor was a stainless steel high temperature Hoke valve (number 421 306Y-316-SS). In addition to a vacuum line for gas handling, the apparatus incorporated a pyrolytic furnace assembly and a gas chromatographic unit. Pressures were measured with a mercury manometer or a McLeod gauge. Gas transfers and distillations were monitored on a Pirani Vacuum Gauge (Consolidated Vacuum Corporation, type GP-140) using Pirani tubes (type GR-001) as the sensing heads. A low pressure line was used to operate the mercury float

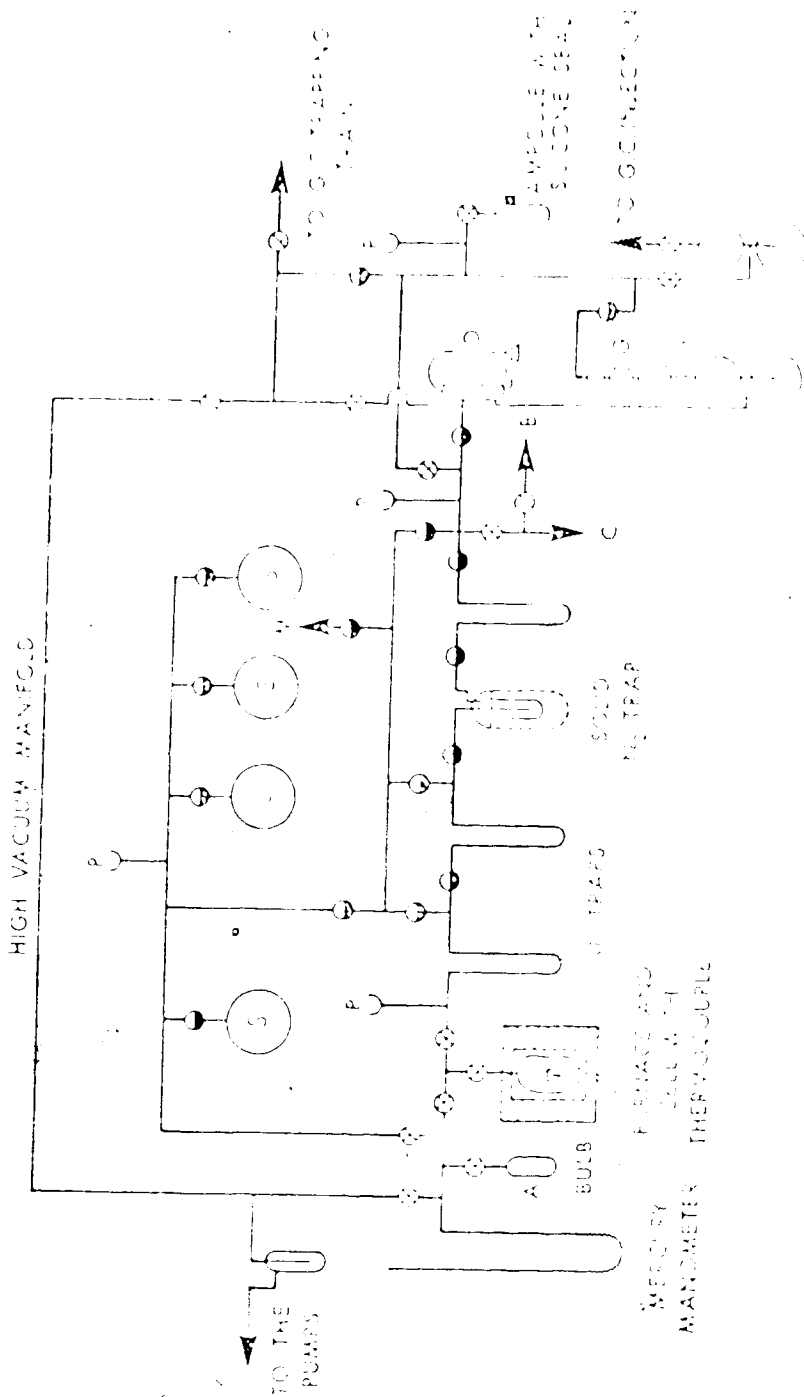


Figure II-1. High Vacuum System.
 A, calibrated bulb; B, outlet to diffusion pump; C, to atmosphere; D, diffusion pump; E, gas burette; F, gauge; G, silicon tube; H, stopcock; I, check valve; J, mercury float valve; K, glass stopcock.

valves and Toepler pumps. The inner surface of the gas handling system was treated with trimethylchlorosilane before use, and every time after being exposed to air in order to deactivate free -OH groups on various surfaces in the system which could cause decomposition of silanes³³.

(2) The auxiliary system (Figure 11-2) was a conventional high vacuum assembly pumped by a two-stage mercury diffusion pump backed by a Cenco Hyvac 7 oil pump. The apparatus was kept grease free by using Delmar mercury float valves, Hoke 425106Y-16-SS valves, or teflon stopcocks (Ace Glass Inc. number 8194) equipped with Viton-A "O" rings. The vacuum system consisted of a distillation train, storage bulbs and a special line lined with a Porapak Q column. The column could be cleaned by a stream of helium, evacuated and used for purification of substrate, as described in Section II-D-3. The auxiliary system was also used for mercury-photosensitized decomposition of substrates in order to prepare authentic samples of disilanes, as described in Section II-E. A cylindrical quartz cell, 10 cm in length and 5 cm in diameter containing a small drop of mercury was attached to the vacuum system via a Hoke valve. A low pressure mercury resonance lamp (Hanovia #687A45) was used as the source of radiation.

Before use, the vacuum system was treated with gaseous trimethylchlorosilane.

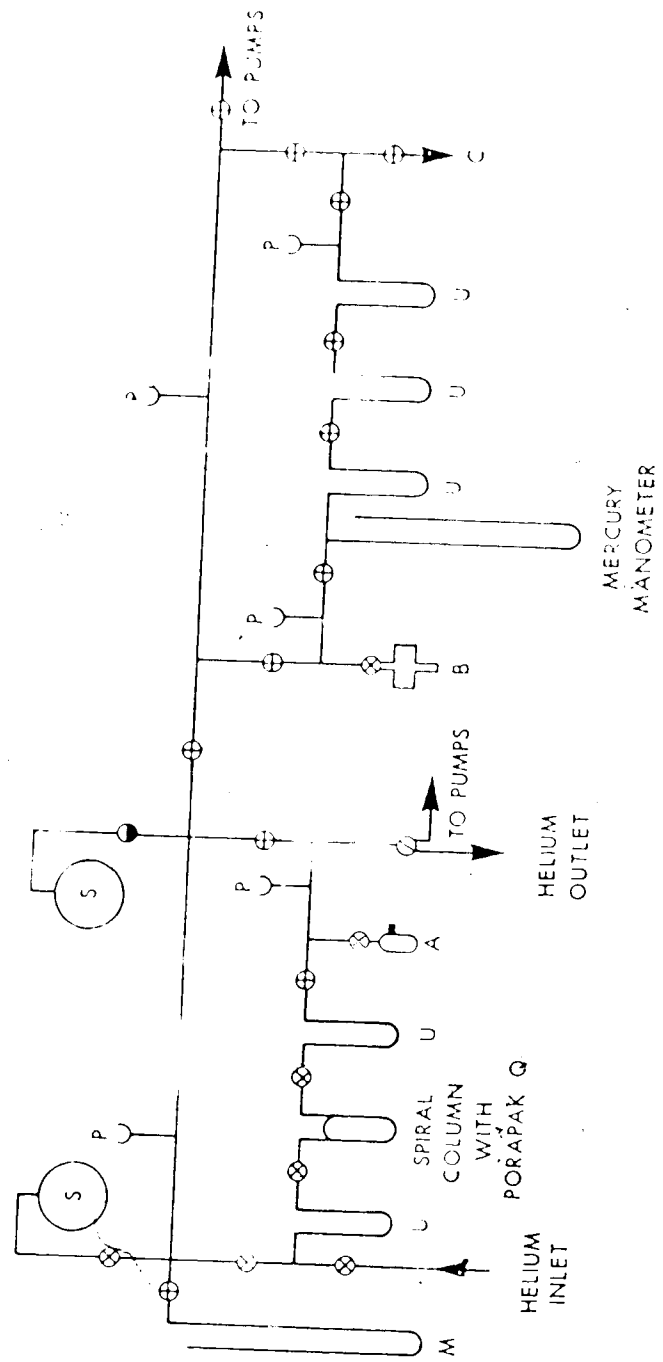


Figure II-2. Auxiliary Vacuum System for Photolysis and Purification of Methylsilane and Dimethylsilane.
 A, sampling ampoule with silicone seal. B, photolysis cell.
 C, to atmosphere. II, mercury manometer. P, Pirani tube.
 S, storage manometer. U, u-traps. U₃ -Hoke valve, G -Teflon valve with "O" rings, G₃ -three-way glass stopcock, G₄ -mercury float valve.

B. Pyrolytic Furnace Assembly

The pyrolytic assembly consisted of a quartz vessel surrounded by an aluminium block furnace as depicted in Figure II-3⁹⁶. The reactor was connected to the vacuum line with a high temperature Hoke valve which in turn was fastened to the furnace block in order to minimize dead space.

The cylindrically-shaped furnace consisted of two halves connected by hinges allowing easy removal from the reaction vessel. The aluminium block was surrounded by a layer of glass wool and transite and, in order to minimize temperature fluctuation and heat loss, the entire unit was wrapped in aluminium foil and placed into a box made of asbestos board. The furnace was heated by means of eight 300-watt pencil heaters arranged in parallel to ensure uniform heating. The pencil heaters were powered and regulated by an API 2-Mode proportional electronic controller. The junction of an iron-constantan thermocouple from the controller was located in a small gap between the reaction vessel and the aluminium block in the middle of the furnace. The temperature of the furnace was maintained to within $\pm 0.2^\circ\text{C}$ and the gradient over the length of the reaction vessel was less than $\pm 0.3^\circ\text{C}$.

Two iron-constantan thermocouples were used to monitor the temperature in the reaction vessel. One was

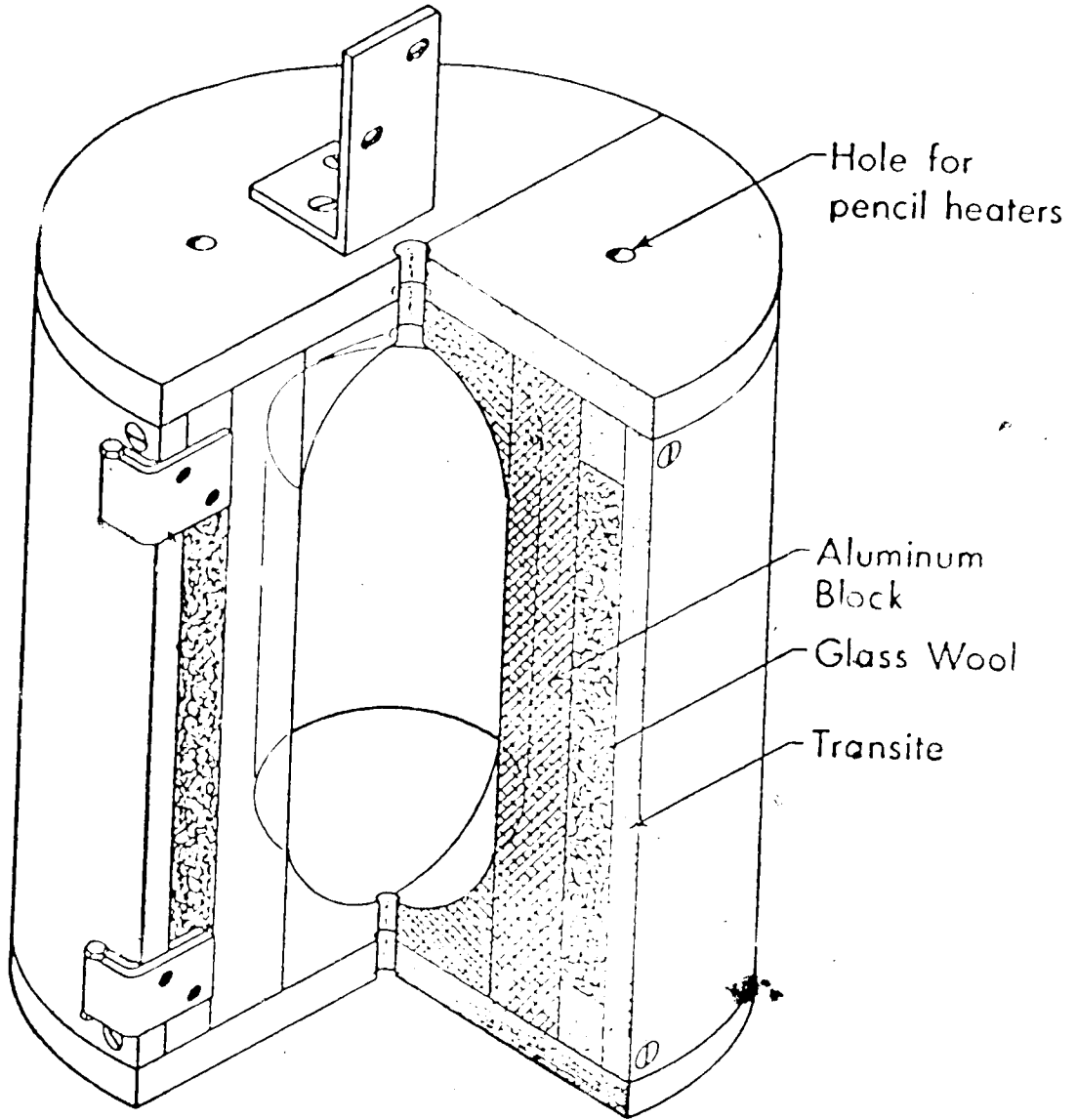


Figure II-3. Sectional View of the Pyrolytic Furnace.

positioned on the outside wall of the vessel and the other in the center of the cell by means of a special thermocouple well. The electromotive force was measured by a Wheelco Instruments potentiometer (Model 310-P), with the reference junctions of the thermocouples at 0°C. A small temperature drop in the cell ($\approx 1.0 - 1.5^\circ\text{C}$) was observed immediately after a fresh reaction mixture was admitted. The temperature rose to the original preset value within 20-40 sec and thereafter remained constant (to within $\pm 0.2^\circ\text{C}$). In short experiments, the reaction temperature was corrected for the initial drop.

Before use, the reaction vessel was treated with a 2:9 mixture of concentrated hydrofluoric and nitric acids, then rinsed with distilled water, acetone and methanol and dried in a vacuum oven at 190°C . After the vessel was attached to the vacuum system and evacuated, it was treated with gaseous trimethylchlorosilane and then thoroughly evacuated to 10^{-6} torr.

Most of the experiments were carried out in a quartz cell of volume 206.6 cc with a surface/volume ratio of about 1.0 cm^{-1} . The inner surface of the cell was coated by a polymer from previous experiments. For investigation of surface effects, a packed cell of volume 153.5 cc with surface/volume ratio of about 21 cm^{-1} was prepared by filling a quartz vessel with quartz tubings the ends of which were fire polished.

C. Analytical Methods

1. Gas Chromatography

The main analytical method employed was gas chromatography with detection by flame ionization or thermal conductivity.

(i) The thermal conductivity gas chromatograph was a component type and was coupled directly to the high vacuum system. The Gow-Mac TR-II-B detector was equipped with W2 filaments and operated at 63°C. The filament current was kept constant at 250 ma by means of a Gow-Mac 9999C power supply, and the results were read out on a Sargent recorder model RS. The carrier gas was helium; it was dried by passage through a column of molecular sieve at -196°C and its flow was regulated by a Hewlett-Packard flow controller (No. 5080-6710).

The thermal conductivity g.c. was used mainly for analyses of the product gases noncondensable at solid nitrogen temperature (-210°C), namely hydrogen and methane. Hydrogen was determined by difference. The thermal conductivity g.c. was also used for separation and identification of condensable products. After passage through the column and detector, the separated components in the effluent could be condensed in a trapping train, from which they could be transferred directly to the high vacuum system and used for mass spectral analysis or preparation of calibration mixtures.

The columns used and the operating conditions are summarized in Table II-1.


TABLE II-1
Thermal Conductivity G.C. Operating Conditions

Column	Dimensions	Flow Rate ^a cc min ⁻¹	Temperature °C	Compounds Analysed
Molecular Sieve 13x, 30-60 mesh	6 ft x 6 mm i.d. glass	35	25	H ₂ , CH ₄
10% Silicone gum Rubber SE-30 on Chromosorb W (AW-DMCS), 60-80 mesh	20 ft x 6 mm i.d. glass	40	50	MeSiH ₃ Me ₂ SiH ₂ Me ₃ SiH (Me ₂ SiH) ₂
Porapak Q 50-80 mesh	5 ft x 6 mm i.d. glass	45	50-160	C ₂ H ₄ , C ₂ H ₆ MeSiH ₃ C ₃ H ₆ , C ₃ H ₈ Me ₂ SiH ₂ Me ₃ SiH MeEtSiH ₂ (MeSiH ₂) ₂

^a Using helium.

(ii) The flame ionization chromatograph was a Hewlett-Packard model 5750 and was used for analysis of the reaction products condensable at liquid nitrogen temperature (-196°C). It was operated in a dual column-dual detector arrangement with temperature programming, as follows: 6 min post-injection interval at 60°C , temperature rise $20^{\circ}\text{C}/\text{min}$ ($60 \rightarrow 165^{\circ}\text{C}$), 20 - 40 min upper limit interval at 165°C . The dual flame detectors were operated at 230°C with hydrogen and oxygen flow rates of 20 cc/min and 200 cc/min, respectively. Helium was the carrier gas; its flow rate was 25 cc/min and it was dried as described previously. Two identical 6' x 1/4" stainless steel columns packed with Porapak Q (50-80 mesh) were used in a dual operation, one for product separation and the other as reference, in order to reduce a baseline drift during temperature programming due to column bleeding. The drift was further reduced by using teflon-coated minimum bleed septums (Unimetrics, catalog No. 2016) in the injection port. The sample was injected with a gas syringe and the results were displayed on a Minneapolis-Honeywell chart recorder model 15307856-01-05-0-000-790-07 009.

Linearity of the detector response for the substrate was determined, and the relative response factors for the products (with respect to the substrate) were obtained by calibration using authentic samples. In g.c. analyses of the



reaction mixtures, the substrate could be used as internal standard, since its concentration was practically unchanged (within experimental error) at conversions below 1. When silicon compounds were burned in the flame of the detector during analysis, a white powder of SiO_2 was formed which deposited on both the jet and collector of the detector. The powder was periodically wiped off and the jet was cleaned by means of a fine wire. It was confirmed, by frequently repeated calibrations, that neither the white deposit nor the cleaning operations affected the relative response factors of the detector.

The compounds which were analyzed by means of the flame ionization g.c. are listed below in the order of their retention times: ethylene, ethane, monomethylsilane, propylene, propane, dimethylsilane, trimethylsilane, methylethylsilane, dimethylethylsilane, 1,2-dimethyldisilane, 1,1,2,2-tetramethyldisilane. Product identifications were accomplished by comparison of their g.c. retention times and mass spectra with those of authentic samples. Since authentic samples of methylethylsilane and dimethylethylsilane were not available, the identification of these compounds was based on analysis of their mass spectra, listed in Appendices I and II.

2. Mass Spectral Analysis

Mass spectra were obtained on Associated Electronics Industries instruments, models MS 2 and MS 12. On both of these instruments, it was possible to carry out gas chromatographic analysis with simultaneous mass spectrometry of each peak as it eluted from the column.

Hydrogen isotope ratios were determined on Associated Electronics Industries Models MS 10 and MS 2 mass spectrometers.

D. Experimental Procedure

1. Pyrolysis

Before the experiment, the reaction vessel was thoroughly evacuated to 10^{-6} torr and its temperature was preset to the desired value. Pure substrate from the storage tank was condensed in bulb A (see Figure II-1) by liquid nitrogen. Bulb A was then warmed to room temperature and the pressure of the substrate was measured with a mercury manometer. The volume of bulb A and that of the adjacent manifold leading to the manometer were calibrated. The manometer pressure was read by means of a cathetometer with a precision better than ± 0.05 torr and the substrate was admitted to the reaction vessel by a momentary opening of the valve attached to the reactor. While the reaction was in progress, the remaining substrate in the manifold was transferred to bulb A. The actual pressure in the reaction vessel

was calculated from the difference. Since the conversions were generally low, 0.1 - 0.5 (1 maximum), any pressure changes in the reaction vessel were negligible and there was no special need for any pressure monitoring device in the reaction vessel. On the contrary, it could be a source of an additional error by increasing dead space of the reactor.

In the experiments with mixtures of gases, the reactant pressures were individually measured and then the components condensed together in bulb A. With the valve to the manifold closed, the bulb was suddenly submerged into hot water bath and allowed to stand for several hours to assure good mixing.

Product Analysis

After pyrolysis, the reaction mixture was passed through two traps at -196°C and -210°C respectively.

(i) The gases noncondensable at -210°C were pumped off with a one-stage mercury diffusion pump and a Toepler pump and measured in a gas burette. The pumps were operated continuously for about 30 minutes after the end of each experiment and during this period readings of the gas burette were taken in 6 minute intervals, in order to get some information about gas evolution from the polymer in the reaction vessel. From the gas burette, the noncondensable gases were transferred quantitatively by means of a second

Toepler pump into the evacuated sample loop of the thermal conductivity g.c. and introduced to the column for analysis.

(ii) The reaction products condensable at -210°C were usually present only in minute quantities (< 0.02 μ moles), very often too small to be measured in a gas burette.

Measurable quantities of this fraction were obtained in the pyrolysis of monomethylsilane at high conversions (> 1) and mass spectrometric analysis indicated the presence of monosilane.

(iii) The entire condensable (-196°C) mixture, consisting of substrate and products, was first measured in a gas burette and then quantitatively transferred into a Pyrex ampoule fitted with a mercury covered Bell Silicone rubber seal. The mixture was allowed to warm up and the internal pressure was raised to 760 torr by introducing helium with a gas syringe. The ampoule contents were mixed by pumping with the gas syringe and a suitably sized sample (5 - 100 μ l) was then withdrawn for injection into the flame ionization g.c. described in Section II-C-1. The injection was usually repeated several times for the same mixture to insure higher precision. Knowing the total amount of sample and relative response factors of the detector for the major components, the composition of the mixture could be determined from the relative peak areas measured with a planimeter.

3. Substrate Purification

Special methods of purifying monomethylsilane and dimethylsilane were developed. The auxiliary vacuum system shown in Figure II-2 was used for this procedure.

(i) Monomethylsilane

A major impurity in monomethylsilane (MMS) was dimethylsilane (DMS) which, although present in quantities less than 1%, was nevertheless one of the reaction products in the pyrolysis of MMS and therefore it was necessary to remove it from the substrate completely. A simple low temperature distillation did not give satisfactory results since the vapor pressures of MMS and DMS are quite similar. An excellent separation, however, was obtained by distilling the mixture through a Porapak Q column and collecting only the first fraction.

The purity of MMS from this fraction was checked by flame ionization g.c., which was capable of detecting impurity levels less than 0.001%, and no traces of DMS were found. A high efficiency of purification was the main advantage of the method since in a single operation, lasting less than 10 minutes, it was possible to obtain pure substrate in quantities sufficient for 10-30 experimental runs (about 20 moles).

The column was a Pyrex spiral trap (6 ft long, 9 mm i.d.) packed with Porapak Q (80-100 mesh). Before use,

6

it was first purged by a stream of dried helium at 150°C for several hours, allowed to cool to room temperature, and then thoroughly evacuated to less than 10^{-5} torr, usually overnight.

Methylsilane (previously distilled at -160°C and degassed at -160°C) was transferred into a B-trap adjacent to the column and its pressure maintained at about 600 torr by means of a low temperature bath of dimethylacetate slush. The Porapak column was operated at 0°C. The impure MMS was admitted into the column and the fraction which passed through within 3 minutes was collected in the second B-trap at -198°C. After a purity check, this fraction was transferred into a storage bulb. The remaining impure MMS was then removed from the distillation line and helium was passed through the heated column in order to prepare it for the next purification cycle.

Monomethylsilane- d_3 was also purified in the same manner.

(ii) Dimethylsilane

The major impurities in dimethylsilane (DMS) were monomethylsilane (MMS), trimethylsilane (TMS), and traces of propane. Since MMS and TMS were both reaction products of the pyrolysis of DMS, they must be removed from the substrate. Removal of MMS and propane was accomplished by a repeated degassing of DMS at -130°C (n-pentane slush). In order to remove TMS, DMS was first distilled at -115°C

(ethanol slush) and then passed through the Porapak Q column, as in the case of MMS. The column was operated at 25°C, the pressure of impure DMS was maintained at about 150 torr by means of a chloroform slush (-64°C), and the fraction of pure DMS eluted in 6 minutes was retained.

E. Materials

The materials used, their source and their purification are listed in Table II-2.

Authentic samples of 1,2-dimethyldisilane and 1,1,2,2-tetramethyldisilane were prepared by the mercury photosensitized decomposition of monomethylsilane (MMS) and dimethylsilane (DMS), respectively, as described by Nay et al.³¹ The photolysis cell in the primary vacuum system (Section II-A) was filled with about 100 mm of substrate silane and irradiated at room temperature for 2 hrs; the disilane product was separated from the substrate by a low temperature distillation at -130°C and -115°C for MMS and DMS, respectively, and purified by preparative g.c. by means of the thermal conductivity gas chromatograph. The columns and conditions used are listed in Table II-1.

TABLE II-2

Materials Used

Material	Supplier	Purification
Helium	Canadian Liq. Air; Linde	Passed through column of molecular sieve at -195°C.
Hydrogen (for g.c.)	Canadian Liq. Air; Linde	None
Oxygen (for g.c.)	Canadian Liq. Air; Linde	None
Methane	Matheson	None
Ethylene	Phillipps Petroleum	Degassed at -186°C. Distilled at -160°C.
Monosilane	Merck, Sharp and Dohme	Degassed at -196°C. Distilled at -160°C.
Monomethylsilane	Merck, Sharp and Dohme	As described in Section II-D-3.
Monomethylsilane-d ₃	Merck, Sharp and Dohme	As described in Section II-D-3.
Dimethylsilane	Peninsular	As described in Section II-D-3.

TABLE II-2 (cont'd)

Materials Used

Material	Supplier	Purification
Trimethylsilane	Chemical Procurement	Degassed at -112°C Distilled at -98°C .
1,2-Dimethyldisilane	Laboratory preparation as described in Section II-E.	Preparative g.c.; conditions as in Table II-1.
1,1,2,2-Tetramethyldisilane	Laboratory preparation as described in Section II-E.	Preparative g.c.; conditions as in Table II-1.
Trimethylchlorosilane	PCR Incorporated	Fractional Distillation at 760 torr; a fraction boiling at $56-58^{\circ}\text{C}$ was collected.

^a Research Grade, purity 99.99%.

CHAPTER III

PYROLYSIS OF MONOMETHYLSILANE

A. Results

The pyrolysis of monomethylsilane was studied in a static system over the range of conditions 340 - 440°C and 40 - 400 torr initial substrate pressure. The investigation was focussed on the initial stages of the reaction (conversions below 1%) where secondary decompositions are minimal. The effects of time, reaction vessel surface, and addition of a free radical scavenger were investigated in order to determine the nature of the processes responsible for the observed products.

1. The Reaction Products and Their Distribution

The following products were observed in the early stages of pyrolysis of monomethylsilane (MMS): hydrogen, 1,2-dimethyldisilane (DMDS), dimethylsilane (DMS), monosilane, methane, and a dark brown polymer deposited on the inner surface of the reaction vessel.

Hydrogen and DMDS were the major reaction products and DMS was a minor product; monosilane and methane were formed occasionally in trace amounts and often could not be detected at all (the detection limits

for SiH_4 and CH_4 were approximately 0.015 and 0.005 μ moles, respectively).

Polymer was another minor reaction product, and since it could not be directly measured and analyzed, its formation created certain complications. Some of the problems associated with polymer formation are reported later; it should be pointed out here, however, that reproducible reaction rates were obtained only in a vessel which was well coated by a polymer from previous runs.

(i) Gaseous Products

The only significant reaction products formed in the initial stages of MMS decomposition (1% conversion) were hydrogen, DMDS and minor amounts of DMS. The ratio H_2/DMDS was approximately 1.15 ± 0.10 , and both products showed a linear dependence on time. The amount of DMS formed was about 5% of that of the major products.

At conversions above 1%, the product distribution was altered considerably. The rates of formation of H_2 and DMS were enhanced whereas that of DMDS declined; also, some methylsilane could be detected among the reaction products.

Product yields as a function of time at 422°C and 127 torr are listed in Table III-1, and illustrated in Figure III-1. The experiments were performed in a

TABLE III-1

Variation of the Product Yields with Time in the
Pyrolysis of MeSiH_3 at 422°C ^d

Time, min	Yields, μ moles				Conversion ^b
	H_2	DMDS	DMS	SiH_4	
3.0	2.18	1.83	0.09	c	0.37
4.0	2.99	d	d	c	0.49
6.0	4.37	3.76	0.20	c	0.69
12.0	9.30	7.57	0.84	0.27	1.51
12.0	8.06	7.29	0.56	0.02	1.32
18.0	13.87	10.51	1.51	0.13	1.77
24.0	19.54	17.55	2.91	0.10	3.32

^a Pressure 124 - 130 torr; cell volume 206.6 cc;
 $S/V = 1.0 \text{ cm}^{-1}$.

^b Based on the yield of H_2 .

^c Too small to measure ($< 0.02 \mu$ mole).

^d Not measured.

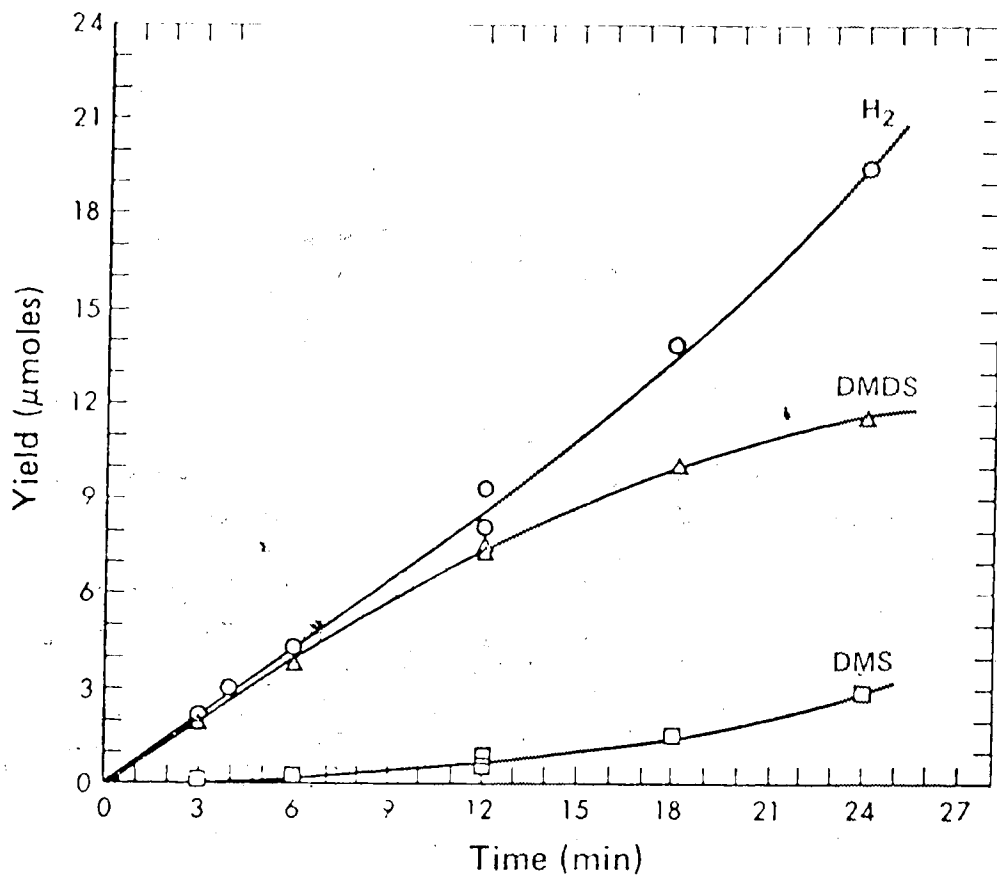


Figure III-1. Product Yields as a Function of Time in the Pyrolysis of MeSiH₃ at 422°C.

reaction vessel of volume 206.6 cc (surface/volume ratio 1.0 cm^{-1}) which was already coated by a polymer.

Upon carrying out the pyrolysis to conversions of 10 - 20% or higher, the reaction system became quite complex and a large variety of new products were formed, not all of which were identified; however, DMS was one of the dominant condensable products and it was present in quantities higher than those of DMDS, indicative of the high thermal stability of DMS. An example of the product yields at conversion of 20.5% is given in Table III-2.

The investigation was therefore limited only to the initial stages of pyrolysis of MMS, i.e. to such conversion where secondary decomposition of the primary products was negligible. Most experiments were carried out to 0.1 - 0.5% conversions, and occasionally as high as 1% in order to obtain sufficient amounts of reaction products for analyses.

(ii) Polymer

Preliminary experiments in a new reaction vessel revealed that the reaction rates were both high and erratic and that only after carrying out several runs to high conversions, after which the inner surface of the vessel became coated by a polymer, did the rates become lower and quite reproducible.

TABLE III-2
 Product Yields in the Pyrolysis of MeSiH₃ at High Conversion

Temp. °C	Time, min	P(MMS), ^a torr	MMS consumed, ^b μ moles	Yield ^c , μ moles		Conversion ^b %
				H ₂	CH ₄	
360	4750.0	88.0	93.9	94.4	5.74	20.5
				17.1	2.02	1.57

^a Initial pressure in a vessel of volume 206.6 cc; S/V = 1.0 cm⁻¹.

^b Based on the yield of H₂.

^c Some other products were formed but were not analyzed.

The chemical composition of the polymer was not analyzed. Although a mass balance between gaseous products and monomethylsilane reacted was attempted, no definite conclusions could be reached since most experiments were carried out at very low conversions where the yield of polymer is extremely small and well within experimental error of the amount of MMS reacted.

The polymer was found to be thermally unstable, since a slow evolution of gases from the coated vessel could be observed upon heating, nevertheless it could not be completely removed from the cell even by a prolonged heating in a vacuum. The rate of degassing, however, was extremely slow when the experiments were carried out to conversions below 10% and the amount of products which could be collected from the decomposing polymer was not sufficient for analysis.

At high conversions however a large quantity of the polymer accumulated in the reaction vessel and it was possible to follow the polymer decomposition for a long period of time (about 8 hrs) and to monitor its rate. In a typical experiment, listed in Table III-2, 8 torr MMS was pyrolyzed for about 79 hrs at 360°C (~20.5% conversion). The reaction vessel was opened to the main vacuum line for 30 min and then the rate of evolution of the light gases was measured.

The light gases evolved from the polymer consisted mainly of hydrogen and methane; some condensable products were also formed in trace quantities, and the presence of lower hydrocarbons (C_2 , C_3) and all methylated monosilanes was confirmed.

The data obtained for the light gases are shown in Table III-3 and plotted in Figure III-2, from which it is seen that the rate of degassing was very steady even after several hours and therefore could be treated quantitatively.

Since hydrogen was also one of the major reaction products of the pyrolysis of MMS, it was necessary to determine the relative importance of hydrogen formation from the thermolysis of the polymer.

After prolonged heating and evacuation of the reaction vessel, the rate of gas evolution declined and then finally became unmeasurably slow or ceased completely. (The time needed to reach this stage could vary from several hours to a few days, depending on the temperature used and the amount of polymer deposited previously.) When such a vessel was used for pyrolysis of MMS at conversions below 1%, no significant degassing from the vessel was observed, indicating that the polymer was only a very minor product and its decomposition was not important compared to the pyrolysis of MMS.

TABLE III-3

The Yield of Gases ^a from Polymer
Decomposition at 360°C as a Function
of Time

Time, min	Yield, μ mole	Time, min	Yield, μ mole
16.0	0.04	225.0	0.67
26.0	0.08	254.0	0.74
36.0	0.11	265.0	0.79
46.0	0.13	290.0	0.85
56.0	0.16	300.0	0.89
66.0	0.19	325.0	0.95
76.0	0.21	335.0	0.99
86.0	0.24	350.0	1.03
96.0	0.27	361.0	1.06
104.0	0.28	371.0	1.08
121.0	0.34	400.0	1.17
131.0	0.38	411.0	1.21
160.0	0.46	420.0	1.24
170.0	0.49	430.0	1.26
180.0	0.53	440.0	1.29
191.0	0.55	450.0	1.31
200.0	0.59	463.0	1.34
213.1	0.63	470.0	1.36 ^b

^a H₂ + CH₄

^b Contains ~ 0.06 μ mole CH₄ and ~ 1.30 μ mole H₂

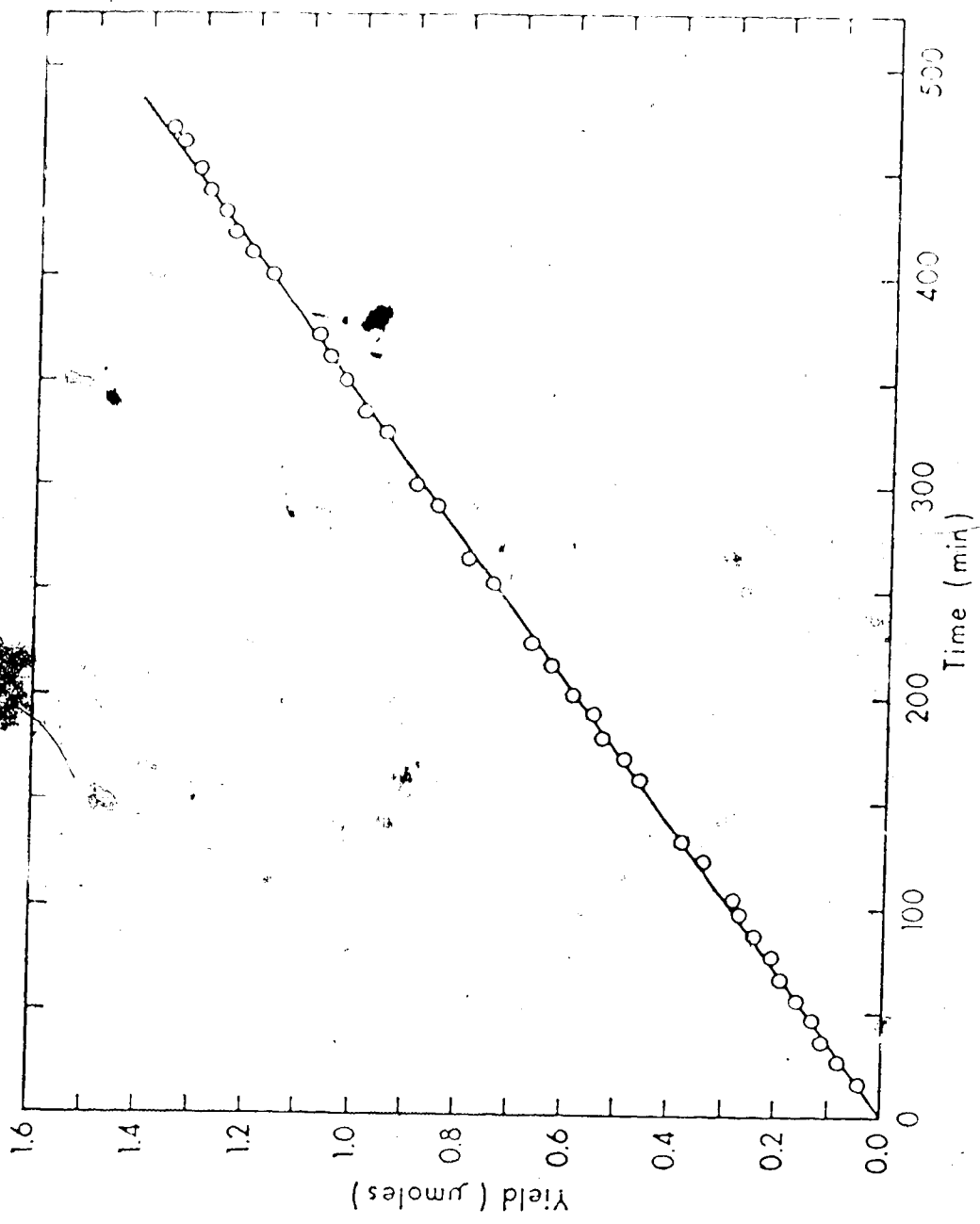


Figure III-2. $H_2 + CH_4$ Yields from Polymer Decomposition at $360^\circ C$ as a Function of Time.

To summarize, reproducible rates could be obtained in a seasoned reaction vessel provided the conversions were kept below 1. In those cases where extensive decomposition of MMS had occurred, or when a large number of experiments had been performed in short consecutive intervals and the polymer deposit was relatively heavy, a simple correction could be made to the observed H_2 yields assuming that the rates of decomposition of the polymer and of the substrate are independent. The procedure is illustrated in Appendix III. Alternatively, the reaction vessel could be heated and evacuated until no gas evolution could be detected.

2. Reaction Order of Hydrogen Formation

In order to obtain some insight into the kinetic features of the decomposition of monomethylsilane, experiments were carried out to determine the initial order of formation of hydrogen. The polymer coated vessel was heated at the reaction temperature and evacuated before each run for at least several hours, usually overnight, in order to minimize any possible contribution from decomposition of the polymer.

The reaction order of hydrogen formation can be calculated using the relationship

$$R(H_2) = k_{H_2} [MMS]^n$$

where $R(H_2)$, k_{H_2} , $[PH_2]$, and n are the initial rate of hydrogen formation, specific rate constant, initial substrate concentration, and order, respectively. In view of the logarithmic plot of rate vs. substrate pressure yields the order of reaction.

The reaction orders were determined over the temperature range 341 - 441°C and the results of the rate data, given in Table III-3 to III-7 are presented in the form of log-log plots in Figures III-3 and III-4.

The orders, determined by least mean square analyses, are summarized in Table III-3 and are seen to increase from unity, at 441°C, to 1.93 at 341°C.

3. Surface Effects and Influence of the Polymer on Surface Activity

The kinetics of gas phase thermal reactions are often complicated by contributions from heterogeneous reactions. Surface reactions are generally very complex phenomena, influenced by surface activity and difficult to control and reproduce, and their occurrence should be minimized in the studies of homogeneous reactions. Surface reactions are particularly prevalent in new, unused reaction vessels, and the walls of the vessel often require a special treatment in order to suppress surface effects; the most usual way is to pyrolyze the substrate repeatedly until the experimental results become

TABLE III-4
 Variation of the Hydrogen Yield with
 Monochloroethane Pressure at Different Temperatures^a

Pressure, mm	Time, hr	H ₂ Yield, g/mole	Conversion, %
441°C			
216.5	1.00	3.00	0.310
171.5	1.01	2.47	0.254
153.7	1.00	2.62	0.267
118.0	1.00	1.57	0.163
104.0	1.00	1.59	0.164
80.0	1.01	1.05	0.109
70.0	1.05	1.18	0.122
57.0	1.50	1.11	0.115
48.0	1.50	0.80	0.083
39.5	2.00	1.02	0.106
32.3	2.00	0.87	0.090
-29°C			
203.5	1.50	2.97	0.308
138.2	1.50	1.76	0.182
94.0	2.00	1.38	0.142
63.7	3.00	1.47	0.152
42.8	4.00	1.24	0.127

^a Cell volume 206.6 cc.

TABLE III-5
Variation of the Hydrogen Yield with
Monomer (Cyclane) Pressure at 421 °C^a

P(MMS), torr	Time, min	H ₂ Yield, mole	Conversion, %
214.5	2.50	2.34	0.229
177.0	2.50	1.87	0.221
147.1	2.50	1.53	0.218
125.7	3.20	1.66	0.277
120.2	3.00	1.48	0.258
100.3	3.05	1.21	0.253
81.4	4.50	1.44	0.371
69.2	4.50	1.18	0.358
55.7	6.00	1.26	0.474
47.1	6.50	1.13	0.504
31.6	9.00	1.05	0.697

^a Cell volume 206.6 cc.

TABLE III-6
 Variation of the Hydrogen Yield with
 Monomer: Plane Pressure at 400°C^a

P(MMS), torr	Time, min	H ₂ Yield, g. mole	Conversion, %
212.3	6.00	1.57	0.176
209.0	6.00	1.50	0.146
201.9	10.00	2.75	0.276
143.5	10.00	1.85	0.253
144.4	10.00	1.73	0.244
135.8	7.10	1.19	0.178
138.6	11.00	1.81	0.266
93.9	10.00	1.09	0.236
91.8	10.00	0.99	0.219
73.7	15.00	1.22	0.337
62.9	15.30	1.03	0.333
61.9	13.00	0.84	0.276
48.5	15.00	0.80	0.335
42.3	20.00	0.87	0.418
33.7	24.00	0.80	0.483

^a Cell volume 206.6 cc.

TABLE III-7
 Variation of the Hydrogen Yield with
 Monomethylsilane Pressure at Different Temperatures^a

P(MMS), torr	Time, min	H ₂ Yield, μ mole	Conversion, %
<u>381°C</u>			
212.8	16.50	1.58	0.147
210.2	11.00	1.09	0.102
145.2	21.50	1.15	0.156
141.5	26.00	1.34	0.187
96.5	30.00	0.94	0.192
65.2	31.00	0.60	0.182
42.9	47.00	0.57	0.263
28.4	90.00	0.73	0.508
<u>361°C</u>			
92.6	148.0	1.26	0.260
62.1	210.0	1.03	0.318
40.5	280.0	0.85	0.402
<u>341°C</u>			
195.8	275.0	2.32	0.220
128.2	325.5	1.34	0.194
84.5	353.0	1.19	0.261

^a Cell volume 206.6 cc.

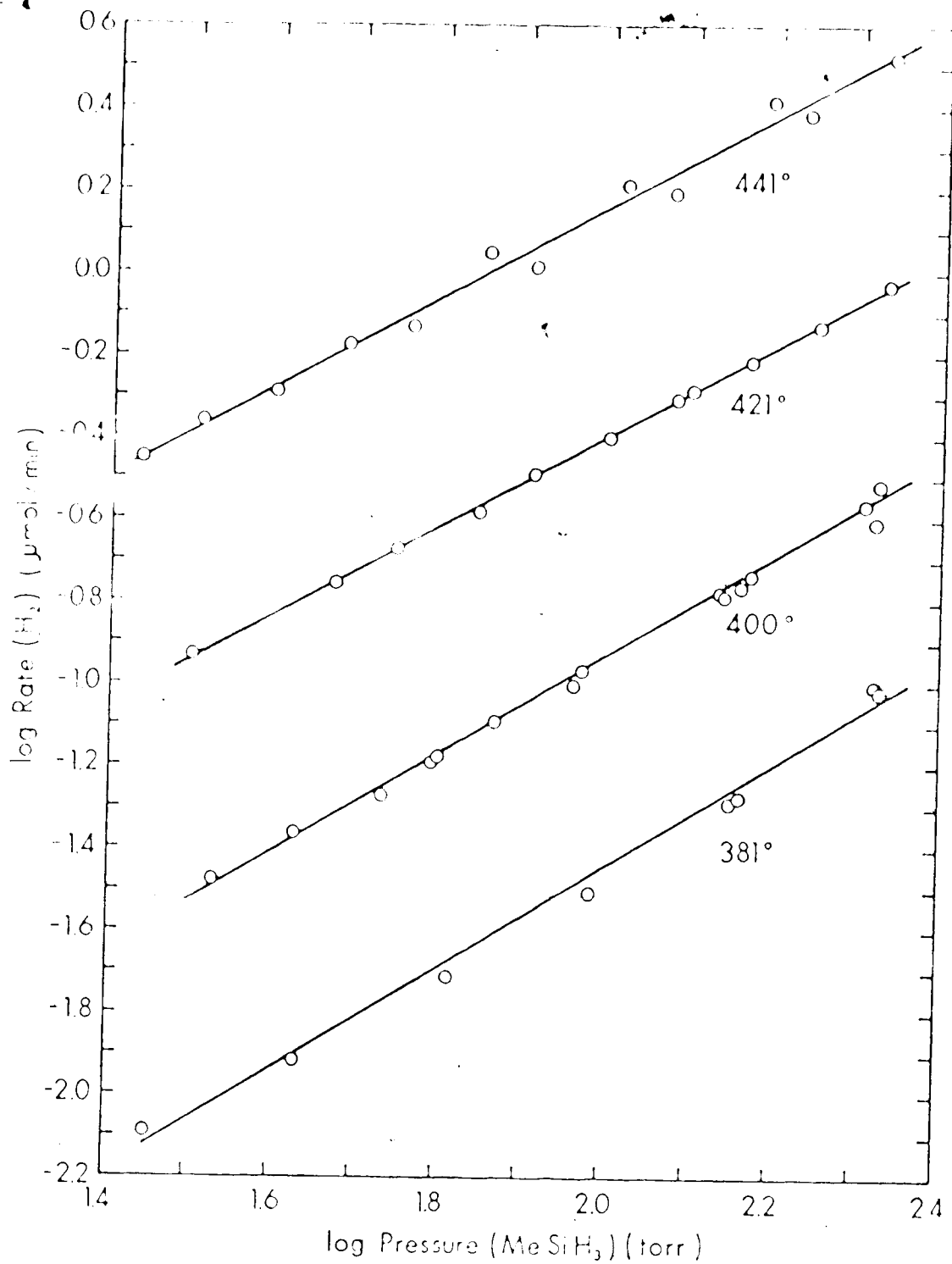


Figure III-3. Order Plots for H₂ Formation in the Pyrolysis of MeSiH₃ at 381, 400, 421 and 441°C.

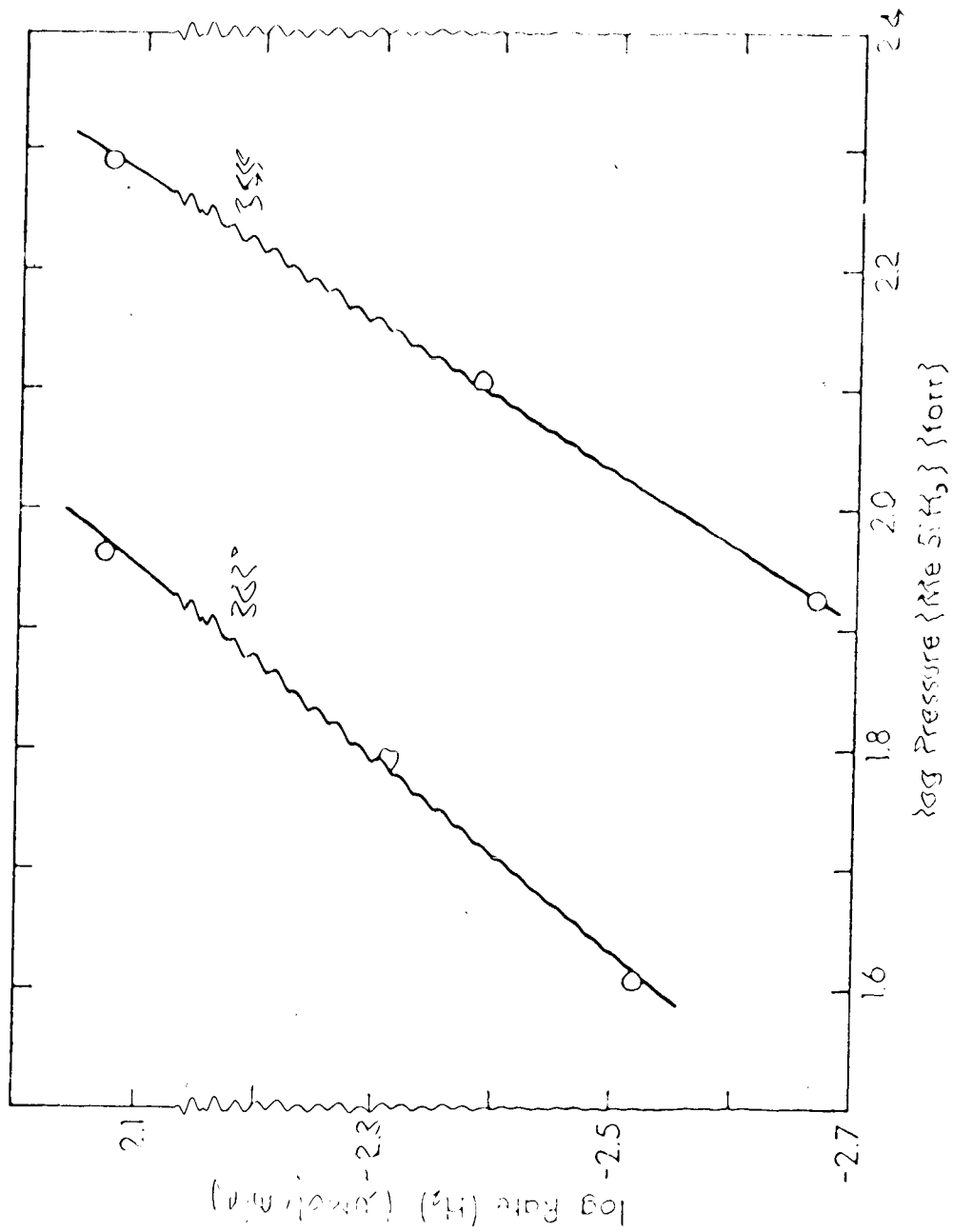


Figure 111-2. Order Plots for H₂ formation in the pyrolysis of MeSiH₃ at 322° and 355°.

TABLE III

Reaction Order of Hydrogen Formation
in the Pyrolysis of Monomethylsilane
at Different Temperatures^a

Temperature	Order
441	1.09 ± 0.04
429	1.19 ± 0.02
421	1.09 ± 0.03
400	1.17 ± 0.02
381	1.27 ± 0.04
361	1.24 ± 0.03
341	1.63 ± 0.04

^a In unpacked reaction vessel of volume
206.6 cc, $\nu = 1.0 \text{ cm}^{-1}$.

formation of the polymer, even when the reaction vessel for both packed and unpacked catalyst was packed with catalyst, some of the reaction product is adsorbed on the walls.

The influence of surfaces on the rate of the reaction is normally investigated in two ways: first, by varying the surface area to volume ratio (S/V) and, secondly, by changing the nature of the surface. Both effects were investigated.

(a) Effect of variation of the Surface Volume Rat

In order to examine the effect of the variation of the surface volume ratio on the reaction rates, the polymerization of methylsilane was carried out at 415°C at various reaction times and initial pressures of the substrate in packed and unpacked reaction vessels having S/V ratios of 27 cm^{-1} and 1.9 cm^{-1} , respectively.

The surface of both vessels was coated by a polymer from previous runs and the vessels were heated at 415°C and evacuated in between experiments, usually overnight. The vessels were initially "seasoned" by repeated polymerizations of about 70 torr MM₀ at 415°C for 10 minutes until the experimental results became reproducible; about 5 to 10 runs were required to attain reproducibility. The required conversions of the seasoning experiments increased with increasing surface area of the

vessel. The disappearance of the reaction vessels, caused by decomposition of the polymer, was monitored before and after each run, and in the run times where evolution of gases were observed, a correction for the loss of solid was applied. (See Appendix III).

Initial time studies were carried out in the packed vessel at 415°C and at initial substrate pressures of 40, 100, 200 and 300 torr, to investigate the nature of the reaction under high conversions. The results, Tables III-9 and III-10, were found to be similar to those obtained in an unpacked vessel at 415°C and 100 torr (see Table III-1 and Figure III-1), confirming the linear dependence of $\log p_0$ and GMS formation on time in both vessels, at conversions below 70%. GMS was again a minor product.

The product yields as a function of MMS pressure at 415°C in the packed and unpacked vessels are listed in Tables III-11 and III-12, respectively. The rates of formation of polymer, GMS and TMS at 415°C and at various MMS pressures in two different vessels are compared in Figures III-8, III-9 and III-10, respectively, using 100 torr as a reference point.

The results indicated that the pyrolysis of MMS might be partly heterogeneous, since the rates of formation of all the products in the packed vessel appeared

TABLE III-9
The Products of Methane Pyrolysis as a Function
of Reaction Time at 410°C^a

Time, min	Yields, μ moles				Conversion, ^b %
	H_2 ^c	CH_4	CM_4	SiH_4	
3.00	2.07	1.92	0.13	0.17	0.50
6.00	1.74	1.65	0.17	0.08	0.48
8.00	2.91	2.4	0.28	c	0.80
10.00	3.11	3.60	0.43	c	1.03
10.00	3.35	2.73	0.32	0.10	0.92
15.00	d	3.94	0.75	e	-
15.00	5.21	d	1.1	c	1.43
15.00	5.30	4.04	0.83	0.22	1.43
23.20	3.67	5.83	1.29	0.15	2.62

^a Pressure of MMO 1.07-1.14 torr; cell volume 113.1 cc; $SiV = 27 \text{ cm}^2$.

^b Based on the yield of H_2 .

^c Too small to measure on gas burette (0.002μ mole).

^d Not measured.

TABLE III
The Effect of Metallo-Precipitates on the Rate of Reaction at 45°C

Time, min	Solid (mg)				Concn. of Ca^{2+} , μM
	Ba_2SO_4	Mg	CaSO_4	CaCO_3	
	20.0% Solution				
1.50	1.12	1.14	0.00	0.00	0.13
3.00	1.15	1.17	0.14	0.00	0.14
4.00	1.91	1.97	0.11	0.00	0.40
5.00	4.28	4.30	0.00	0.00	0.84
6.00	4.43	4.40	0.00	0.00	0.81
7.50	6.13	4.93	0.41	0.00	1.04
8.00	6.16	5.10	0.47	0.00	1.04
10.00	10.10	7.86	0.33	0.00	1.41
	50.0% Solution				
2.00	0.35	0.19	0.00	0.00	0.14
5.00	1.05	0.97	0.00	0.00	0.80
10.00	1.41	1.13	0.00	0.00	1.07
12.50	1.64	1.06	0.17	0.00	1.20
15.00	2.10	1.67	0.185	0.00	1.54

^a Cell volume 15.15 cc; $0.1 \times 27 \text{ cm}^3$.
^b Based on the weight of the precipitate.
^c Too small to measure in gas burette; less than 0.1 ml.

TABLE I

Product Yield as a Function of Time (mole-% of
 H_2 at 47°C and 1.00 atm)

P, Measured, torr	Time, min	Yield, %		
		H_2	DMF	DM
344.4	2.50	3.05	4.65	0.123
363.4	2.00	3.64	3.65	0.155
364.4	2.50	3.71	3.17	0.147
383.4	2.50	3.30	2.16	0.100
384.4	2.00	2.33	2.17	0.100
389.4	2.50	1.86	1.84	0.086
405.4	3.00	2.91	3.13	0.165
403.7	6.00	4.40	4.32	0.28
404.7	2.50	1.76	1.74	0.081
404.4	2.50	1.26	1.20	0.048
454.7	2.50	1.17	1.16	0.054
453.7	3.00	1.03	0.94	0.055
481.0	6.00	1.76	1.59	0.110
481.7	2.50	0.53	0.43	0.020
471.7	2.50	0.35	0.23	0.011
471.4	6.00	1.18	1.01	0.050

$V_0 = 153.6$ cc, $STP = 01$ cm $^{-1}$.

TABLE III-17
 Product Yields as a Function of Pressure and
 Reaction Time in the Unpacked Vessel^a

P (Bar), torr	Time, min	Yields (mmole)		
		Et_2	DMDS	DMG
468.1	2.50	7.43	4.70	0.44
460.3	10.00	20.87	18.13	0.65
400.7	2.00	3.63	3.20	0.10
404.3	2.00	3.46	2.76	0.074
407.1	2.00	3.03	2.76	0.060
347.5	2.50	1.98	1.85	0.051
324.0	2.50	4.15	3.43	0.30
301.1	2.50	1.53	b	b
254.3	2.50	1.31	0.95	0.023
138.5	2.50	1.25	0.78	0.022
147.0	12.00	4.93	4.23	0.090
109.1	2.50	0.80	0.66	0.010
62.4	2.50	0.47	0.46	0.033
49.3	2.50	0.32	0.42	0.004
46.9	2.50	b	0.38	0.00
45.4	2.50	0.36	0.31	0.00

^a Volume 236.6 cc, S/V = 1.0 cm⁻³.

^b Not measured.

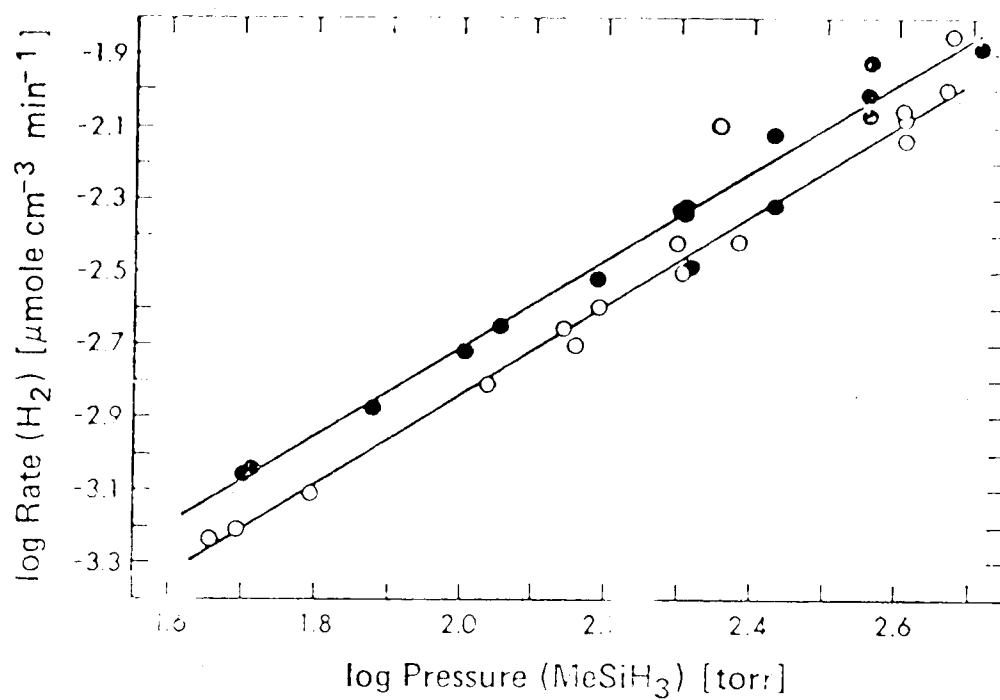


Figure III-5. Rate of H₂ Formation as Function of MeSiH₃ Pressure at 415°C in Reaction Vessels of Different S/V Ratios; ○ , 1.0 cm⁻¹; ● , 27 cm⁻¹.

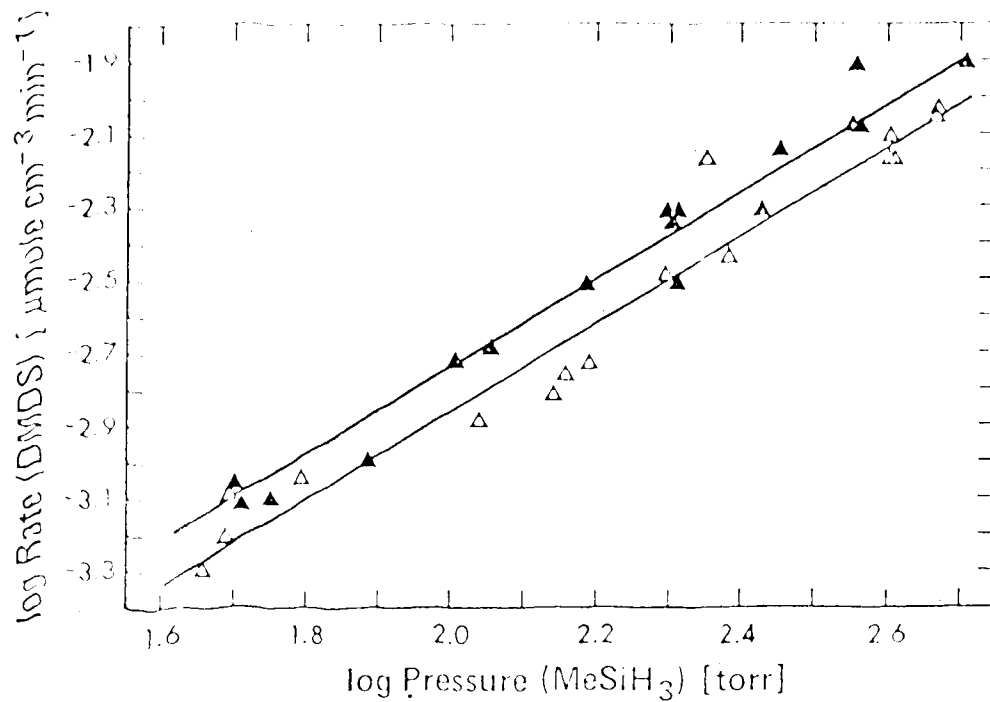


Figure III-6. Rate of DMDS Formation as Function of MeSiH₃ Pressure at 415°C in Reaction Vessels of Different S/V Ratios; Δ , 1.0 cm⁻¹; \blacktriangle , 21 cm⁻¹.

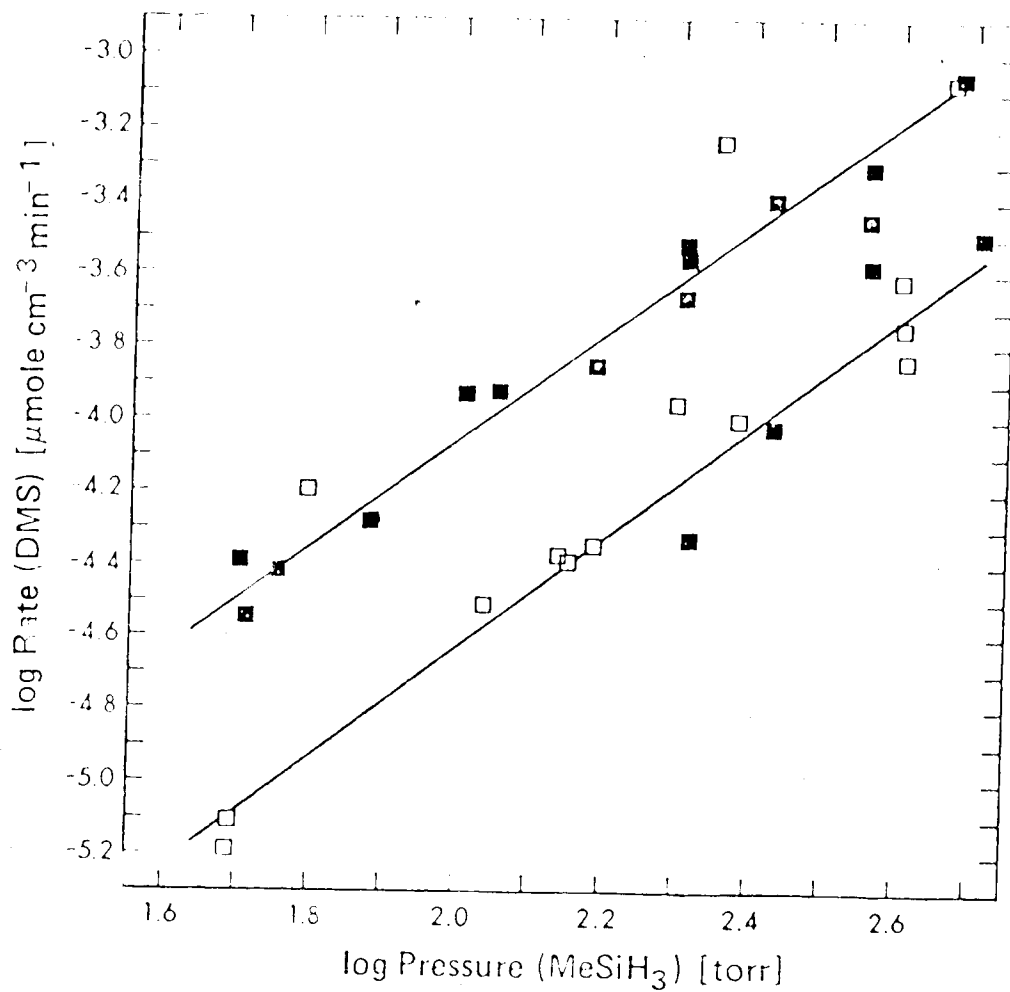


Figure III-7. Rate of DMS Formation as Function of MeSiH₃ Pressure at 415°C in Reaction Vessels of Different S/V Ratios; □, 1.0 cm⁻¹; ■, 21 cm⁻¹.

to be generally faster than those in the unpacked vessel; the minor product, DMS, was affected the most by a change in the S/V ratio.

The results, however, are not very conclusive in view of the large scatter of the data: Figures III-5 to III-7 show that some results in the packed vessel were low and essentially not different from those in the unpacked vessel, while on the other hand, some experiments in the unpacked vessel were unusually fast.

Even though the observed scatter was partly due to experimental errors, it was nevertheless possible to establish a certain correlation between the large deviation from the "expected" rates and the mode of treatment of the reaction vessel before the experiment: when the polymer was freshly deposited on the surface of the vessel, the reaction rates tended to decrease and the effect of S/V ratio on the reaction rate became less apparent; prolonged heating and evacuation of the reaction vessels, on the other hand, caused an increase in the reaction rates. The effect of the nature of the surface on the reaction rates is examined in the next section in more detail.

(ii) Effect of the Nature of the Surface

The insensitivity of a reaction rate on the surface/volume ratio does not necessarily imply a

complete absence of surface reactions, since a heterogeneous reaction could escape detection if a radical-chain mechanism which is both surface-initiated and surface-terminated were involved⁹⁷. A change in the nature of the surface, however, could indicate the presence of such radical-chain processes since as a rule the nature of the walls affects the rates of wall-initiation and wall-termination of the chain differently⁹⁸.

A very limited choice of reaction vessel surfaces was available for this investigation, mainly because polymer deposition on the surface of the vessel occurred with every run, and after several experiments, regardless of the initial treatment, the surfaces eventually became identical.

The effects of changing the nature of the surface were studied in two ways: (a) starting with a new cell, the effect of gradually increasing polymer deposition on the reaction rate was investigated and (b) the thermal stability of the polymer was examined since it was not known to what extent polymer decomposition affected the nature of the surface.

(a) The investigation of the effect of increased polymer deposit was carried out in a packed quartz vessel (volume 153.5 cc, $S/V = 21 \text{ cm}^{-1}$), which was first washed and treated as described in Section II-B, and then a

silicon mirror was deposited by repeatedly pyrolyzing monosilane to completion (hydrogen and a silicon mirror were the only products observed when 100 torr SiH₄ was pyrolyzed at 490 C for about 48 hrs). The vessel was then thoroughly evacuated to 10⁻⁶ torr and no degassing could be observed. The silicon mirror surface was chosen since it was assumed to be inert, both in the pyrolysis of monosilane³⁸ and disilane⁵⁷.

In order to determine how the thermal decomposition of MMS was affected by increasing polymer deposition in the cell, a repetitive series of experiments was carried out under identical reaction conditions in the silicon-coated reaction vessel.

The results, listed in Table III-13, are illustrated in Figure III-8, where the product yields are plotted vs the serial number of the run (i.e. the aggregate reaction time in the vessel) to show how the rates of formation of all the products are suppressed as the extent of polymer deposition increases. For comparison, products obtained in a "seasoned" packed vessel under the same conditions, are included.

From Table III-13 and Figure III-8 it can be seen that the yields of DMS and monosilane were affected the most by polymer deposition and that of DMDS, the least.

TABLE II-13
 Effect of Polymer Deposition on the Product Yields in
 Successive Pyrolyses of MeSiH_3 at $415^\circ\text{C}^{\text{a}}$

Experiment Number	$P(\text{MeSiH}_3)$, torr	Yields, μ moles			
		H_2	MDS	DMS	SiH_4
1	68.3	9.90	3.69	3.30	1.66
2	67.4	5.82	3.70	2.06	0.85
4 ^b	73.3	3.94	2.80	0.81	c
5	66.4	c	2.62	0.50	c
6	65.6	2.61	2.31	0.36	0.20
7	69.0	2.82	2.47	0.43	0.15
d	68.0	1.86	1.76	0.08	0.02

^a Time, 10.00 min; cell volume 153.5 cc; $S/V = 21 \text{ cm}^{-1}$; silicon-mirror surface.

^b The reaction mixture from experiment number 3 was accidentally lost.

^c Not determined.

^d "Seasoned" vessel.

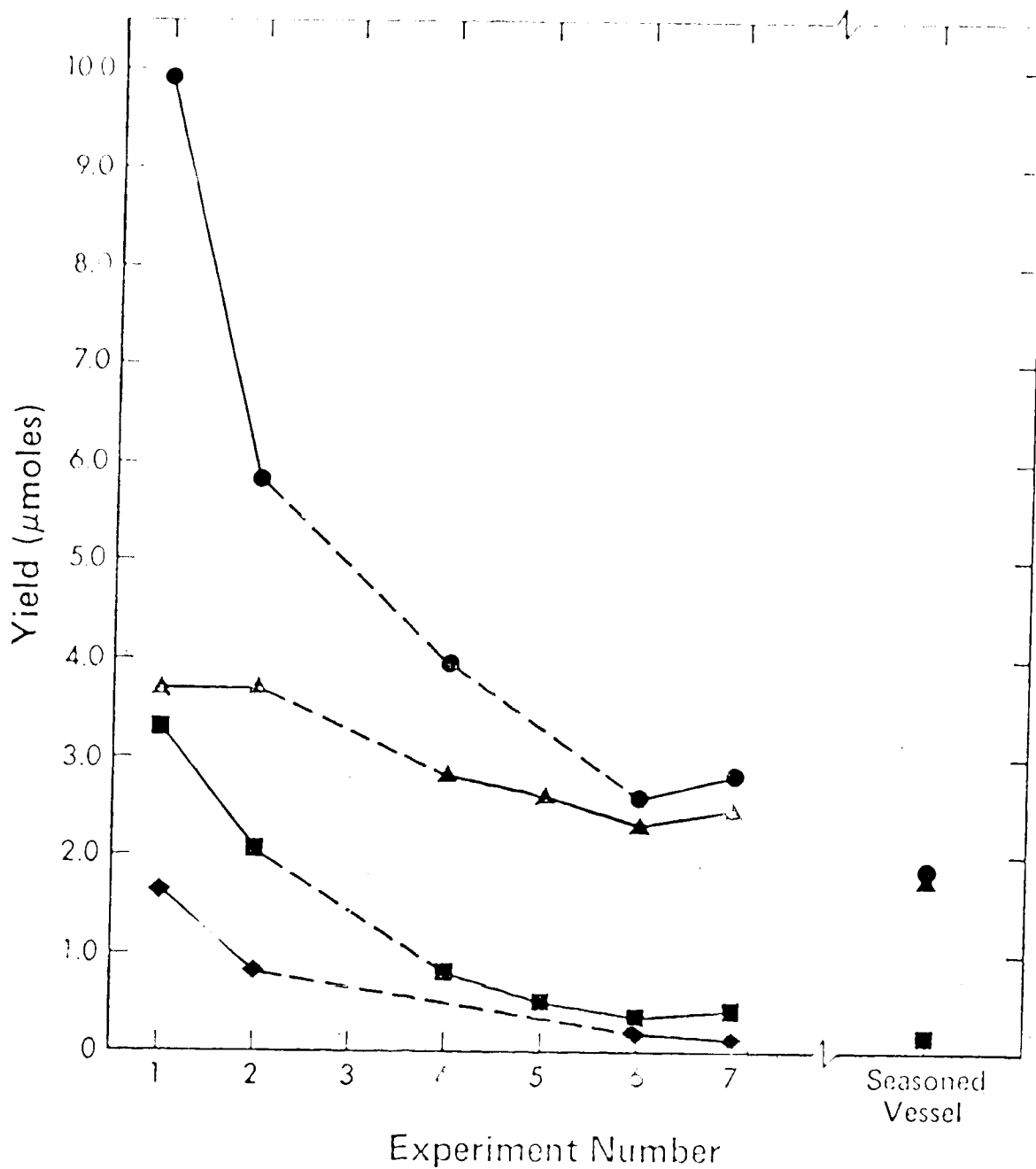


Figure III-8. Effect of Increased Polymer Deposition on the Product Yields in Successive Pyrolyses of MeSiH_3 at 415°C .

●, H_2 ; ▲, DMDS; ■, DMS; ◆, SiH_4 ;
 —, consecutive experiments;
 ---, non-consecutive experiments.

It appears that some heterogeneous processes, and probably radical chain reactions, are involved in the pyrolysis of MMS and that the polymer is able to deactivate the surface to a high extent.

(b) With regard to the thermal stability of the polymer, it should be recalled at this point that it decomposed slowly when heated in vacuum, liberating light gases. This may indicate that the character of the polymer and consequently that of the surface may have been changed by prolonged heating.

Indeed, it was observed that the rate of MMS pyrolysis obtained in a "seasoned" vessel which had been continuously heated at the reaction temperature and evacuated for a period of several days (or even at shorter periods if the temperature was raised) was always faster than that in subsequent runs.

Typical results are illustrated in Table III-14.

4. Effect of Added Ethylene

In order to determine the molecular or free radical nature of the primary steps in the reaction, the pyrolysis of monomethylsilane was carried out in the presence of ethylene.

Ethylene is a molecule well known for its behaviour as a radical scavenger, and is thermally stable

TABLE III-14

Effect of Polymer Treatment in a "Seasoned" Vessel^a on the Rate of Pyrolysis of Monomethylsilane at 415°C

P(MMS), torr	Time, min	Yield, μ mole		Rate, μ mole/min		Vessel Treatment	
		n ₂	DMS	n ₂	DMS		
400.9	2.00	11.10	6.09	5.55	3.05	0.20	3
409.	2.51	8.00	6.14	3.19	2.45	0.15	3
405.0	2.50	7.29	6.08	2.92	2.43	0.12	3
400.7	2.00	3.63	3.13	1.62	1.60	0.050	3
407.6	2.00	3.03	2.76	1.52	1.39	0.029	3
404.8	2.00	3.46	2.76	1.73	1.35	0.037	3

^a Cell volume 206.6 cc; S/V = 1.0 cm⁻¹; cell seasoned as described in Section III-A-3f.

^b Heated at 415°C and evacuated for 1 month.

^c Heated at 500°C and evacuated for 24 hrs.

^d freshly coated by polymer before experiment: 55 torr MMS (pyrolyzed at 415°C for 30 min, the mixture discarded, and the vessel evacuated for 30 min at 415°C).

at the temperatures used for the pyrolysis of MMS. Thus no hydrogen was detected when 460.5 torr of ethylene was heated at 415°C for 10 min, and only a negligible trace of methane (< 0.01 mole) was formed. Small quantities of propylene and butene were detected but these did not interfere analytically with the products from the pyrolysis of MMS.

Before each run, the reaction vessel was heated at 500°C and evacuated for 16 hrs; the effect of added ethylene on the rate of pyrolysis of MMS was investigated at 415°C and 360°C at constant MMS pressures of about 405 and 278 torr, respectively. The variation of the rates of formation of hydrogen and DMDS with pressure of added ethylene is shown in Table III-15, and the data at 415°C are illustrated in Figure III-9.

The results show that addition of ethylene to the system has a profound effect on the product yields: the rates of formation of H_2 and DMDS decrease very rapidly initially and then level off to constant values (above ca 5% added ethylene); DMS is completely suppressed. Some additional reaction products were formed, the most prominent of which was identified as methylethylsilane by its mass spectrum given in Appendix I.

TABLE III-15
 Effect of Added Ethylene on the Product Yields
 in the Polymerization of MgCl_2^a

Pressure, Torr	C_2H_4	C_2H_4 molar	Yields, % male		
			H_2	OMS	OMS
409.0	-	-	8.00	6.14	0.27
405.0	-	-	7.29	6.08	0.31
402.4	0.10	0.52	4.31	4.16	c
412.0	0.20	0.93	3.57	2.38	c
408.0	4.09	1.94	4.58	d	d
410.0	1.06	1.90	3.92	2.08	c
400.4	21.40	4.96	2.85	1.93	c
404.6	41.36	9.07	2.53	1.64	c
392.0	100.0	20.1	2.38	1.89	c
407.0	10.0	20.0	2.45	1.91	c
400.0	84.1	16.3	2.63 ^(e)	1.96 ^(e)	c
360°C ^f					
274.6	68.9	20.0	1.36	1.01	c
378.0	46.2	14.2	1	1.09	c
287.0	30.9	9.9	1	1.08	c

^a Cell vol. = 206.6 cc. ($\text{S/V} = 1.0 \text{ cm}^{-1}$) was evacuated at 500°C for 16 hrs before each run, except (e).

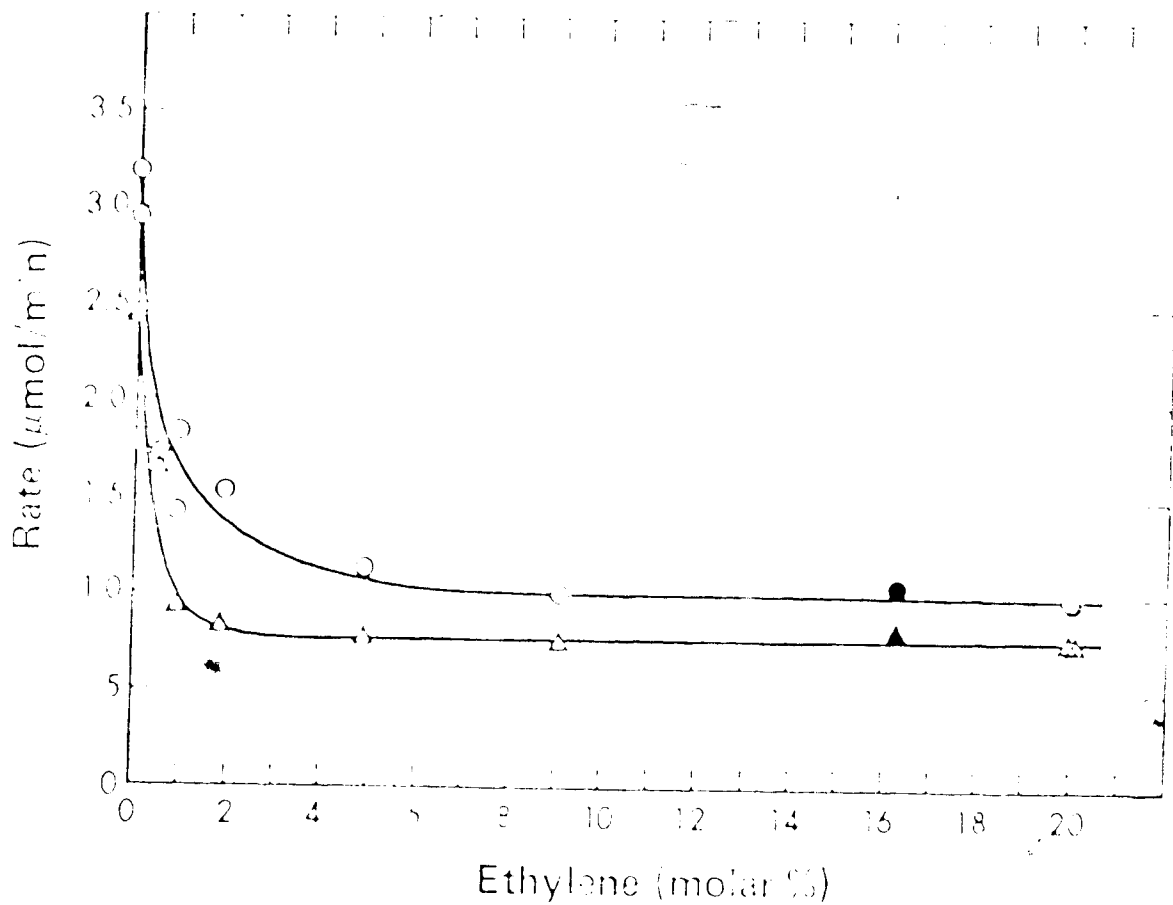
^b Time, 2.50 min.

^c No OMS formed.

^d Not measured.

^e Cell freshly coated by polymer before experiment.

^f Time, 100.0 min.



111. Effect of Adsorption on the Rate of Product Formation in the Reaction of C_2H_4 with NiSO_4 at 4.5 Torr. of C_2H_4 and 1.0×10^{-2} Torr. of NiSO_4 at 4.5 Torr. of C_2H_4 and 1.0×10^{-2} Torr. of NiSO_4 and evaluated at 5.0 Torr. of C_2H_4 and 1.0×10^{-2} Torr. of NiSO_4 .
 ○ - H_2 , △ - H_2O from a reactor coated with a polymer.
 ● - H_2 , ▲ - H_2O from a reactor coated with a polymer.

Figure III-9 also shows that the rates of formation of H_2 and DMDS in the level-off region were not dependent on the nature of the surface of the reaction vessel. It is seen that in the presence of a high concentration of C_2H_4 , the rates in a vessel freshly coated with polymer were the same as those obtained in the vessel evacuated for 16 hrs at 500°C.

It was concluded that the limiting hydrogen and DMDS yields formed at higher pressures of ethylene were of molecular origin, and that about 10% ethylene in the mixture was sufficient to eliminate contributions from radical reactions within the temperature range examined in this study.

Since the molecular reaction rates were not affected by the nature of the surface of the reaction vessel, it can be further concluded that the molecular process is not heterogeneous.

5. Arrhenius Parameters for the Molecular Process

The pyrolysis of MMS was carried out in the presence of about 10% ethylene in the range 340 to 440°C and 40 to 400 torr MMS. Conversions were kept below 1% and the vessel was evacuated overnight before each experiment.

The results are presented in Table III-16.

TABLE III-16
 The Monometallic Ethylene System: The Yields of H₂ and GMS as Functions
 of MeSiH₃ Pressure and Time at Different Temperatures, and the Calculated
 First Order Rate Constants for H₂ and GMS Formation^a

Temperature, °C	P(CH ₃ SiH ₃), torr	Time, min	$\frac{C_{2H_4}}{MeSiH_3}$	H ₂ , moles	GMS, moles	k_{H_2} , s ⁻¹	k_{GMS} , s ⁻¹
440	278.3	2.50	0.111	8.17	6.24 ^a	4.22×10^{-5}	2.22×10^{-5}
441	133.4	2.50	0.107	3.95	3.03	4.25×10^{-5}	3.25×10^{-5}
440	43.0	2.50	0.107	1.22	0.96 ^e	4.05×10^{-5}	3.21×10^{-5}
421	282.3	3.00	0.107	2.87	2.25	1.15×10^{-5}	9.25×10^{-6}
420	62.7	6.50	0.107	1.33	1.10	1.14×10^{-5}	3.42×10^{-6}
415	404.6	2.50	0.100	2.53	1.84	8.55×10^{-6}	6.40×10^{-6}
415	277.9	2.50	0.195	1.75	1.31	6.73×10^{-6}	6.53×10^{-6}
415	194.9	2.50	0.195	1.21	0.91	3.62×10^{-6}	5.77×10^{-6}
415	58.4	10.00	5.554	1.46	^b	3.67×10^{-6}	
401	406.3	4.00	0.107	1.50	1.14	3.13×10^{-6}	2.39×10^{-6}
399	192.7	8.00	0.111	1.30	1.18	2.85×10^{-6}	2.49×10^{-6}
400	90.9	16.00	0.107	1.23	1.07	2.87×10^{-6}	2.49×10^{-6}
380	189.3	30.00	0.107	1.17	$(1.00)^c$	6.77×10^{-7}	5.73×10^{-7}
380	57.3	125.00	0.111	1.57	1.21 ^c	7.21×10^{-7}	5.26×10^{-7}

TABLE III-16 (cont'd)
 The Monomethylsilane-Ethylene System: The Yields of H₂ and DMDS as Function
 of MeSiH₃ Pressure and Time at Different Temperatures, and the Calculated
 First Order Rate Constants for H₂ and DMDS Formation^a

Temperature °C	P(CH ₃ SiH ₃), torr	Time, min	$\frac{C_2H_4}{MeSiH_3}$	H ₂ , moles	DMDS, moles	k _{H₂} , s ⁻¹	k _{DMDS} , s ⁻¹
360	278.2	100.0	0.166	1.34	1.09	1.54×10^{-7}	1.25×10^{-7}
360	280.7	100.0	0.110	1.36	1.08	1.54×10^{-7}	1.23×10^{-7}
360	84.6	340.0	0.111	1.35	1.05	1.49×10^{-7}	1.15×10^{-7}
361	38.1	792.0	0.111	1.48	1.13 ^c	1.57×10^{-7}	1.19×10^{-7}
340	398.4	370.0	0.111	1.55	1.00	3.25×10^{-8}	2.03×10^{-8}
340	127.6	910.0	0.111	0.92	0.85	2.44×10^{-8}	2.25×10^{-8}

^a Cell volume 206.6 cc

^b Not analyzed.

^c Traces of DMS present.

(i) Order of Formation of Hydrogen and DMDS

From the data in Table III-16, the logarithms of the rates of H_2 and DMDS formation were plotted against the logarithms of initial MMS pressure, and the corresponding order plots at different temperatures are shown in Figure III-10.

The reaction orders, derived from the slopes of the order plots by least mean squares analyses, are listed in Table III-17. The formation of both products was found to be first order with respect to monomethylsilane at all temperatures; the sole exception was hydrogen at 340°C, and the observed deviation from unity was probably an experimental error since the value is based on two points only.

(ii) Rate Constants and Arrhenius Parameters for Hydrogen and DMDS Formation

In the presence of 10% ethylene, the formation of H_2 and DMDS was first order with respect to MMS, thus

$$\text{Rate}(H_2) = \frac{\Delta[H_2]}{\Delta t} = k'_{H_2} [MMS], \quad \text{and}$$

$$\text{Rate}(DMDS) = \frac{\Delta[DMDS]}{\Delta t} = k'_{DMDS} [MMS],$$

where $\Delta[H_2]$, $\Delta[DMDS]$ are the product yields in concentration units, Δt is the reaction time, k'_{H_2} and k'_{DMDS} are the individual first-order rate constants at a certain

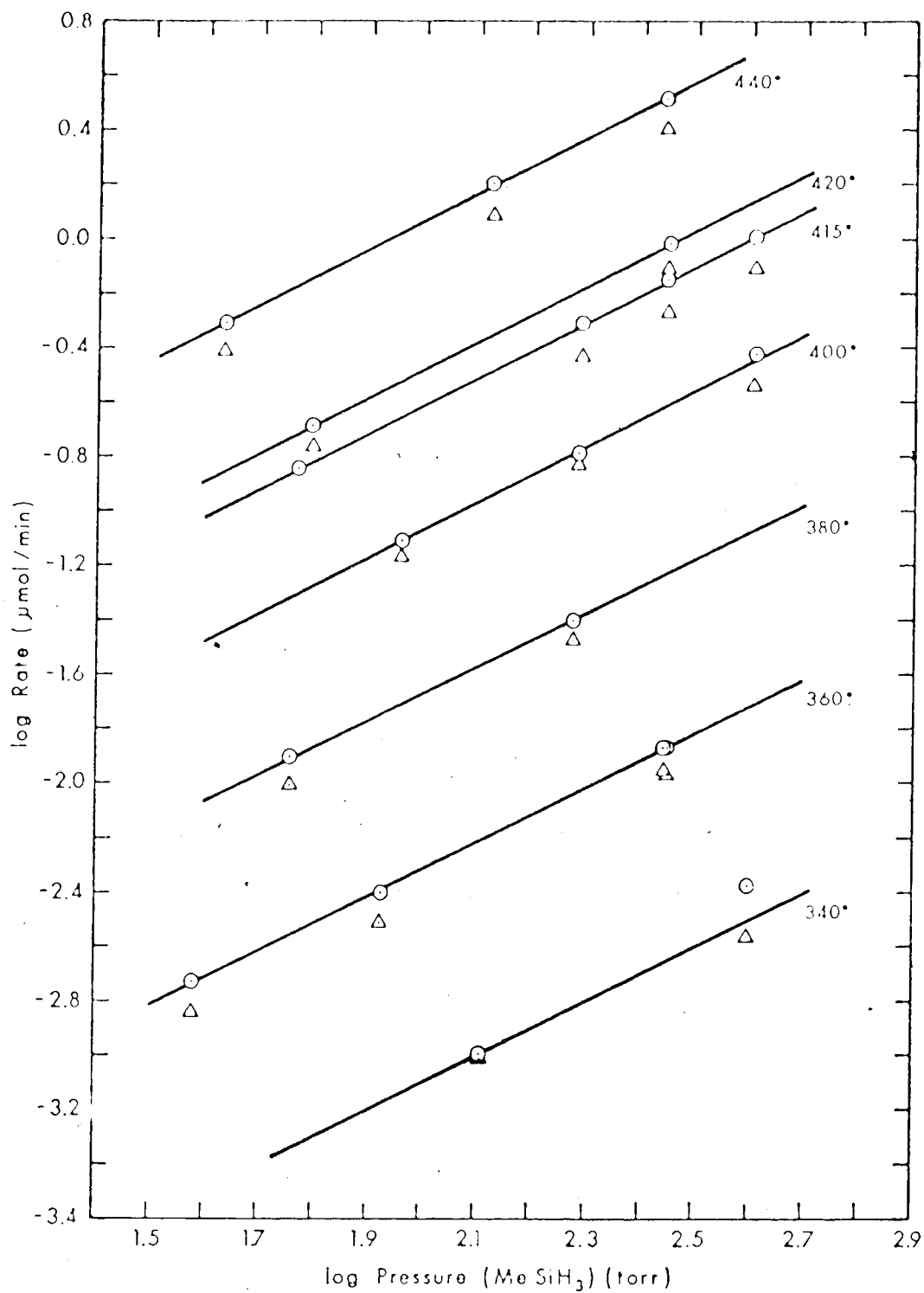


Figure III-10. Order Plots for H₂ and DMDS at Different Temperatures in the Presence of ~ 10% Ethylene; ○ -H₂, △ -DMDS.

TABLE III-17
Monomethylsilane-Ethylene System: Orders
of Formation of Hydrogen and DMDS

Temperature	Order	
	H ₂	DMDS
440	1.02	1.004
420	1.03	0.96
415	1.00	1.03
400	1.01	0.97
380	0.95	1.03
360	0.99	1.02
340	1.25	0.92

reaction temperature (with the prime indicating the presence of ethylene), and $[MMS]$ is the substrate concentration.

Since the conversions were well below 10, it is reasonable to assume that the concentration of the substrate was unchanged, i.e.

$$[MMS] = [MMS]_{\text{initial}}$$

The calculated rate constants k'_{H_2} , k'_{DMDS} are listed in Table III-16.

The activation energies and pre-exponential factors associated with H_2 and DMDS formation were calculated from the slopes and intercepts of the Arrhenius plots, using the logarithmic form of the Arrhenius equation,

$$\log k = \log A - \frac{E_a}{2.3 RT}$$

where k is the rate constant, A is the pre-exponential factor, E_a , the activation energy, T , absolute temperature, and R the gas constant (1.987 cal/deg mole).

The Arrhenius plots for H_2 and DMDS formation in the presence of ethylene are shown in Figure III-11 and the corresponding Arrhenius parameters obtained by least mean squares analyses are presented in Table III-18.

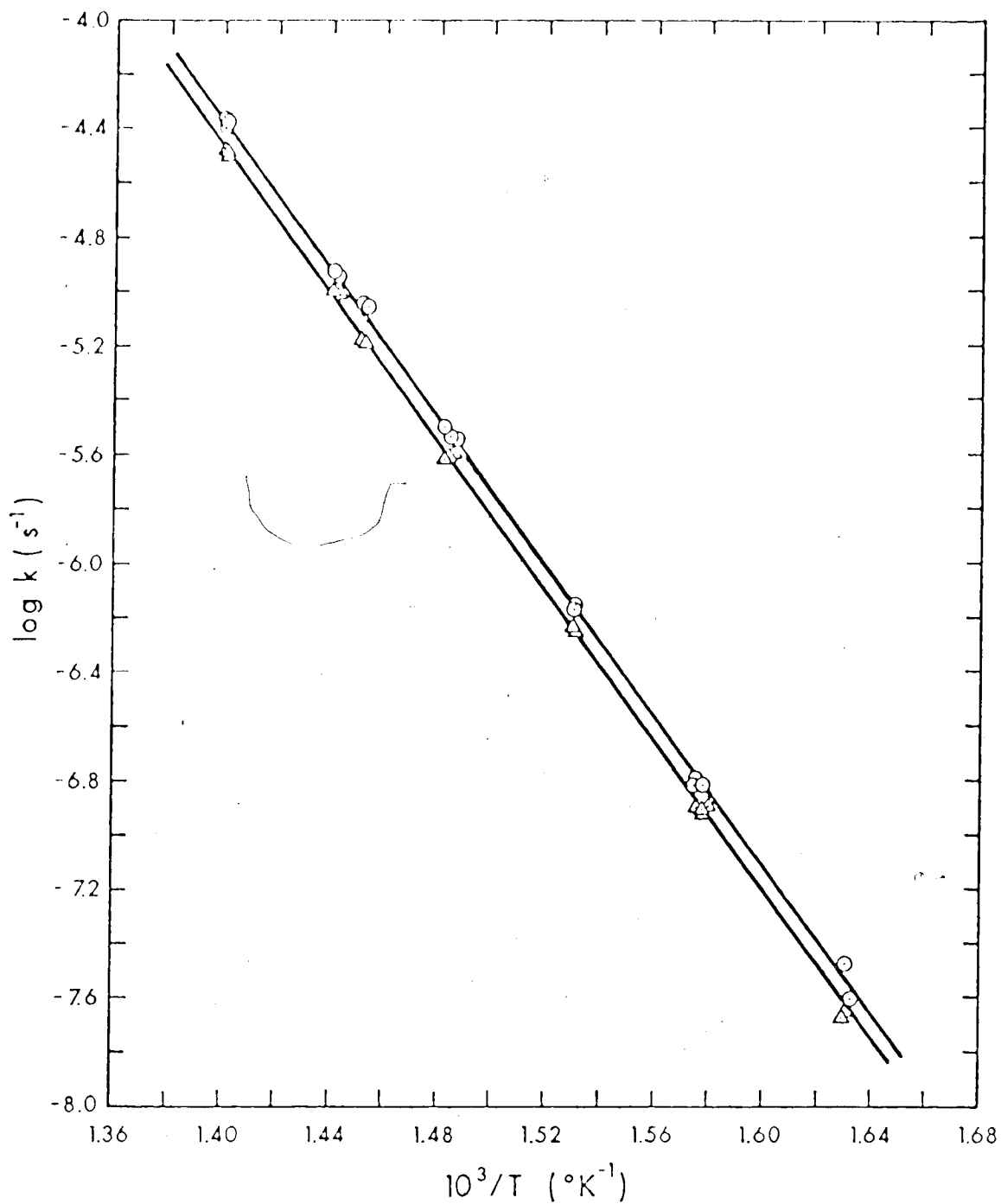


Figure III-11. Arrhenius Plots for H_2 and DMDS Formation from the Pyrolysis of MeSiH_3 in the Presence of $\sim 10\%$ Ethylene; \circ - H_2 , \triangle - DMDS.

TABLE III-18
Arrhenius Parameters for H₂ and DMDS
Formation in the Monomethylsilane-Ethylene System

Product	log A (s ⁻¹)	E _a , kcal/mole
H ₂	15.02 ± 0.10	63.27 ± 0.31
DMDS	14.87 ± 0.12	63.15 ± 0.35

C. Isotopic Labelling Experiments

In order to establish whether the Si-H or C-H bonds were involved in the production of hydrogen, isotopically labeled monomethylsilane- d_3 (CH_3SiD_3) was pyrolyzed both in the presence and absence of 10% ethylene, and the isotopic composition of hydrogen was analyzed. The results are presented in Table III-19.

It was found that about 97% of the hydrogen fraction was D_2 . Since the isotopic purity of monomethylsilane- d_3 used was reported^{31,46,61} to be about $97.0 \pm 0.5\%$, the results indicated that hydrogen was formed solely by splitting of Si-H bonds.

E. Discussion

In the initial stages of the pyrolysis of monomethylsilane (MMS), hydrogen and 1,2-dimethyldisilane (DMDS) were formed as major products and dimethylsilane (DMS) as a minor product. When a free radical scavenger, ethylene, was added to the reaction system, the formation of H_2 and DMDS was partially suppressed and that of DMS was totally suppressed.

The results suggest that at least two different processes leading to H_2 and DMDS formation must participate in the pyrolysis of MMS. One, a radical process, is suppressed by the addition of ethylene, and the other, a

TABLE III-19
 Isotopic Distribution of Hydrogen from the
 Pyrolysis of Monomethylsilane-d₃

Temperature, °C	P(CH ₃ SiD ₃), ^a torr	Time, min	H ₂ , μ moles	H ₂	
				HD	D ₂
401 ^b	370.1	12.75	3.44	0.58	4.66
403 ^b	284.5	20.00	2.52	0.45	4.51
415 ^b	170.1	18.00	4.70	0.03	4.47
401 ^c	364.2	12.00	4.94	0.7	2.1
401 ^c	251.7	12.00	3.27	1.32	1.95

^a Cell volume 206.6 cc.

^b 9.90% Ethylene in the mixture.

^c Without ethylene.

molecular process, leads to the formation of nonscavengable H_2 and DMS.

In spite of the apparent simplicity of the overall reaction, the kinetics of the pyrolysis were found to be complex. The main complications arose from the occurrence of heterogeneous reactions, as indicated by the dependence of the reaction rates on the mode of treatment of the reaction vessel. Although a great deal of effort was expended in order to eliminate surface reactions, only partial success was achieved and therefore this aspect of the pyrolysis will only be briefly discussed. In the presence of ethylene however, the rates were not surface dependent, and the resulting kinetic data on the molecular process can be treated quantitatively.

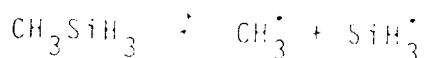
1. The Primary Reaction Steps

The hydrogen fraction from the pyrolysis of monomethylsilane- d_3 (CH_3SiD_3) consisted almost entirely of D_2 , Table III-19. Thus C-H bond cleavage is not important and can be neglected as a primary reaction step.

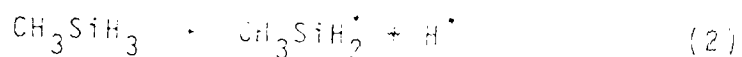
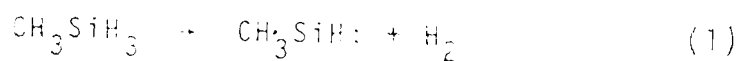
Cleavage of the Si-C bond can also be eliminated as a primary step in the pyrolysis of MMS, since no significant yields of methane were observed. The rate of H-abstraction by CH_3 radicals from Si-H bonds is

known to be extremely rapid⁶¹. (The formation of small amounts of methane, which were occasionally detected, can be explained by slow thermal decomposition of the polymer.)

The present experimental data do not agree with the results of Davidson et al.⁵⁶, who claimed analytical and kinetic evidence for the occurrence of Si-C cleavage,



The results of this study conclusively show that in the primary steps of the pyrolysis of MMS, only the silicon-hydrogen bonds are broken. MMS may decompose either by elimination of molecular H₂ yielding methylsilylene, reaction (1), or by dissociation of a single silicon-hydrogen bond forming an H atom and a methylsilyl radical, reaction (2).



The results indicate that both primary steps (1) and (2) occur and that these steps can be distinguished by adding ethylene to the system.

A possible reaction mechanism for the pyrolysis of MMS will now be proposed in order to elucidate the effect of added ethylene.

(c) Possible Reaction Mechanism

From the experimental results and the literature data available on the reactivity of ethyl radicals and silylenes, the reaction scheme shown in Table III is proposed for the pyrolysis of MMS.

The proposed mechanism is consistent with the formation of the major reaction products, C_2H_4 and C_2H_2 , under the various conditions employed. It does not, however, provide a satisfactory explanation for the formation of the minor product, C_2H_6 , since the species Y^{\cdot} in reaction (9) is unspecified; reaction (9) will be discussed later in more detail (see Section III.2.4.2).

Reactions (1), (3) and (4) correspond to the molecular process and are assumed to be unaffected by the addition of ethylene.

It is suggested that the radical process is represented by reactions (5) - (9) in the absence of ethylene, and by reactions (2) - (10) - (12) in the presence of high concentrations of ethylene.

In neat MMS pyrolysis, a free radical process is operative and contributes to the yields of C_2H_4 and C_2H_2 formed by the molecular process. According to the scheme, this radical chain is initiated by primary step (2), propagated by reactions (5) and (6), and terminated by methylsilyl radicals either by self-combination,

TABLE III-26
Reaction Scheme for the Pyrolysis of MeSiH_3

Reaction Step	Temp. (°C)	Ref.
Molecular processes:		
$\text{MeSiH}_3 + \text{MeSiH}_3 \rightarrow \text{MeSiH}_2 + \text{H}_2$ (1)	14.55-21.7	b
$\text{MeSiH}_3 + \text{MeSiH}_3 \rightarrow (\text{MeSiH}_2)_2$ (3)	14.55-21.7	b
$\text{MeSiH}_3 \rightarrow \text{polymer}$ (4)	14.55-21.7	b
Radical process:		
Initiation		
$\text{MeSiH}_3 \xrightarrow{\text{wall}} \text{MeSiH}_2^\cdot + \text{H}^\cdot$ (2)	14.55-21.7	b
(a) No Ethylene:		
Propagation		
$\text{H}^\cdot + \text{MeSiH}_3 \rightarrow \text{H}_2 + \text{MeSiH}_2^\cdot$ (5)	14.55-21.7	b
$\text{MeSiH}_2^\cdot + \text{MeSiH}_3 \rightarrow (\text{MeSiH}_2)_2 + \text{H}^\cdot$ (6)	14.55-21.7	b
Termination		
$2 \text{MeSiH}_2^\cdot \rightarrow (\text{MeSiH}_2)_2$ (7)	14.55-21.7	b
$\text{MeSiH}_2^\cdot \xrightarrow{\text{wall}} \text{products}$ (8)	14.55-21.7	b
$\text{MeSiH}_2^\cdot + \text{X} \rightarrow \text{Me}_2\text{SiH}_2$ (9)	14.55-21.7	b

TABLE III-20 (cont'd)

Reaction Scheme for the Pyrolysis of MeSiH₃

Reaction Step	log A ^a	E _a , kcal/mole
(b) Ethylene added:		
H ⁺ + C ₂ H ₄ + C ₂ H ₅	10.0 ^b	11.1 ^c
MeSiH ₂ + C ₂ H ₄ + MeSiH ₂ CH ₂ CH ₂	17.0 ^c	2.5 ^c
C ₂ H ₅ ⁺ and MeSiH ₂ CH ₂ CH ₂ ⁺ + stable products		

^a A-factors for unimolecular and bimolecular reactions are in units of s⁻¹ and M⁻¹s⁻¹, respectively.

^b Measured in this work.

^c Estimated from literature data; see text.

reaction (7), or by diffusion to the walls, reaction (8).

In the presence of ethylene, hydrogen atoms and methylsilyl radicals from the primary step (2) are scavenged in reactions (10) and (11), where ethyl and dimethylethyl radicals, respectively, are formed. Although these radicals may undergo further addition, abstraction, recombination or disproportionation reactions to form stable products, reaction (12), it is assumed that no significant amounts of H_2 or DMDS will be formed in these processes.

Thus, if steps (5)-(9) could be effectively eliminated by high concentrations of ethylene, the radical process will no longer contribute to the yields of H_2 and DMDS, and these products will then be formed solely by the molecular process.

The effect of ethylene on the pyrolysis of MMS will now be discussed in detail.

3. Effect of Added Ethylene on the Molecular and Radical Processes

According to the reaction scheme in Table III-20, the yields H_2 and DMDS in the presence of ethylene will correspond to the molecular process, if the following conditions are fulfilled:

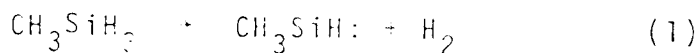
- (a) the molecular process, i.e. reactions (1), (3) and (4), is unaffected by the addition of ethylene; and
 (b) reactions (5)-(9) are suppressed by ethylene, and the subsequent reactions of ethyl and β -methylethylsilyl radicals, (12), do not form any additional H_2 or DMDS.

Each of these possibilities will now be discussed.

(i) Molecular Process, Reactions (1), (3) and (4)

(a) Reaction (1)

The primary reaction step (1),



represents a unimolecular decomposition of the thermally activated substrate molecule, the rate constant of which is pressure dependent in the fall-off region (see Section I.B).

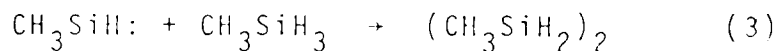
The experimentally measured first order rate constants for H_2 and DMDS formation in the presence of ethylene, listed in Table III-16, were determined in a broad pressure range of approximately 40 - 400 torr. They were, within experimental error, independent of total pressure and therefore represent the limiting high pressure values.

Moreover, an RRKM calculation of the fall-off curve for the rate constant of reaction (1) confirmed that the present investigation was carried out in the high pressure region⁹⁹.

Thus it can be concluded that at pressures above 40 torr, the rate of reaction (1) is unaffected by the addition of ethylene.

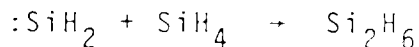
(b) Reaction (3)

Reaction (3),

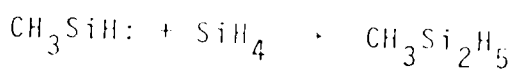


represents insertion of methylsilylene into the Si-H bond of the substrate. In order that spin be conserved in the primary reaction step (1), MeSiH: must be produced in the singlet state which is very likely the ground electronic state by analogy with $:\text{SiH}_2$ ⁵⁵.

Although the rate of reaction (3) has not been reported, one can deduce from the following considerations that it must be very fast. The Arrhenius parameters for insertion of $:\text{SiH}_2$ into SiH_4 ,

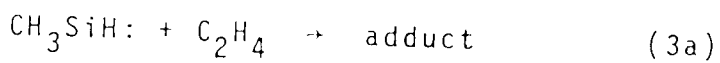


are $E_a = 1.3 \pm 1.1$ kcal/mol and $\log A(\text{M}^{-1}\text{s}^{-1}) = 9.7 \pm 0.4$ ⁶⁶, and the preexponential factor for insertion of methylsilylene into monosilane,



was calculated to be $\log A(\text{M}^{-1}\text{s}^{-1}) = 10.1^{77}$. The latter reaction is also very rapid and its activation energy is likely to be very small. The rate of insertion of MeSiH: into MeSiH_3 , reaction (3), should therefore be fast and feature a similar A-factor and low E_a^{68} .

In the presence of ethylene, addition of methylsilylene across the double bond, reaction (3a),



might be expected to occur in parallel and in competition with reaction (3)^{62,86}; however, the limiting yields of DMDS were unaffected by increasing concentrations of C_2H_4 (see Table III-15), indicating that methylsilylene is not very reactive toward ethylene.

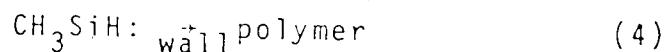
Moreover, from the available information on the reactivity of various silylenes, it can be deduced that the rate of reaction (3a) should be very slow in comparison with reaction (3). For example, Attwell and Weyenberg⁵⁹ reported that the relative reactivity of $\text{Me}_2\text{Si:}$ towards a series of substrates follows the trend benzene < ethylene << dimethoxytetramethyldisilane < < 1,3-dienes,

and that ethylene cannot compete with 1,3-butadiene for $\text{Me}_2\text{Si}:$. Jenkins, Ring et al.⁶⁹ have shown that for MeSiH : the rate of addition to 1,3-butadiene is comparable with the rate of insertion into Si-H bonds, and also reported that for the most reactive silylene, $:\text{SiH}_2$, the rate of insertion into Si-H bonds is about four times faster than the rate of addition to 1,3-butadiene.

On the basis of these results it can be deduced that addition reaction (3a) cannot compete with insertion reaction (3), and therefore reaction (3) will not be affected by the addition of ca 10% of ethylene to the reaction system.

(c) Reaction (4)

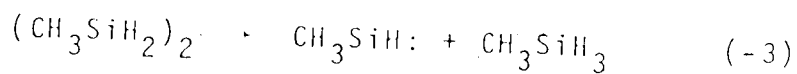
Reaction (4),



is one of several reactions which might lead to the formation of polymer. Polymer was formed mainly in the later stages of the pyrolysis of MMS; in the initial stages, however, (at conversions below 1%) it was only a very minor product.

The rate of reaction (4) will depend on the concentration of MeSiH : which can be estimated from the following considerations. DMDS is less thermally stable than the substrate, MMS, and the main mode of decomposition

of DMDS is via elimination of methylsilylene⁵⁸, i.e. reaction (-3),



the Arrhenius parameters of which can be estimated from recently published data^{27,77} to be $\log A_{-3}(\text{s}^{-1}) = 14.0$ and $E_{-3} = 50.0 \text{ kcal/mol}$. Together with the previously estimated Arrhenius parameters for reaction (3), $\log A_3(\text{M}^{-1}\text{s}^{-1}) = 10$, $E_3 = 1 \text{ kcal/mol}$ ^{66,68}, the equilibrium constant K_{-3} at 400°C is:

$$K_{-3} = \frac{k_{-3}}{k_3} = \frac{[\text{MeSiH:}][\text{MMS}]}{[\text{DMDS}]} \approx 1.5 \times 10^{-12} \text{ M}$$

Thus at ~ 0.20 conversion the equilibrium concentration of MeSiH: is very small, of the order of $\sim 3 \times 10^{-15} \text{ M}$, and since the rate of reaction (4) is expected to be diffusion controlled, small quantities of ethylene should have no effect.

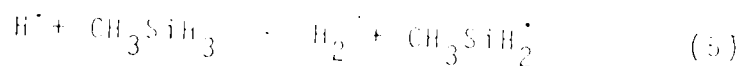
Thus it can be concluded that the rates of the molecular reactions (1), (3) and (4), are unaffected by the addition of ethylene. We shall now turn our attention to the effect of ethylene on radical processes.

(ii) Radical Reactions

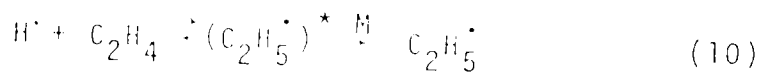
(a) Scavenging of H atoms

Hydrogen atoms, formed in the primary reaction step (2) or by reaction (6) (see Table III-20), can react

either with the substrate, reaction (5),



and propagate the chain or can be scavenged by added ethylene, reaction (10):



Several values for the room temperature rate constant k_5 have been reported, $2.1 \pm 0.5 \times 10^8 \text{ M}^{-1} \text{ s}^{-1}$ ¹⁰⁰, $6.9 \pm 1.2 \times 10^8 \text{ M}^{-1} \text{ s}^{-1}$ ⁷⁵, $1.8 \pm 0.5 \times 10^8 \text{ M}^{-1} \text{ s}^{-1}$ ⁷⁵ and $3.1 \times 10^8 \text{ M}^{-1} \text{ s}^{-1}$ ¹⁰¹, where the last two refer to the analogous $\text{D} + \text{CH}_3\text{SiH}_3$ system. Obi et al. ¹⁰¹ have also estimated the activation energy E_5 to be 2.3 - 3.7 kcal/mol, assuming an A-factor in the range $5 \times 10^9 - 5 \times 10^{10} \text{ M}^{-1} \text{ s}^{-1}$ per Si-H bond.

The addition of H atoms to ethylene, (10), has been thoroughly investigated and the reported high pressure rate constants at room temperature ^{102,103} are in good agreement, yielding an average value of $6.9 \pm 1.1 \times 10^8 \text{ M}^{-1} \text{ s}^{-1}$, E_{10} is 1.5 - 2.0 kcal/mol ^{103,104} and $\log A_{10} (\text{M}^{-1} \text{ s}^{-1}) = 10.0 \pm 0.1$ ¹⁰⁵.

Thus the room temperature rate constant ratio $k_{10/5}$ is about 2, in good agreement with the experimentally determined value of $k_{10/5} = 1.72$ ¹⁰¹ where k_{10} refers to the $\text{D} + \text{C}_2\text{D}_4$ reaction. Since $E_{10} = 1.75 \text{ kcal/mol}$,

$A_{10} = 10^{10.0} \text{ M}^{-1} \text{ s}^{-1}$ and $E_5 = 3.0 \text{ kcal/mol}$, then
 $A_5 = 10^{10.6} \text{ M}^{-1} \text{ s}^{-1}$, and at 400°C $k_{10}/k_5 \approx 0.64$.

Thus, within the temperature range used in this work, the rate constants for reactions (5) and (10) are not very different, and ethylene therefore cannot compete very efficiently with MMS for H atoms.

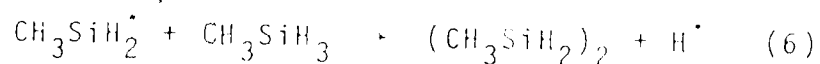
This relative inefficiency of ethylene in scavenging H atoms is further increased in the present study by the relatively low concentrations of C_2H_4 used (see Table III-16). Thus, at 400°C and for a mixture containing ~10% ethylene, the relative rates R_{10}/R_5 will be approximately

$$\frac{R_{10}}{R_5} = \frac{k_{10}[\text{C}_2\text{H}_4]}{k_5[\text{MMS}]} = 0.64 \frac{[10\%]}{[90\%]} = 0.07$$

i.e. only ~7% of H atoms present in the system will be scavenged by ethylene and the remaining 93% will react with the substrate by (5) yielding H_2 .

This simple calculation however is not compatible with experimental observations. Figure III-9 shows that in the presence of ~1% ethylene the rate of H_2 formation has already dropped to about 50% of its original value, and at 6% added C_2H_4 it was almost 70% lower; further increases in the ethylene concentration did not have any apparent effect.

Since this high efficiency of ethylene cannot be explained simply in terms of scavenging of H atoms, it must be related to a suppression of the rate of H atom formation in the chain propagation step (6):



If the chain length is large, then the majority of H atoms formed in the system will come from the chain propagation step (6) and the chain propagation reactions (5) and (6) will be the major source of H_2 formed in the radical process; the other contribution from the chain initiation step (2) will be only minor. In other words, since the chain length, λ , is defined as

$$\lambda = \frac{\text{Rate(Propagation)}}{\text{Rate(Initiation)}}$$

the individual contributions from the initiation and propagation steps $\text{H}_2, \text{Rad}^{\text{Init}}$ and $\text{H}_2, \text{Rad}^{\text{Prop}}$ respectively can be expressed as:

$$\frac{\text{H}_2, \text{Rad}^{\text{Init}}}{\text{H}_2, \text{Rad}^{\text{Prop}}} = \frac{1}{\lambda}$$

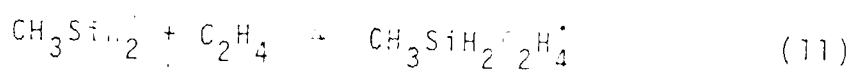
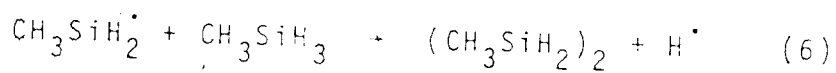
Thus, if λ is very large the relative contribution from the initiation step will be very small. That this is indeed the case is evident from the large decrease in H_2 yields in the presence of small concentrations of ethylene; direct evidence for the presence of a long chain will be presented later (Section III.8.3.4).

In the next section it will be shown that ethylene is a highly efficient scavenger of methylsilyl radicals, and that even small concentrations of C_2H_4 , e.g. 5 - 10%, can effectively suppress reaction (6) and thus eliminate the contribution $H_2^{Prop. Rad.}$.

Furthermore, it will be shown (Section III.B.4.v) that the rate of the chain initiation reaction (2) is very small in comparison with that of the molecular reaction (1), and therefore the H_2 yields measured in the presence of ethylene can be assumed to be formed by the molecular process only, i.e. by reaction (1).

(b) Scavenging of Methylsilyl Radicals

Methylsilyl radicals formed in the primary reaction step (2) or by reaction (5), can either react with the substrate, reaction (6), or be scavenged by added ethylene, reaction (11):



Neither reaction has been investigated kinetically.

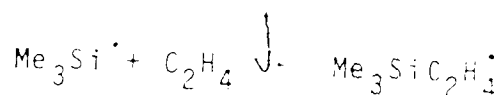
From the most recent data on bond dissociation energies in silicon compounds^{13,15,17} however, one may estimate $D(MeSiH_2-H)$ 90 and $D(MeSiH_2-SiH_2Me)$ 80 kcal/mol, and thus reaction (6) will be approximately 10 kcal/mol endothermic. E_6 will probably be higher

than 10 kcal/mole, since

$$E_0 = \Delta H_0^\ddagger + E_{-0} = 10 + E_{-0}$$

where ΔH_0^\ddagger is the enthalpy change of the reaction, and E_{-0} is the activation energy of the reverse reaction. A value of $E_0 = 13 - 15$ kcal/mol is quite plausible since in the analogous $\text{SiH}_3^\cdot + \text{SiH}_4$ system, the activation energies for the forward and reverse reactions have been estimated to be 15³⁹ and 3 kcal/mol³², respectively. The maximum value of the A factor for the $\text{SiH}_3^\cdot + \text{SiH}_4$ reaction has been estimated to be $\sim 10^{10} \text{ M}^{-1} \text{ s}^{-1}$ ³⁹.

The rate of addition of methylsilyl radicals to ethylene, reaction (11), can also be estimated. Choo and Gaspar⁴⁰ found that the rate of addition of trimethylsilyl radicals to ethylene,

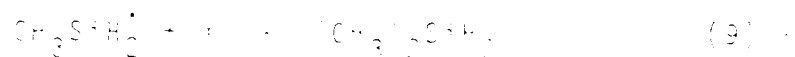


is much faster than that of simple alkyl radical addition to ethylene. They measured the activation energy and A factor, 2.5 ± 0.2 kcal/mole and $10^{7.0 \pm 0.2} \text{ M}^{-1} \text{ s}^{-1}$, respectively, and reported that the rate of addition of SiH_3^\cdot to ethylene was even more rapid than that of the $\text{Me}_3\text{Si}^\cdot$ radical. Similarly, Pollock et al.³² found that the addition of disilyl radicals to ethylene is several orders of magnitude faster than that of corresponding

a $\text{Et}_2\text{Si}^\cdot$ radical. At room temperature the rate constants for addition of disilyl and triethylsilyl radicals to ethylene are $4 \times 10^5 \text{ M}^{-1} \text{ s}^{-1}$ and $1 \times 10^6 \text{ M}^{-1} \text{ s}^{-1}$, respectively.

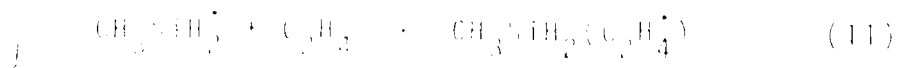
The rate of addition of methylsilyl radicals to ethylene, (11), is probably of the same order of magnitude as that of disilyl radicals and much faster than that of $\text{Me}_3\text{Si}^\cdot$ radicals, which may be considered as a lower limit for k_{11} . Therefore, using the measured Arrhenius parameters for the $\text{Me}_3\text{Si}^\cdot + \text{C}_2\text{H}_4$ reaction, and the estimated values for reaction (6), $E_6 = 23 \text{ kcal/mol}$, $A_6 = 10^{10} \text{ M}^{-1} \text{ s}^{-1}$ (vide supra), it follows that $R_{11}/R_6 = 3 \times 10^3$ at 400°C .

Thus, in the presence of ca 10% ethylene, $k_{11}/k_t = 3 \times 10^2$, and therefore the chain cannot be sustained. Since the concentration of methylsilyl radicals will be greatly reduced, the other DMS-forming reactions in the radical process (i.e. termination reactions (7) and (8)), will also be suppressed. The total suppression of DMS, formed via



is direct evidence for efficient scavenging of methylsilyl radicals.

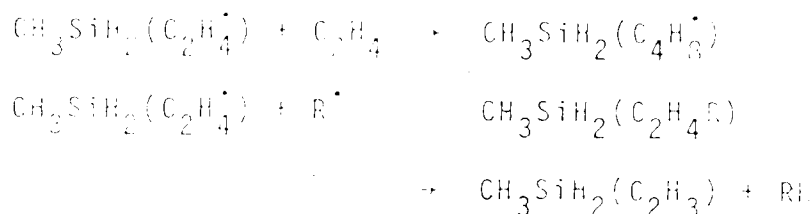
When methylsilyl radicals react with ethylene,



1-ethylethylsilyl radicals are formed. These undergo further reactions, the most important of which is abstraction of H atoms from the substrate



to form methylethylsilane. Other possible reactions are addition to ethylene, recombination and disproportionation.



These are minor processes, however, and the nature of the products could not be established. It is reasonable, however, to assume that none of these processes will lead to the formation of DMDS.

Thus it can be concluded that in the presence of ethylene, the observed DMDS yields will correspond solely to the contribution from the molecular process.

(ii) Arrhenius Parameters for H₂ and DMDS Formation in the Presence of Ethylene

It has been shown that the DMDS yields formed in the pyrolysis of MMS in the presence of ethylene

arise exclusively from the molecular process, i.e. reactions (1) and (3); (1) is the rate-determining step. Since some decomposition of DMDS might have occurred even at low conversions, $k_{\text{DMDS, Molec.}}$ (see Table III-16) should be $\approx k_1$.

The Arrhenius parameters for H_2 formation in the presence of ethylene (Table III-18) are the same, within experimental error, as those for DMDS and would therefore appear that $k_{\text{H}_2, \text{Molec.}} = k_{\text{DMDS, Molec.}} = k_1$.

The errors in the rate constant parameters are commensurate with the errors in the H_2/DMDS ratios, (Table III-16): which were consistently higher than unity (1.27 ± 0.10) and it would appear that the hydrogen yields in the presence of C_2H_4 may contain a very small contribution from the radical primary step (2). Therefore $k_{\text{H}_2, \text{Molec.}} = k_1$.

The radical contribution to the H_2 yields in the presence of ethylene are very small however and we conclude that the measured Arrhenius parameters for H_2 and DMDS formation in the presence of C_2H_4 relate solely to the rate constant k_1 of the molecular primary step (1); these results will now be used to elucidate the radical processes occurring in the absence of ethylene.

Pyrolysis in the Absence of Ethylene: the Radical Process

In the pyrolysis of neat MMS, the molecular and radical processes both contribute to the formation of H_2 and DMDS. To a good approximation these processes may be considered to be independent of each other, and thus in the absence of ethylene the yields of H_2 and DMDS may be expressed as the sum of the individual contributions from the molecular and radical processes.

The radical yields of H_2 and DMDS may thus be calculated from the total yields given in Tables III-4 to III-7 and Tables III-11 and III-12 by subtracting the molecular yields obtained from the Arrhenius parameters for the molecular process, listed in Table III-18.

The results for hydrogen at different temperatures are listed in Tables III-21 to III-25, and the radical yields of all products at 415°C in the unpacked and packed vessels are given in Tables III-26 and III-27, respectively.

(c) The Reaction Orders for the Products of the Radical Process

The reaction order for products formation by the radical process was determined from the slope of conventional $\log(\text{rate})$ versus $\log(\text{substrate concentration})$ plots by least-square analysis. The orders for H_2 , Rad

TABLE III-21
 Yields of hydrogen from the Molecular and Radical Processes in the
 Pyrolysis of Monomethylsilane at 441°C and 429°C^a

P(MMS), torr	MMS, 10 ³ M	Time, s	H ₂ Yield, μ moles		Rate, M s ⁻¹	
			Total	Radical	10 ⁷ H ₂ , Total	10 ⁸ H ₂ , Rad
441°C						
171.5	3.84	60.6	2.47	2.175	1.96	2.36
118.0	2.65	60	1.57	1.420	1.27	1.21
80.8	1.81	60.6	1.05	0.994	0.34	0.45
57.6	1.29	90	1.11	1.059	0.60	0.27
39.5	0.87	120	1.02	0.969	0.41	0.21
429°C						
203.5	4.64	90	2.97	1.79	1.60	6.35
138.2	3.15	90	1.76	1.22	0.94	2.90
94.0	2.15	120	1.38	1.01	0.56	1.50
63.7	1.46	180	1.41	1.07	0.38	0.91
42.8	0.98	240	1.24	0.92	0.25	0.65

^a C e 206.6 cc.

TABLE III-22
 Yields of Hydrogen by the Molecular and Radical Processes in the
 Pyrolysis of Monomethylsilane at 421°C^a

P(MMS), torr	MMS, 10 ³ M	Time, s	H ₂ Yield, μ moles		Rate, M s ⁻¹		
			Total	Molecular Radical	10 ⁸ H ₂ , Total	10 ⁹ H ₂ Rad	
214.3	4.95	150	2.34	1.83	0.51	7.55	16.4
177.0	4.09	150	1.87	1.51	0.36	6.03	11.5
147.1	3.40	150	1.53	1.26	0.27	4.94	8.78
125.7	2.90	192	1.66	1.38	0.28	4.19	7.16
120.2	2.77	180	1.48	1.23	0.25	3.98	6.64
100.3	2.32	183	1.21	1.05	0.16	3.20	4.31
81.4	1.88	270	1.44	1.25	0.19	2.58	3.35
69.2	1.60	270	1.18	1.065	0.115	2.11	2.06
55.7	1.29	360	1.26	1.14	0.11	1.69	1.44
47.1	1.09	390	1.18	1.05	0.13	1.40	1.66
31.6	0.73	540	1.05	0.972	0.078	0.94	0.70

^a Cell volume 206.6 cc.

TABLE III-23
 Yields of Hydrogen by the Molecular and Radical Processes in the
 Pyrolysis of Monomethylsilane at 400°C^a

P(MMS), torr	MMS, 10 ³ M	Time, s	H ₂ Yield, μ moles		Rate, M s ⁻¹		
			Total	Molecular Radical	10 ⁷ H ₂ , Total	10 ⁸ H ₂ , Rad	
212.3	5.06	360	1.84	1.07	0.77	2.48	10.3
209.0	4.98	360	1.50	1.06	0.44	2.02	5.97
202.9	4.83	600	2.75	1.71	1.04	2.22	8.40
148.5	3.54	600	1.85	1.25	0.60	1.49	4.83
144.4	3.44	600	1.73	1.22	0.51	1.40	4.15
135.8	3.23	426	1.19	0.84	0.35	1.36	3.97
138.6	3.30	660	1.81	1.28	0.53	1.33	3.86
93.9	2.24	600	1.09	0.79	0.30	0.88	2.41
91.8	2.18	600	0.99	0.77	0.22	0.80	1.75
73.7	1.75	900	1.22	0.93	0.29	0.66	1.55
62.9	1.50	918	1.03	0.81	0.22	0.54	1.16
61.9	1.47	780	0.84	0.68	0.16	0.52	1.01
48.5	1.16	900	0.80	0.61	0.19	0.43	1.01
42.3	1.01	1200	0.87	0.71	0.16	0.35	0.63
33.7	0.80	1440	0.80	0.68	0.12	0.27	0.40

^a Cell volume 206.6 cc.

TABLE III-24
 Yields of Hydrogen by the Molecular and Radical Processes in the
 Pyrolysis of Monomethylsilane at 380°C^a

P(MMS), torr	MMS, 10 ³ M	Time, s	H ₂ Yield, μ moles		Rate, M s ⁻¹		
			Total Molecular	Radical	10 ⁹ H ₂ , Total	10 ⁹ H ₂ , Rad	
212.8	5.22	990	1.58	0.74	0.84	7.73	4.12
210.2	5.15	660	1.09	0.49	0.60	7.99	4.41
145.2	3.56	1290	1.15	0.64	0.51	4.32	1.93
141.5	3.47	1560	1.34	0.78	0.56	4.16	1.75
96.5	2.37	1800	0.94	0.61	0.33	2.53	0.88
65.2	1.60	1860	0.60	0.43	0.17	1.57	0.45
42.9	1.05	2820	0.57	0.425	0.145	0.98	0.25

^a Cell volume 206.6 cc.

TABLE III-25
 Yields of Hydrogen by the Molecular and Radical Processes in the
 Pyrolysis of Monomethylsilane at 361°C and 341°C^a

P(MMS), torr	MMS, 10 ³ M	Time, s	H ₂ Yield, μ moles		Rate, M s ⁻¹	
			Total	Molecular Radical	10 ¹⁰ H ₂ , Total	10 ¹⁰ H ₂ , Rad
<u>361°C</u>						
92.6	2.35	8880	1.26	0.66	6.87	3.29
62.1	1.57	12600	1.03	0.62	3.95	1.56
40.5	1.02	16800	0.85	0.53	2.45	0.91
<u>341°C</u>						
195.8	5.11	16500	2.32	0.52	6.81	5.29
128.2	3.35	19500	1.34	0.41	3.32	2.32
84.5	2.21	33180	1.19	0.44	1.73	1.09

^a Cell volume 206.6 cc.

TABLE III-26
 Product Yields by the Molecular and Radical Processes in the Pyrolysis of Monomethylsilane at
 415°C in the Unpacked Vessel^a

P(MMS), corr	MMS, 10 ³ M	Time, s	H ₂ Yield, μ moles		DMS Yield, μ moles		DMS Yield, μ moles	Rate, μ s ⁻¹						
			Tot	Rad	Tot	Rad		10 ⁵ $\dot{r}_{2,Tot}$	10 ⁵ $\dot{r}_{DMS,Tot}$					
409.7	9.34	120	3.63	1.735	1.895	3.20	1.34	1.86	0.10	14.6	7.53	12.9	7.50	4.03
404.8	9.44	120	3.46	1.79	1.67	2.76	1.38	1.38	0.074	4.0	6.74	11.1	5.56	2.39
407.9	9.50	120	3.03	1.64	1.19	2.76	1.42	1.34	0.090	12.2	4.81	11.1	5.43	2.42
241.5	5.62	150	1.98	1.40	0.58	1.85	1.08	0.77	0.052	6.39	1.93	5.07	2.49	1.53
198.5	4.62	120	1.58	0.92	0.66	1.33	0.71	0.62	0.045	6.37	2.67	5.38	2.52	1.52
154.8	3.61	150	1.31	0.83	0.48	0.95	0.64	0.11	0.023	4.23	1.56	3.07	2.36	0.74
133.5	3.23	150	1.15	0.80	0.35	0.76	0.62	0.16	0.022	3.78	1.13	2.52	2.52	0.71
144.2	3.36	720	4.93	3.75	1.18	4.23	2.69	1.34	0.330	3.32	0.79	2.64	0.90	0.61
109.1	2.54	150	0.80	0.59	0.21	0.66	0.46	0.20	0.010	2.53	0.53	2.13	0.56	0.31
42.3	1.15	150	0.32	0.267	0.053	0.42	0.21	0.21	0.004	1.03	0.17	1.36	0.63	0.13
43.9	1.14	180	-	-	-	0.38	0.245	0.135	0.004	-	-	1.02	0.55	0.11
45.4	1.06	150	0.36	0.29	0.07	0.31	0.23	0.08	0.004	0.57	0.19	0.83	0.22	0.11

^a Cell volume 206.6cc; S/V = 1.0 cm⁻¹.



TABLE III-27
 Yields of Products by the Molecular and Radical Processes in the
 Pyrolysis of Monomethylsilane at 415°C in the Packed Vessel^a

P(MMS), torr	PMS 10 ³ M	Time, s	M ₂ Yield, μ moles		MMS Yield, μ moles			M ₂ Yield, μ moles	M ₂ Total Yield		M ₂ Total Yield % of MMS			
			Tot	MST	Tot	MST	MST		M ₂ Total	% of MMS				
514.3	12.0	150	5.05	2.27	2.73	4.63	1.75	2.93	0.123	21.9	12.1	20.3	12.7	0.534
363.5	8.46	120	3.64	1.27	2.37	3.65	0.98	2.67	0.153	19.8	12.9	19.6	14.5	0.321
361.4	8.41	150	3.71	1.59	2.12	3.17	1.23	1.94	0.133	16.1	9.19	13.8	8.42	0.504
268.3	6.25	120	2.33	0.93	1.40	2.17	0.72	1.45	0.100	12.7	7.53	11.8	7.66	0.543
205.4	4.78	240	2.91	1.15	1.46	3.13	1.12	2.01	0.17	7.90	3.96	8.50	5.46	0.462
203.7	4.74	360	4.42	2.16	2.26	4.32	1.66	2.66	0.28	8.00	4.10	7.82	4.61	0.557
203.3	4.73	150	1.76	0.87	0.89	1.74	0.67	1.07	0.080	7.64	3.85	7.56	4.63	0.343
154.1	3.59	150	1.17	0.66	0.51	1.16	0.51	0.65	0.054	5.03	2.21	5.04	2.81	0.235
113.5	2.64	180	1.03	0.585	0.445	0.94	0.45	0.49	0.055	3.73	1.61	3.40	1.77	0.199
102.0	2.37	360	1.76	1.12	0.64	1.50	0.87	0.71	0.11	3.19	1.15	2.66	1.29	0.133
76.0	1.77	150	0.51	0.33	0.18	0.40	0.25	0.15	0.020	2.22	0.80	1.74	0.64	0.037
56.4	1.31	150	-	-	-	0.30	0.19	0.11	0.014	-	-	-	1.29	0.46
51.7	1.20	150	0.35	0.23	0.12	0.29	0.18	0.11	0.011	1.52	0.53	1.26	0.50	0.043
50.4	1.17	480	1.56	0.69	0.39	0.97	0.535	0.435	0.050	1.47	0.53	1.32	0.57	0.063

^a Volume 153.5 cc, S/V = 21 cm⁻¹.

determined at different temperatures are given in Table III-28 and for $H_{2,Rad}$, $DMDS_{Rad}$ and DMS at 415°C in the packed and unpacked reaction vessels in Table III-29.

It is evident that the reaction order for $H_{2,Rad}$ is between 1.5 and 2.0 depending on the experimental conditions. Similar data for $DMDS_{Rad}$ and DMS are available for one temperature only and exhibit considerable scatter; at 415°C, the orders both appear to be approximately 1.5, similar to that for $H_{2,Rad}$.

The orders found for $H_{2,Rad}$, 1.5-2.0, are in the expected range for a radical chain process. Considering that the order for $H_{2,Molec}$ is 1.0 (Table III-17) and that the order of $H_{2,Total}$ is slightly greater than unity, Table III-8, it would appear that a substantial portion of total H_2 yield is formed in the radical chain.

The sequence of radical reactions which are assumed to take place in the pyrolysis of MMS,

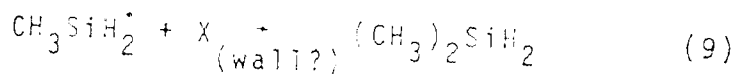
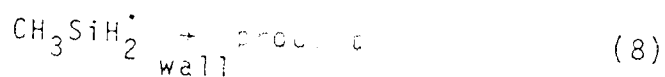
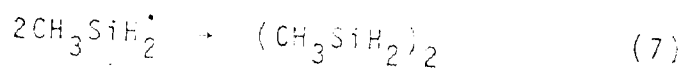
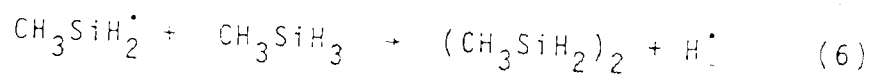
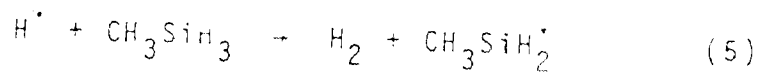
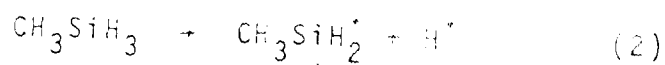


TABLE III-28
Reaction Orders for H_2, Rad in the Pyrolysis of
 $MeSiH_3$ at Different Temperatures ^a

Temperature, °C	Order
441	1.74±0.13
429	1.47±0.14
421	1.65±0.07
400	1.59±0.07
381	1.65±0.08
361	1.55±0.17
341	1.88±0.04

^a In an unpacked reaction vessel of
volume 206.6 cc, $S/V = 1.0 \text{ cm}^{-1}$.

TABLE III-23
 Reaction Orders for H_2 , Rad, $DMDS_{Rad}$ and
 DMS in the Pyrolysis of $MeSiH_3$ at $415^\circ C$

Product	Order	
	Packed Vessel ^a	Unpacked Vessel ^b
H_2 , Rad	1.51 ± 0.06	1.65 ± 0.10
$DMDS_{Rad}$	1.62 ± 0.06	1.32 ± 0.22
DMS	1.32 ± 0.12	1.59 ± 0.09

^a Volume 153.5 cc, $S/V = 21 \text{ cm}^{-1}$.

^b Volume 206.6 cc, $S/V = 1.0 \text{ cm}^{-1}$.

involves a free radical chain which is initiated unimolecularly by reaction (4) and propagated bimolecularly by reactions (5) and (6). The chain can be terminated either quadratically by reaction (7) or linearly on the walls of the reactor by reaction (8).

It can be shown that the reaction order for the products of such a chain reaction will depend mainly on the type of termination of the chain. Thus, if it is assumed that the products are formed predominantly by the chain propagation reactions (i.e., assuming a long chain length), then the usual steady-state approximations predict that the reaction order for $H_{2,Rad}$ and $DMDS_{Rad}$ will be 3/2 if the chain is terminated quadratically by (7), or 2 if the chain termination is linear, (8). The experimental reaction orders for $H_{2,Rad}$ and $DMDS_{Rad}$ however are between 1.5 and 2.0, and therefore it would seem that both quadratic and linear termination of the chain must participate in the reaction mechanisms.

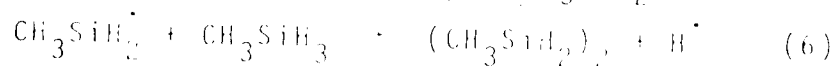
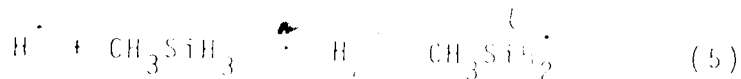
We will return to the chain termination reaction after discussing the chain propagation steps.

(ii) Chain Propagation

The participation of a free radical chain mechanism in the synthesis of CH_3CHO has been already suggested by Ring et al.³⁰ and is confirmed by the present

work (cf. Section III.B.11.1).

Propagation of a free radical chain by reactions such as (5) and (6)



cannot be facile owing to the high activation energy of reaction (6) and can be operative only at elevated temperature. Thus, in the mercury ($^3\text{P}_1$) photosensitized decomposition of MeSiH_3 and Me_2SiH_2 ³¹, both H atoms and the corresponding silyl radicals were present, but the product quantum yields indicated that no chains were operative at room temperature. In the case of dimethylsilane, the H_2 quantum yields increase rapidly above 250°C, indicating the onset of a chain reaction. Similarly, radical chain reactions are claimed to be present in the pyrolysis of SiH_4 at ca 400°C^{39,88}, but not at low temperatures³⁷.

The values of the rate constants k_5 and k_6 have been estimated to be (Section III.3.3.1):

$$k_5 (\text{M}^{-1}\text{s}^{-1}) \approx 10^{10.6} \exp(-3000/\text{RT})$$

$$k_6 (\text{M}^{-1}\text{s}^{-1}) \approx 10^{10} \exp(-13000/\text{RT})$$

The chain is propagated by H atoms and methylsilyl radicals; the relative concentrations of which can be estimated from the rate constants k_5 and k_6 by

$$\frac{R_5}{R_6} = \frac{k_5 [H^\cdot] [MMS]}{k_6 [MeSiH_2^\cdot] [MMS]} = \frac{k_5}{k_6} \frac{[H^\cdot]}{[MeSiH_2^\cdot]}$$

By solving the kinetics of the radical process applying the steady state approximations, it can be shown that if a long chain length is operative (i.e. $H_{2, Rad}$ and $DMDS_{Rad}$ are formed mainly by the chain propagation reactions), the rates of both propagation steps (5) and (6) are approximately the same, i.e. $R_5/R_6 \approx 1$. Hence,

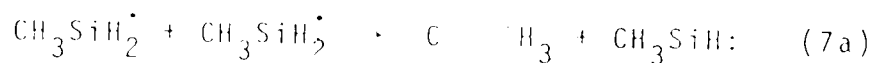
$$\frac{[MeSiH_2^\cdot]}{[H^\cdot]} \approx \frac{k_5}{k_6} \approx 7 \times 10^3 \quad \text{at } 400^\circ\text{C}$$

Since the concentration of methylsilyl radicals is much higher than that of H atoms (cf. Section III.B.4.v) the chain will be terminated almost exclusively by methylsilyl radicals.

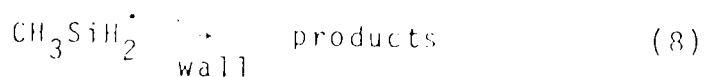
(iii) Chain Termination

The metathetical reaction (5) of hydrogen atoms is highly efficient, $k_5 = 10^{10.6} \exp(-3,000/RT)^{101}$, and therefore under the experimental conditions employed in this study will go to completion. This leaves the

$\text{CH}_3\text{SiH}_2\dot{\text{C}}$ radical as the chain terminating species via the bimolecular combination and disproportionation reactions,



or on heterogeneous wall



The value of k_{7a}/k_7 has been estimated to be 0.1 at 25°C³² but at elevated temperatures it may be higher and may also be pressure dependent in the 40-400 torr range. Both reactions (7) and (7a) will be represented by a quadratic term in the overall rate equation and reaction (8), a linear term.

No information is available on the nature of the products of reaction (8). In any case, since the chain length is large, the products of this termination step are very minor and can be neglected.

(iv) Formation of Dimethylsilane

Dimethylsilane, a minor product of the pyrolysis of MMS, must be formed in the radical process since

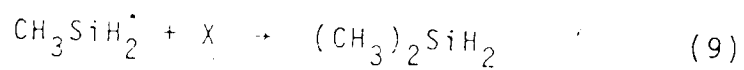
(a) it can be completely scavenged by ethylene (cf.

Table III-15), and

(b) there is an excellent correlation between the rates of formation of DMS and those of $H_{2, Rad}$ and $DMDS_{Rad}$. The plots of $Rate(H_{2, Rad})$ vs. $Rate(DMS)$ and $Rate(DMDS)_{Rad}$ vs. $Rate(DMS)$, shown in Figure III-12 are linear and pass through the origin.

Since DMS is definitely not formed by the molecular process, its presence could serve as a criterion for the occurrence of radical reactions, and may also be used to estimate their importance.

At present, however, the mechanism of DMS formation is not very clear. In the reaction scheme proposed, Table III-20, reaction (9) describes the formation of DMS



but the exact nature of the species "X" cannot be defined since DMS might be formed in a partly or fully heterogeneous process. Although "X" is very likely the substrate, other species such as DMDS, the methylsilyl radical, methylsilylene or even polymer must also be considered.

If "X" is the substrate, reaction (9a) would form a silyl radical which would undergo further reactions, such as (9a-1) and (9a-2), forming monosilane and

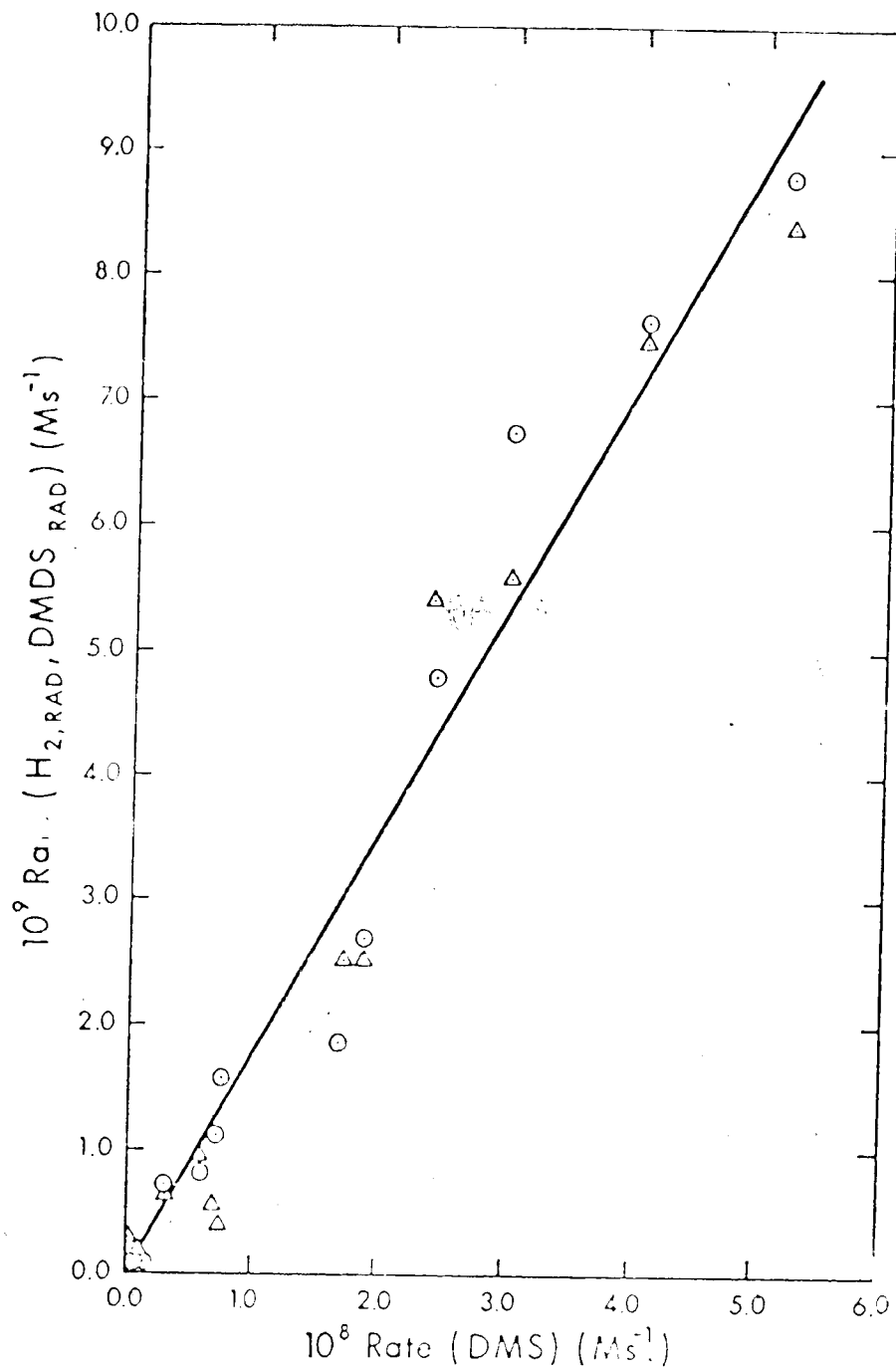
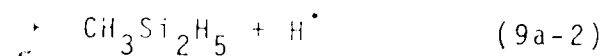
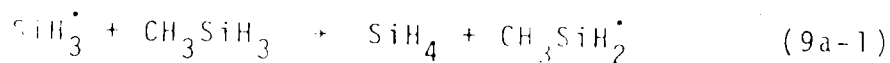
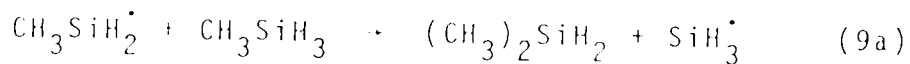


Figure III-12. Correlation Between the Products of the Radical Process in the Pyrolysis of MeSiH_3 at 415°C : Rate $(\text{H}_2)_{\text{Rad}}$ (○) and Rate $(\text{DMDS})_{\text{Rad}}$ (Δ) versus Rate (DMS).

methyldisilane:



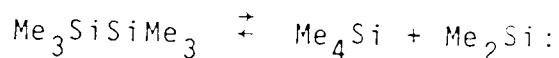
Monosilane, SiH_4 , was detected among the reaction products, and its yields were found to correlate to a certain degree with those of DMS (cf. Figure III-8 and Table III-1).

Negligible traces of methyldisilane were also detected.

If reaction (9a) is responsible for the formation of DMS, then methylsilyl radicals must be able to abstract a methyl group from the substrate. This type of metathetical reaction has been proposed by others. Thus, in early work on the pyrolysis of Me_6Si_2 , Davidson and Stephenson¹⁰⁶ detected Me_4Si and suggested that it was formed by abstraction of a methyl group by a $\text{Me}_3\text{Si}^\bullet$ radical,



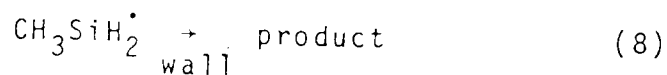
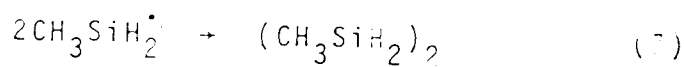
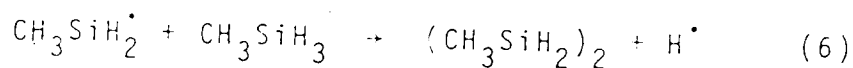
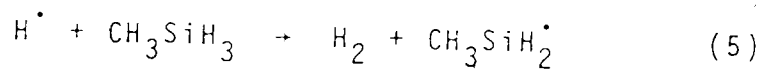
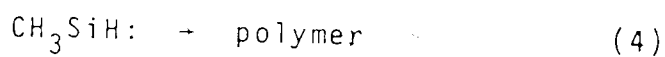
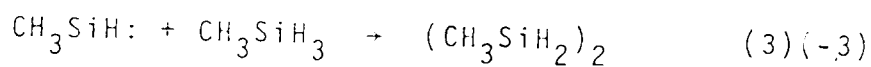
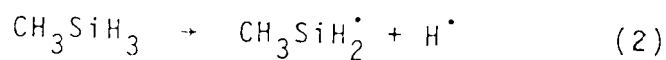
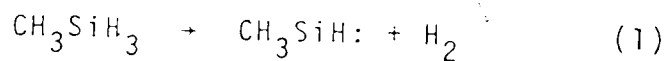
Frangopol and Ingold⁹⁰, however, expressed skepticism about this type of reaction, and recently Davidson et al.¹⁷ offered an alternative reaction for the formation of Me_4Si :

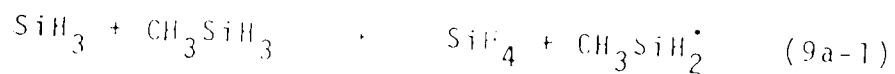
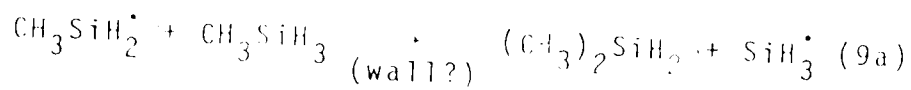


Further work is obviously needed in order to elucidate the modes of formation of DMS and SiH_4 in the pyrolysis of MMS. At present, we feel that reactions (9a) and (9a-1) are the most probable sources of DMS and SiH_4 , and are of the opinion that reaction (9a) is probably heterogeneous, (cf. Chapter IV).

(v) Rate Constants and Arrhenius Parameters for the Radical Process

It has been shown that the nature and the kinetics of formation of the products formed in the pyrolysis of MMS can be rationalized by postulating radical and molecular processes which occur simultaneously and independently. The proposed reactions are:





The rate expressions derived from this mechanism using steady-state assumptions, however, are too complex to be solved analytically. The main complication arises from the presence of two chain terminating steps, (7) and (8).

Were the radical chain terminated by only one process, i.e. quadratic or linear, the rate expressions would be more simple and amenable to kinetic interpretation. We shall now examine these two cases separately, bearing in mind that the actual situation may involve the simultaneous occurrence of both steps.

In the case that the chain is terminated quadratically, the rate expressions are:

$$R(\text{H}_2)_{\text{Total}} = (k_1 + k_2)_{\text{quad}} [\text{MMS}] + \left\{ k_6 \left(\frac{k_2}{k_7} \right)^{\frac{1}{2}} \right\}_{\text{quad}} [\text{MMS}]^{\frac{3}{2}} \quad (14)$$

$$R(\text{DMDS})_{\text{Total}} = (k_1 + k_2)_{\text{quad}} [\text{MMS}] + \left\{ k_6 \left(\frac{k_2}{k_7} \right)^{\frac{1}{2}} \right\}_{\text{quad}} [\text{MMS}]^{\frac{3}{2}} - R(\text{polymer}) \quad (15)$$

$$R(\text{DMS}) = k_{9a} \left(\frac{k_2}{k_7} \right)^{\frac{1}{2}}_{\text{quad}} [\text{MMS}]^{\frac{3}{2}} \quad (16)$$

and for the case of linear termination,

$$R(\text{H}_2)_{\text{Total}} = (k_1 + k_2) \text{lin} [\text{MMS}] + \left(k_6 \frac{2k_2 \text{lin}}{k_8} \right) [\text{MMS}]^2 \quad (17)$$

$$R(\text{DMDS})_{\text{Total}} = k_1 \text{lin} [\text{MMS}] + \left(k_6 \frac{2k_2 \text{lin}}{k_8} \right) [\text{MMS}]^2 + R(\text{polymer}) \quad (18)$$

$$R(\text{DMS}) = \left(k_9 \frac{2k_2 \text{lin}}{k_8} \right) [\text{MMS}]^2 \quad (19)$$

(In the following discussion, the superscripts quad and lin will refer to the quadratic and linear termination mechanisms, respectively.)

The rate expressions for hydrogen, (14) and (17), contain two terms, one of which is first order and the other, of higher order, both with respect to MMS; it is significant that the coefficients of the first order terms are identical in both cases. The rate expressions for DMDS, (15) and (18), are very similar to those for H_2 , except they contain an additional term corresponding to polymer formation. (The rate constant k_2 does not appear in the first order term of eq (18) since the products of the chain termination reaction (8) have been neglected; if it is assumed that, for each two methylsilyl radicals terminated on the wall, one DMDS molecule is formed, then the first order terms of (18) and (17) will be the same.)

The kinetic expressions for $R(H_2)$, (14) and (17), are mathematically the most simple and since the experimental data on H_2 (in Tables III-21 to III-27) are extensive and accurate, a more detailed analysis of the kinetics of H_2 formation will now be attempted.

Rearranging (14) and (17) gives

$$\frac{R(H_2)_{Total}}{[MMS]} = (k_1 + k_2)^{quad} + \left\{ k_6 \left(\frac{k_2}{k_7} \right)^{1/2} \right\} [MMS]^{1/2} \quad (20)$$

and

$$\frac{R(H_2)_{Total}}{[MMS]} = (k_1 + k_2)^{lin} + \left\{ k_6 \frac{2k_2}{k_7} \right\} [MMS] \quad (21)$$

Equations (20) and (21) predict a linear relationship between $R(H_2)_{Total}/[MMS]$ and $[MMS]^{1/2}$ and $[MMS]$, respectively, and identical intercepts yielding $k_1 + k_2$ directly.

The data in Tables III-21 to III-26 were used for the kinetic plots, representative examples of which are illustrated in Figure III-13.

The predicted linear relationships (20) and (21) hold, and each limiting case appears to be a reasonable approximation.

The first order rate coefficients corresponding to the intercepts of eqs (20) and (21) were determined by least mean squares analyses, and the results at different temperatures are listed in Table III-30; the values of

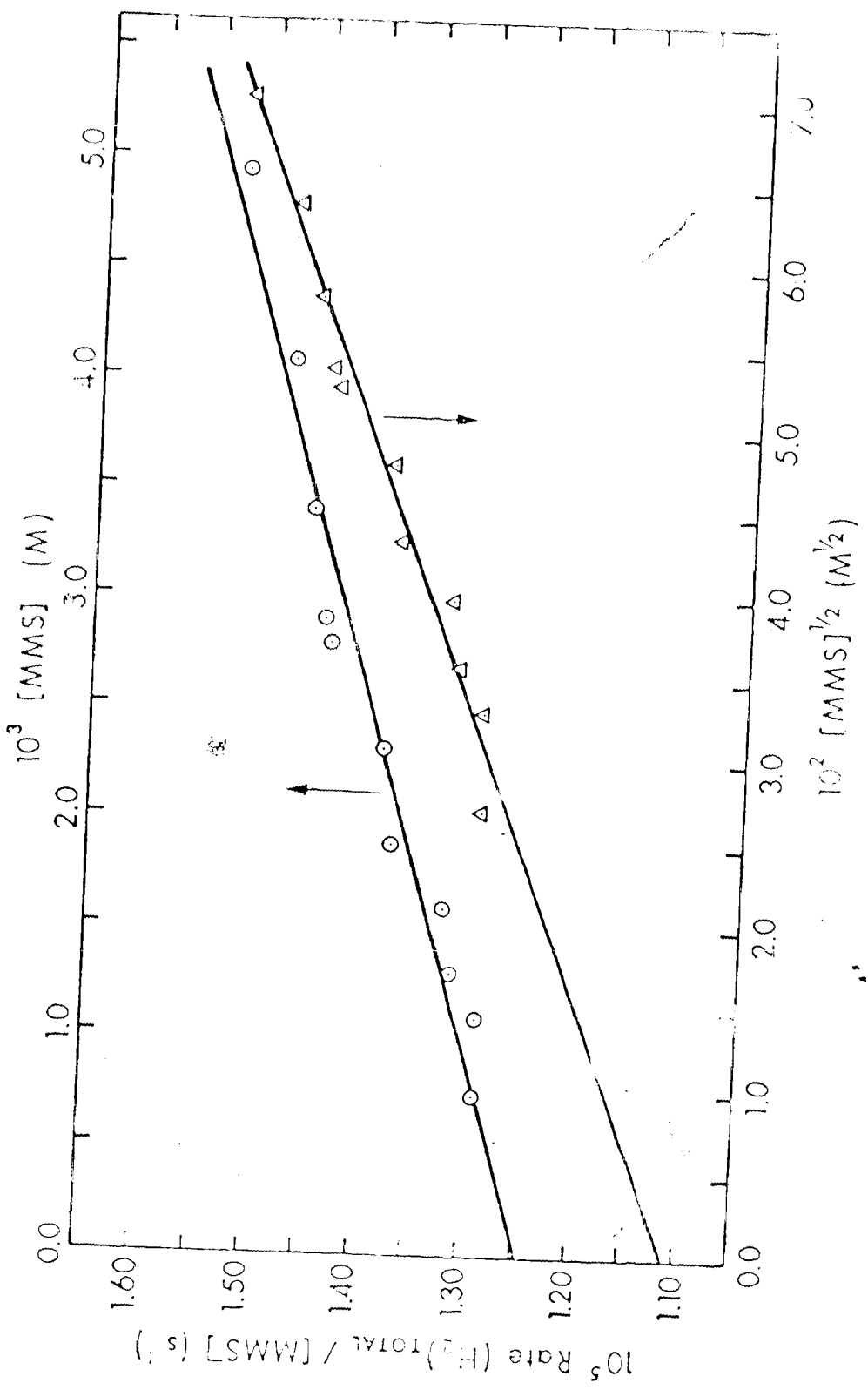


Figure III-13. Rate $(H_2)_{\text{TOTAL}} / [MMS]^{1/2}$ versus $[MMS]^{1/2}$, (O), and $[MMS]$, (Δ), at 421°C.

TABLE III-30
 Pyrolysis of MeSiH_3 ^a: First-Order Rate Constant,
 k_1 , for H_2 Formation as a Function of Temperature

Temperature, °C	k_1 molec. l ⁻¹ s ⁻¹	Rate constant (k_1+k_2) quad ^c s ⁻¹	(k_1+k_2) lin ^d s ⁻¹
441	4.20×10^{-5}	$4.26 \pm 0.17 \times 10^{-5}$	$4.47 \pm 0.08 \times 10^{-5}$
429	-	$1.61 \pm 0.18 \times 10^{-5}$	$2.14 \pm 0.09 \times 10^{-5}$
421	1.16×10^{-5}	$1.11 \pm 0.02 \times 10^{-5}$	$1.25 \pm 0.01 \times 10^{-5}$
415	8.67×10^{-6}	$6.24 \pm 1.02 \times 10^{-6}$	$8.84 \pm 0.11 \times 10^{-6}$
400	2.95×10^{-6}	$2.61 \pm 0.19 \times 10^{-6}$	$2.61 \pm 0.19 \times 10^{-6}$
381	7.00×10^{-7}	$4.98 \pm 0.96 \times 10^{-7}$	$7.83 \pm 0.38 \times 10^{-7}$
361	1.54×10^{-7}	$1.30 \pm 0.34 \times 10^{-7}$	$2.03 \pm 0.21 \times 10^{-7}$
341	2.85×10^{-8}	$(-2.78 \pm 1.00 \times 10^{-8})$	$3.68 \pm 0.12 \times 10^{-8}$

^a Unpacked vessel; 206.6 cc; $S/V = 1.0 \text{ cm}^{-1}$.

^b In the presence of 1% ethylene (Table III-16).

^c Intercept of eq. (20).

^d Intercept of eq. (21).

k_1^{molec} , the first order rate constant for H_2 formation obtained in the presence of ethylene, are also included for comparison.

Inspection of Table III-30 shows that the kinetically derived values of k_1+k_2 from the linear or the quadratic termination mechanism are in reasonably good agreement with k_1^{molec} , except for $(k_1+k_2)^{\text{quad}}$ at the lowest temperature, 341°C; here the negative value of $(k_1+k_2)^{\text{quad}}$ is probably due to experimental error (only three points were available for the plot). The calculated coefficients represent limiting cases, with $(k_1+k_2)^{\text{quad}}$ and $(k_1+k_2)^{\text{lin}}$ being lower and higher limits, respectively, of the actual case, i.e. $(k_1+k_2)^{\text{quad}} < (k_1+k_2) < (k_1+k_2)^{\text{lin}}$. It is significant that these rate coefficients are very close to k_1^{molec} ; this implies that k_2 must be relatively small. We shall return to this point later.

The logarithms of the rate coefficients k_1+k_2 in Table III-30 were then plotted versus $1/T$, Figure III-14, and the activation energies and A factors derived by least mean squares analyses of the slopes and intercepts are given in Table III-31.

If it is assumed that the quadratic and linear termination steps participate to the same extent, the values of the Arrhenius parameters are

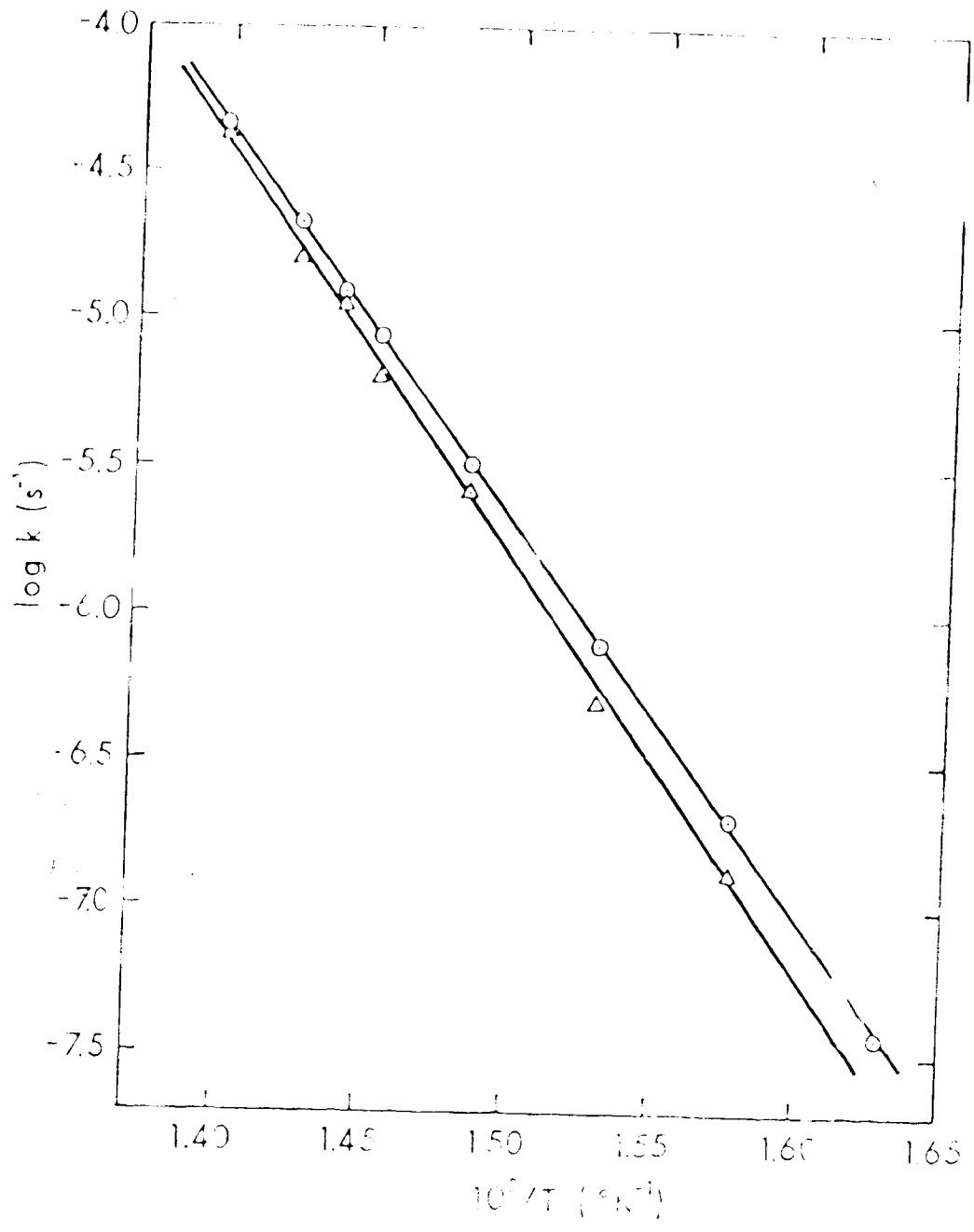


Figure III- Arrhenius Plots for the First Order Reaction Constants $(k_1 + k_2)$ in O_2 and $(k_1 + k_2)^{\text{aq}}$, Δ , based on Hydrogen Formation.

TABLE III-31
Arrhenius Parameters for Hydrogen Formation in
the Pyrolysis of Monomethylsilane

Rate Constant, s^{-1}	$\log A (s^{-1})$	E_a , kcal/mol
$(k_1+k_2)^{quad}$	15.40 ± 0.44	64.75 ± 1.37
$(k_1+k_2)^{lin}$	14.42 ± 0.13	61.35 ± 0.41
$k_1^{molec.}^a$	15.02 ± 0.10	63.27 ± 0.31

^a From experiments with added ethylene
Table III-18.

$$\log A_1 = 14.91 \quad \text{and} \quad E_1 = 63.06 \text{ kcal/mol}$$

which are in excellent agreement with those of the molecular process (cf. Table III-18).

The rate constant k_2 must therefore be small compared to k_1 and must thus be neglected in the calculations involving $(k_1 + k_2)$ without introducing any significant error. (This also implies that the chain length must be considerably long (cf. Sections IIIB.3.ii and III.B.4.vii)).

The Arrhenius parameters of the radical chain reaction for the two extreme cases of chain termination can now be calculated. Since $k_1 \gg k_2$, only the higher order terms in (14) and (17) correspond to H_2 formation by the radical chain process.

The rate coefficients $(k_6 \frac{k_2}{k_7})^{\text{quad}}$ and $(\frac{2k_2}{6k_8})^{\text{lin}}$, obtained from least squares analyses of the slopes of the kinetic plots of equations (20) and (21), respectively, are listed in Table III-32 as a function of temperature.

If the data in Table III-32 are normalized to the same concentration units, then the rate constant ratios for the linearly and quadratically terminated chains are found to be of a comparable order of magnitude.

TABLE III-32
 Apparent Rate Constants for H_2, Rad as a Function of
 Temperature for Linear and Quadratic Termination
 of the Chain^a

Temperature,	$k_6 (k_2/k_7)^{1/2}$, quad $M^{-1} s^{-1}$	$(k_6 + 2k_2/k_8)^{1/2}$, $M^{-1} s^{-1/2}$
441	$1.19 \pm 0.40 \times 10^{-4}$	$1.46 \pm 0.37 \times 10^{-3}$
429	$2.55 \pm 0.39 \times 10^{-4}$	$2.74 \pm 0.35 \times 10^{-3}$
421	$5.85 \pm 0.34 \times 10^{-4}$	$5.95 \pm 0.40 \times 10^{-4}$
415	$8.37 \pm 1.47 \times 10^{-5}$	$6.07 \pm 1.14 \times 10^{-4}$
400	$2.67 \pm 0.37 \times 10^{-5}$	$2.64 \pm 0.36 \times 10^{-4}$
381	$1.31 \pm 0.48 \times 10^{-5}$	$1.34 \pm 0.11 \times 10^{-4}$
367	$3.29 \pm 0.83 \times 10^{-6}$	$3.34 \pm 1.11 \times 10^{-5}$
341	$2.24 \pm 0.17 \times 10^{-6}$	$1.88 \pm 0.03 \times 10^{-5}$

^a Cell volume 206.6 cc, $S/V = 1.0 \times 10^{-3} m^{-1}$.

The Arrhenius plots of the data in Table III-27 are shown in Figure III-15; the values of $\log A$ and $\log k$ for the two limiting cases of chain termination were determined by least squares analyses and are given in Table III-27.

In spite of the relatively large errors associated with the calculated Arrhenius parameters, the overall activation energy for H_2 formation by the radical process is nevertheless close to ~ 41 kcal/mol and the A factor is probably between 10^9 ($M^{-1/2}s^{-1}$) and 10^{10} ($M^{-1}s^{-1}$).

From these results it is now possible to decide whether the chain initiation step, reaction (2), is a homogeneous gas phase reaction, or whether it is a heterogeneously catalysed process.

(vi) Chain Initiation Step: Homogeneous or Heterogeneous?

It will be recalled that the rate of pyrolysis of MMS is strongly dependent on the nature of the surface but not on the S/V ratio. It has also been shown that the heterogeneity of the decomposition is associated with the radical process which is characterized by a long radical chain. These observations indicate that both initiation and termination of the chain are at least partly heterogeneous.

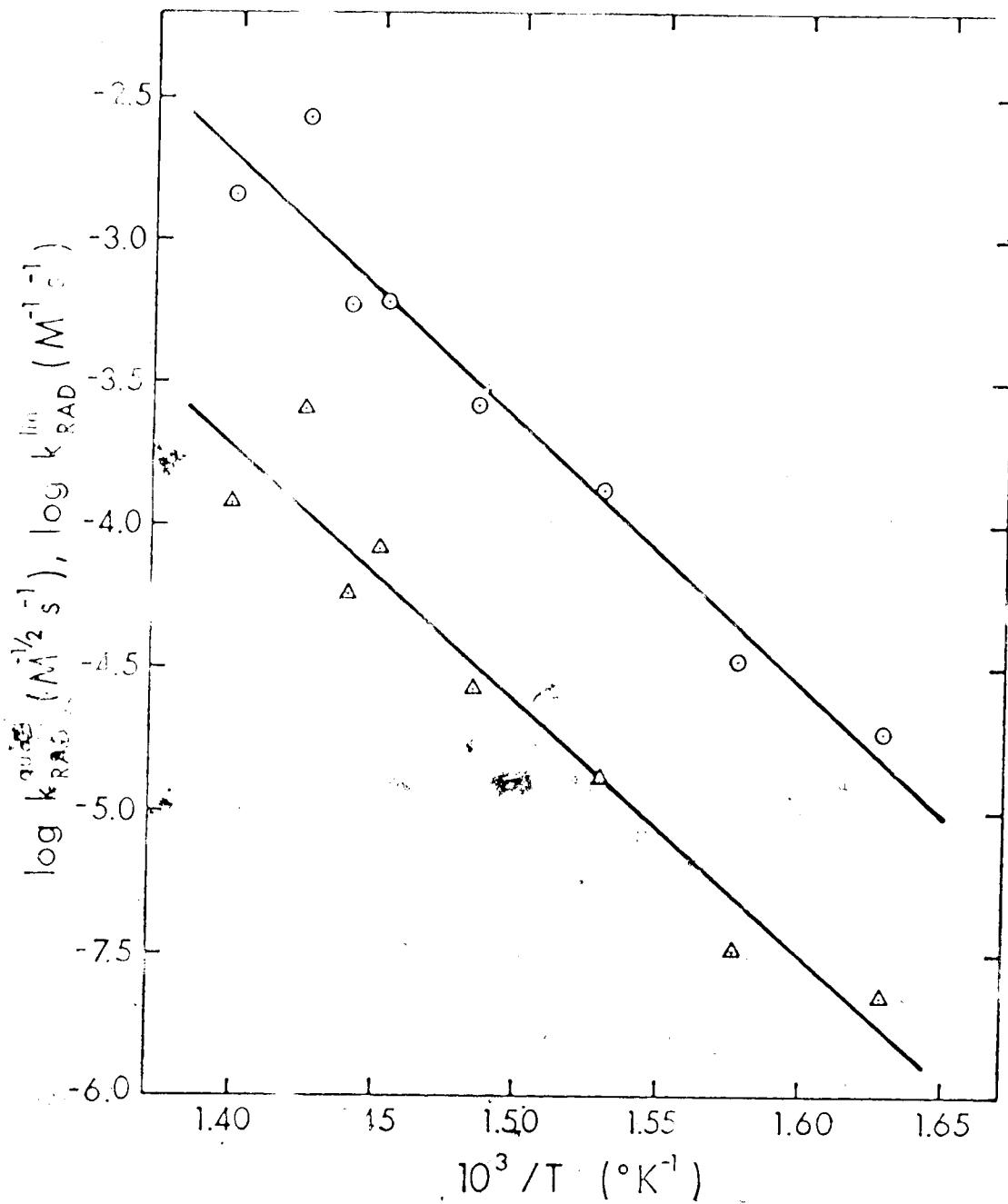


Figure III-75. Arrhenius Plots for the Rate Constants $\{k_6 2k_2/k_3\}^{\text{lin}}$, \odot , and $\{k_6 (k_2/k_7)^{1/2}\}^{\text{quad}}$, \triangle , based on Hydrogen Formation.

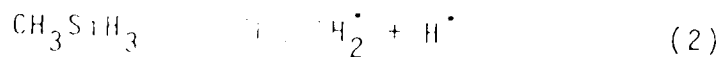
TABLE III-3
 Apparent Arrhenius Parameters for H_2, Rad in the
 Pyrolysis of $MeSiH_3$ for Two Extreme Cases
 of Chain Termination

Rate Constant	$\log A$	$E_a,$ kcal/mol
$(k_6 \frac{k_2}{k_7})^{1/2}$ quad	8.8 ± 1.5^a	40.9 ± 4.4
$(k_6 \frac{2k_2}{k_3})^{1/2}$ lin	10.3 ± 1.3^b	42.4 ± 4.0

^a In units of $M^{-1/2} s^{-1}$.

^b In units of $M^{-1} s^{-1}$.

More compelling evidence for the heterogeneous nature of the chain initiation reaction (2)



can be obtained from the E_2 and estimated Arrhenius parameters for this reaction.

If (2) is a homogeneous gas phase reaction, then E_2 should be approximately equal to the bond dissociation energy $D(\text{MeSiH}_2\text{-H}) \approx 90 \text{ kcal/mol}$ ¹³, since E_{-2} will be close to zero. With regard to A_2 , Benson¹⁰⁷ has estimated values of ca. 10^{15+1} s^{-1} for this type of homogeneous gas phase decomposition.

If, on the other hand, reaction (2) is a heterogeneous process, E_2 is expected to be considerably lower than $D(\text{MeSiH}_2\text{-H})$.

The values of E_2 and A_2 can be estimated from the Arrhenius parameters for the radical process, Table III-33.

First, if it is assumed that the chain is terminated quadratically, the rate constant for H_2 formation by the radical process is

$$k_{\text{Rad}}^{\text{quad}} = k_6 \left(\frac{k_2}{k_7} \right)^{1/2}$$

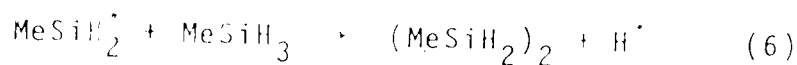
and therefore

$$E_{\text{Rad}}^{\text{quad}} = E_6 + \frac{1}{2}(E_2 - E_7) \approx 41 \text{ kcal/mol} \quad (24)$$

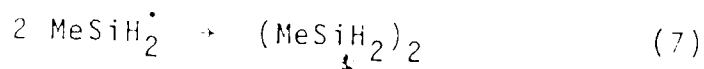
and

$$\log A_{\text{Rad}}^{\text{quad}} (\text{M}^{-1} \text{s}^{-1}) = \log A_6 + \frac{1}{2}(\log A_2 - \log A_7) \approx 9 \quad (25)$$

The Arrhenius parameters for reaction (6)



have been estimated (cf. Section III.B.3.b.ii) to be $E_6 \approx 13$ kcal/mol and $\log A_6 (\text{M}^{-1} \text{s}^{-1}) \approx 10$, and those for reaction (7),



to be $E_7 \approx 1$ kcal/mol and $\log A_7 (\text{M}^{-1} \text{s}^{-1}) \approx 10$, (cf. Section III.B.4.v). The E_2^{quad} is calculated to be ≈ 57 kcal/mol, which is considerably lower than $D(\text{MeSiH}_2\text{-H}) \approx 90$ kcal/mol; similarly $A_2^{\text{quad}} \approx 10^8 \text{ s}^{-1}$, which is seven orders of magnitude smaller than the preexponential factor associated with a gas phase homogeneous decomposition.

Now let us consider the second case, assuming that the free radical chain is terminated linearly: the rate constant is

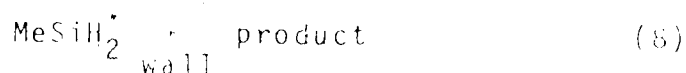
$$-k_{\text{Rad}}^{\text{lin}} = k_6 \frac{2k_2}{k_8}$$

and thus

$$E_{\text{Rad}}^{\text{lin}} = E_6 + E_2 - E_8 \approx 41 \text{ kcal/mol} \quad (26)$$

$$\text{and } \log A_{\text{Rad}}^{\text{lin}} (\text{M}^{-1} \text{s}^{-1}) = \log A_6 + \log A_2 - \log A_8 + \log 2 \approx 10 \quad (27)$$

Although no information is available on reaction (8),



it is very likely that the activation energy for such a process is very small, and thus E_8 may be neglected in eq. (26). Since $E_6 \approx 13 \text{ kcal/mol}$, then $E_2 \approx 28 \text{ kcal/mol}$. A_2^{lin} cannot be estimated since A_8 is unknown; however, for a rate of initiation comparable with a quadratic mechanism, A_2^{lin} should be several orders of magnitude smaller than $A_2^{\text{quad}} (\approx 10^8 \text{ s}^{-1})$.

Thus the kinetic treatment of each case of chain termination leads to the same conclusion, namely, that the activation energy E_2 for the chain initiation reaction is between 28 and 57 kcal/mol which is considerably lower than $D(\text{MeSiH}_2\text{-H}) \approx 90 \text{ kcal/mol}$, and the preexponential factor in each case is incompatible with that normally associated with a homogeneous gas phase reaction. Therefore the chain initiation reaction (2) must be a heterogeneous process.

Other and more detailed studies of the heterogeneous reactions involved in the pyrolysis of

MMS are necessary in order to elucidate the mechanism of the radical process and particularly the formation of the minor products.

vii. Length of the Radical Chain

The length of the radical chain λ can be estimated from

$$\lambda = \frac{R_{\text{propagation}}}{R_{\text{termination}}}$$

where $R_{\text{propagation}}$ can be approximated by $R_{\text{H}_2, \text{quad}}$ provided the chain is sufficiently long; only the quadratic termination rate will be considered since we have no data on the rate of linear termination.

The steady state concentration of methylsilyl radicals is given by

$$[\text{MeSiH}_2\cdot]_{\text{quad}} = \left\{ \frac{k_2}{k_7} \right\}^{\frac{1}{2}} \text{quad} [\text{MMS}]^{\frac{1}{2}}$$

$$\text{and } [\text{MeSiH}_2\cdot]_{\text{lin}} = \left\{ \frac{2k_2}{k_8} \right\} \text{lin} [\text{MMS}]$$

Using the data in Table III-32 and since $k_6 = 10^{10} \exp(-13000/RT) \text{ M}^{-1} \text{ s}^{-1}$, one can calculate $[\text{MeSiH}_2\cdot]_{\text{quad}} = 3 \times 10^{-13} \text{ M}$ and $[\text{MeSiH}_2\cdot]_{\text{lin}} = 2 \times 10^{-11} \text{ M}$ at 400°C and $[\text{MMS}] = 5 \times 10^{-3} \text{ M}$. The average value of $\sim 3 \times 10^{-12} \text{ M}$ will be used in the following calculations.

$R_{\text{termination}}$ can now be estimated from the Arrhenius parameters of reaction (7),



$E_7 = 1 \text{ kcal/mol}$ and $A = 10^{10} \text{ M}^{-1} \text{ s}^{-1}$ 33,34,37,89,90

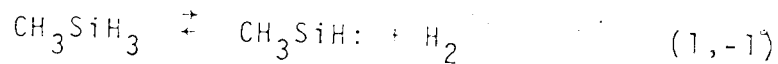
Thus at 400°C

$$R_{\text{termination}} = k_7 [\text{MeSiH}_2 \cdot]^2 = 5 \times 10^9 [3 \times 10^{-12}]^2 = 5 \times 10^{-14} \text{ M s}^{-1}$$

and since, from Table III-23, $R_{\text{propagation}} \approx R_{\text{H}_2, \text{Rad}} = 8 \times 10^{-8}$, the chain length \bar{x} is approximately 10^6 .

5 Some Thermochemical Implications of the Arrhenius Parameters for the Molecular Process

It has been shown that the rate data for H_2 and DMDS obtained in the pyrolysis of MMS in the presence of ethylene refer to the molecular step



having the following average rate parameters (cf. Table III-18):

$$\log k_1 (\text{s}^{-1}) = (14.95 \pm 0.11) - (63200 \pm 330) / 2.3RT$$

Let us now consider the thermochemical implications of these results.

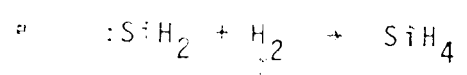
(i) The Activation Energy

The enthalpy change for reaction (1), ΔH_1^0 , is related to the activation energies (E_1, E_{-1}) of the forward and reverse reactions by

$$\Delta H_1^0 = \Delta E_1 + \Delta nRT = (E_1 - E_{-1}) + \Delta nRT \approx E_1 - E_{-1} \quad (28)$$

where the term ΔnRT allows for the change in the number of moles, but it is approximately compensated for by the temperature correction which should be applied to E_1 .

Unfortunately the activation energy E_{-1} for insertion of methylsilylene into hydrogen, reaction (-1), has not been measured; it can be estimated however on the basis of the analogous reaction,



for which the rate constant has been determined⁶⁶:

$$\log k (\text{M}^{-1} \text{s}^{-1}) = (9.1 \pm 0.4) - (5500 \pm 1000)/2.3RT$$

Thus, if it is assumed that $E_{-1} \approx 6$ kcal/mol, then

$$\Delta H_1^0 = E_1 - E_{-1} = 63 - 6 = 57 \text{ kcal/mol}$$

Alternatively, the enthalpy change ΔH_1^0 is related to the enthalpies of formation by

$$\Delta H_1^0 = \Delta H_f^0(\text{MeSiH:}) + \Delta H_f^0(\text{H}_2) - \Delta H_f^0(\text{MeSiH}_3) \quad (29)$$

Using the reported values of $\Delta H_f^0(\text{MeSiH}_3)$, -4 kcal/mol^{13, 14, 18} and $\Delta H_f^0(\text{MeSiH}_2)$, 53.1 kcal/mol⁷⁷,

$$\Delta H_1^0 = 53 + 4 = 57 \text{ kcal/mol},$$

which is consistent with the above calculation.

The enthalpies of formation used above may not be very accurate, however, since Vanderwieles, Ring and O'Neal⁷⁷, in their calculation of $\Delta H_f^0(\text{MeSiH}_2) = 53.1$ kcal/mol, used $\Delta H_f^0(\text{MeSiH}_3) = 1.0$ kcal/mol, suggested by Potzinger and Lampe¹¹ for the bond additivity scheme. Using this value for $\Delta H_f^0(\text{MeSiH}_3)$,

$$\Delta H_1^0 = 53 - 1 = 52 \text{ kcal/mol}$$

which in turn implies that E_{-1} should be approximately 11 kcal/mol, a considerably higher value than the one assumed before.

Since the present thermochemical data are obviously inaccurate, the mean value

$$\Delta H_1^0 \approx \frac{1}{2}(57 + 52) = 55 \text{ kcal/mol}$$

will be used in the following discussion.

Reaction (1) involves splitting of two Si-H bonds in monomethylsilane and formation of a hydrogen molecule, and thus the enthalpy change ΔH_1^0 is related to the bond dissociation energies by

$$\Delta H_1^0 = D(\text{MeSiH}_2\text{-H}) + D(\text{MeSiH-H}) - D(\text{H-H}) \quad (30)$$

The value of $D(\text{H-H}) = 104.2$ kcal/mol is well established,¹⁰⁸ and $D(\text{MeSiH}_2\text{-H})$ can be estimated from recently published data as follows.

From electron impact studies, Pottinger et al.¹³ concluded that the first Si-H bond dissociation energies in SiH_4 , MeSiH_3 , Me_2SiH_2 and Me_3SiH are approximately the same and equal to 89 ± 4 kcal/mol. These results are in excellent agreement with those of Berkley et al.⁶¹ who reported that the activation energies for H atom abstraction by methyl radicals from the Si-H bond in silane, mono-, di-, and trimethylsilane are the same but that for SiH_4 is 1 kcal/mol lower. Walsh and Wells¹⁹ have investigated the gas phase reaction between iodine and trimethylsilane and measured $D(\text{Me}_3\text{Si-I}) = 90.0 \pm 2.6$ kcal/mol; a similar value, $D(\text{Me}_3\text{Si-H}) = 88$ kcal/mol, has been determined by Davidson and Howard¹⁷ from the pyrolysis of Me_6Si_2 . Thus an average value of $D(\text{MeSiH}_2\text{-H})$ of 90 ± 3 kcal/mol can be used with a high degree of confidence.

Using eq (30) we can therefore calculate the second bond dissociation energy $D(\text{MeSiH-H})$:

$$\Delta H_1^0 = D(\text{MeSiH}_2\text{-H}) + D(\text{MeSiH-H}) - D(\text{H-H}) \quad (30)$$

$$55 = 90 + D(\text{MeSiH-H}) - 104$$

$$D(\text{MeSiH-H}) = 69 \text{ kcal/mol}$$

Although the error might be as high as 6 kcal/mol (but probably less), this value nevertheless indicates a large drop from the first to the second BDE in monomethylsilane, of approximately 20 kcal/mol.

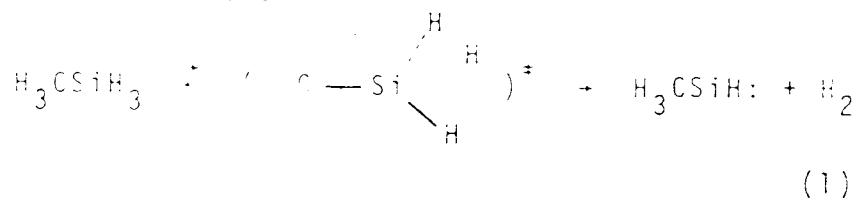
This large decrease appears to be a general trend in silicon chemistry, and has not been observed for carbon compounds. Thus in the cases of SiH_4 , SiCl_4 ¹⁹ and Me_4Si ²⁷, differences of approximately 35, 55 and 65 kcal/mol, respectively, have been calculated.

Some specific stabilizing effect must therefore be present in divalent silicon species, a qualitative explanation of which has been suggested by Walsh and Wells¹⁹.

(ii) The Preexponential Factor

The preexponential factor of reaction (1), $\log A(\text{s}^{-1}) = 14.95$, may yield some information about the nature of the transition state.

The most probable configuration of the transition state is a three-centered cyclic intermediate which may be visualized as follows:



$$\begin{aligned}
 A_1 &= 10^{14.95} \text{ s}^{-1} && \text{- Pre-exponential factor of reaction (1)} \\
 e &= 2.718 && \text{- Base of natural logarithms} \\
 k &= 1.358 \times 10^{-16} \text{ erg deg}^{-1} && \text{- Boltzmann constant} \\
 h &= 6.626 \times 10^{-27} \text{ erg s} && \text{- Planck constant} \\
 T &= 670^\circ\text{K} && \text{- Mean reaction temperature} \\
 R &= 1.987 \text{ cal deg}^{-1} \text{ mol}^{-1} && \text{- gas constant}
 \end{aligned}$$

from which $\Delta S_1^\ddagger = 6.3 \text{ e.u.}$

Since the activation entropy is rather large and positive, the transition state may be classified as "loose".

The activation entropy, ΔS_1^\ddagger , is the difference between the molar entropy of the transition state, S_\ddagger^0 , and that of the reactant, S_{MMS}^0 , i.e.,

$$\Delta S_1^\ddagger = S_\ddagger^0 - S_{\text{MMS}}^0 \quad (32)$$

The molar entropies can be calculated directly from the known molecular parameters by the methods of statistical mechanics. The absolute value of S_{MMS}^0 can be therefore determined "exactly", but the same is not possible for S_\ddagger^0 since the required molecular data (e.g. structural parameters, fundamental vibrational frequencies, symmetry, etc.) are not available for the transition state. One may nevertheless estimate these transition state parameters and calculate the corresponding activation entropy in order to verify the correctness of the assumed model.

On the basis of the suggested configuration of the transition state, let us first examine which degrees of freedom will contribute the most to the activation entropy.

From statistical mechanics, we know that the molar entropy S can be expressed in terms of the molar partition function Q as

$$S = k \ln Q + k \left(\frac{E_0}{kT} \right) \quad (33)$$

$$\text{and } Q = \frac{q_{\text{tran}}^N}{N!} q_{\text{rot}}^N q_{\text{vib}}^N q_{\text{elec}}^N e^{-E_0/kT} \quad (34)$$

where k is the Boltzmann constant, N is Avogadro's number, E_0 is the zero point energy and q_{tran} , q_{rot} , q_{vib} , q_{elec} are the molecular partition functions for translation, rotation, vibration and electronic excitation. The standard molar entropy will therefore be the sum of the contributions from the different degrees of freedom,

$$S^0 = S_{\text{tran}}^0 + S_{\text{rot}}^0 + S_{\text{vib}}^0 + S_{\text{elec}}^0$$

and similarly from eq (32) we obtain

$$\Delta S_{\ddagger}^0 = \Delta S_{\text{tran}}^{\ddagger} + \Delta S_{\text{rot}}^{\ddagger} + \Delta S_{\text{vib}}^{\ddagger} + \Delta S_{\text{elec}}^{\ddagger}$$

Since both monomethylsilane and the transition state complex are expected to remain in their singlet ground electronic states, there will be no contribution from electronic excitation to ΔS_1^\ddagger

The translational contribution to ΔS_1^\ddagger will also be zero since no change in the molecular weight has taken place in the formation of the transition state:

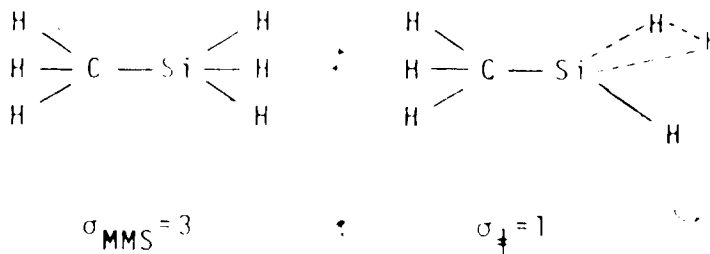
$$\Delta S_{\text{tran}}^\ddagger = \frac{3}{2}R \ln \frac{M_1^\ddagger}{M_{\text{MMS}}} = \frac{3}{2}R \ln 1 = 0 \quad (37)$$

External rotation of a nonlinear molecule will contribute to the entropy of activation by

$$\Delta S_{\text{rot}}^\ddagger = R \ln \left[\frac{(I_A I_B I_C)_{\ddagger}^{\frac{3}{2}}}{(I_A I_B I_C)_{\text{MMS}}^{\frac{3}{2}}} \frac{\sigma_{\text{MMS}}}{\sigma_{\ddagger}} \right] \quad (38)$$

where $I_A I_B I_C$ is the product of the principal moments of inertia and σ is the total symmetry number. Since the mass of a hydrogen atom is extremely small, the moments of inertia of the transition state complex $(I_A, I_B, I_C)_{\ddagger}$ will not be very different from those of the reactant $(I_A, I_B, I_C)_{\text{MMS}}$ and thus rotation will not contribute significantly to ΔS_1^\ddagger except if some change in the symmetry numbers $\sigma_{\ddagger}, \sigma_{\text{MMS}}$ occurs. The CH_3SiH_3 molecule has one threefold symmetry axis and hence $\sigma_{\text{MMS}} = 3$; since this symmetry is destroyed when the transition state is formed,

$$\sigma_{\ddagger} = 1.$$



From eq (38) we therefore obtain

$$\Delta S_{\text{rot}}^{\ddagger} \approx R \ln \left(\frac{\sigma_{\text{MMS}}}{\sigma_{\ddagger}} \right) = R \ln \frac{3}{1} = +2.2 \text{ e.u.}$$

Finally, we will examine the contribution from the vibrational modes (including hindered rotation) to ΔS_{\ddagger} . From statistical mechanics the following expression can be derived for the vibrational entropy of a harmonic oscillator of frequency ω (cm^{-1}):

$$S_{\text{vib}}^0 = R \left[\frac{x}{e^x - 1} - \ln(1 - e^{-x}) \right] \quad (39)$$

where $x = hc\omega/kT$. To calculate the total vibrational entropy of the molecule, the contribution from each fundamental vibrational frequency must be considered, and the summation must be taken over all vibrational modes.

To estimate the vibrational contribution $\Delta S_{\text{vib}}^{\ddagger}$ to the activation entropy, however, we may consider only those vibrational frequencies of the reactant which will

be most likely affected by formation of the transition state (i.e. the stretching and bending frequencies of the Si-H bonds, ν_{SiH}) and leave the other frequencies unchanged.

Since the transition state is "loose", we expect a lowering of these vibrational frequencies and estimate

$$\nu_{\text{SiH}}^{\ddagger} = \frac{2}{3} \nu_{\text{SiH, MMS}}$$

According to transition state theory, one vibrational mode in the activated complex corresponds to the "reaction coordinate" and must be omitted in the calculation of $\Delta S_{\text{vib}}^{\ddagger}$.

The data used for the calculation of $\Delta S_{\text{vib}}^{\ddagger}$ are shown in Table III-34; the fundamental frequencies of CH_3SiH_3 were taken from the literature¹¹⁰. Benson¹¹¹ has tabulated the absolute entropies of a harmonic oscillator using eq (39), and these data have been used to estimate how the frequency shift will contribute to the vibrational entropy of activation.

From Table III-34 it is seen that the main contribution to the vibrational entropy of activation comes from the weakened bending modes of the Si-H bonds of the transition state.

The individual contributions to the entropy of activation are summarized in Table III-35 where it is

TABLE III-31
 Estimated Contributions from some Fundamental Vibrations of CH_3SiH_3 to the
 Entropy of Activation at 600K

Mode	Degeneracy	Frequency, cm^{-1}		Vib Entropy, e.u.		ΔS^\ddagger , vib, e.u.
		MMS ^a	(MMS) ^b	$\frac{S^\ddagger}{S}$	$\frac{S^\ddagger}{S}$	
CH_3 sym.str.	1	2928				
SiH_3 sym.str.	1	2169 + 1450		0.2 + 0.4		+0.2
CH_3 sym.def.	1	1266				
SiH_3 sym.def.	1	946 + 630		1.0 + 1.7		+0.1
Si-C stretch	1	701				
Torsion	1	200				
CH_3 asym.str.	2	2982				
SiH_3 asym.str.	2	2166 ± 1450	R.C. ^d	3.2 ± 5.4		+0.2
CH_3 asym.def.	2	1412				+0.2
SiH_3 asym.def.	2	943 ± 630		2.0 ± 3.4		+0.4
CH_3 rock	2	870				
SiH_3 rock	2	540 ± 360		3.6 ± 5.2		+0.3

^a Taken from Reference 110.

^b Estimated: $w_4 = \frac{2}{3} w_{\text{MMS}}$

^c Determined from the tabulated data of Benson(11).

^d One of these doubly degenerate modes is taken as the reaction coordinate.

TABLE III-13
 Contributions to the Entropy of Activation
 at 600 K^a

Modes	Calculated	Observed
Translation	0	0
Rotation	0	0
Symmetry ^b	+2.2	0
Electronic excitation	0	0
Vibration ^c	+3.9	0
Total, calculated	+6.1	
observed		+6.3

^a Mean Reaction Temperature.

^b Calculated from the symmetry numbers σ in the rotational partition function and may be interpreted as the degeneracy of the reaction path.

^c Cf. Table III-14.

seen that the major factors responsible for the large increase in entropy are the changes in the symmetry numbers and vibrational frequencies.

The calculated entropy of activation is in good agreement with the experimental value and therefore the suggested structure of the transition state appears to be a reasonable model.

CHAPTER IV

PYROLYSIS OF DIMETHYLSILANE

A. Experimental

A preliminary study of the pyrolysis of dimethylsilane (DMS) has been carried out in the temperature and pressure ranges 440 - 500 °C and 41 - 395 torr respectively, using the same static system as described previously. The effects of reaction time, surface and addition of ethylene have been investigated.

1. The Reaction Products

The following products have been observed in the initial stages of the pyrolysis: hydrogen, 1,1,2,2-tetramethyldisilane (TMDS), trimethylsilane (TMS), monomethylsilane (MMS), methane, and a solid polymeric deposit.

Hydrogen and TMDS were the major reaction products, TMS and MMS were minor products; methane was formed only in small amounts, its yield being approximately 1% of those of the major products. Reproducible reaction rates were observed only in a vessel which was well coated by polymer from previous runs.

2. Time Study

The variation of the yields of the gaseous products with time has been investigated at 490°C and at $P = 125$ torr dimethylsilane. The reaction vessel (200 cm^3 , $S/V = 1.0 \text{ cm}^{-1}$), coated by a polymer from previous runs, was heated at 490°C and evacuated overnight before each experiment in order to minimize thermal decomposition of the polymer. The rate of degassing from the coated vessel was monitored after each run for at least 30 min and found to be negligible.

The results of the time study, listed in Table IV-1 and plotted in Figure IV-1, show that the yields of H_2 , TMDS, TMS and MMS were all linear functions of time at conversions below 0.8. Furthermore, a close correspondence between the yields of H_2 and TMDS and between those of TMS and MMS was observed.

3. Effect of the Nature of the Surface

As in the thermal decomposition of MMS (cf. Section III.A.3), the rate of pyrolysis of DMS was found to be dependent on the conditions of the reactor surface, particularly on the extent of polymer deposition.

TABLE IV-1
 Product Yields as a function of Time in the Hydrolysis of Ve_2SiH_2 at 130 °C

Time, min	P (DMS), torr	H_2	Yields, mols TMS	Yields, mols TMS	CH_4	Conversion %
5.00	125.6	1.27	0.274	1.291	0.000	2.133
5.00	127.1	1.28	0.273	0.277	0.000	1.232
10.00	126.3	2.56	0.559	0.559	0.000	3.467
15.00	124.7	3.94	0.826	0.823	0.041	7.09
15.60	125.3	4.09	1.16	1.15	0.054	1.753
20.00	124.3	6.27	2.56	2.57	0.175	1.753
20.00	122.9	5.93	2.68	2.10	0.249	1.753

^a Cell volume 206.6 cc, S/V = 110 cm^{-1} .

^b Calculated from H_2 yield.

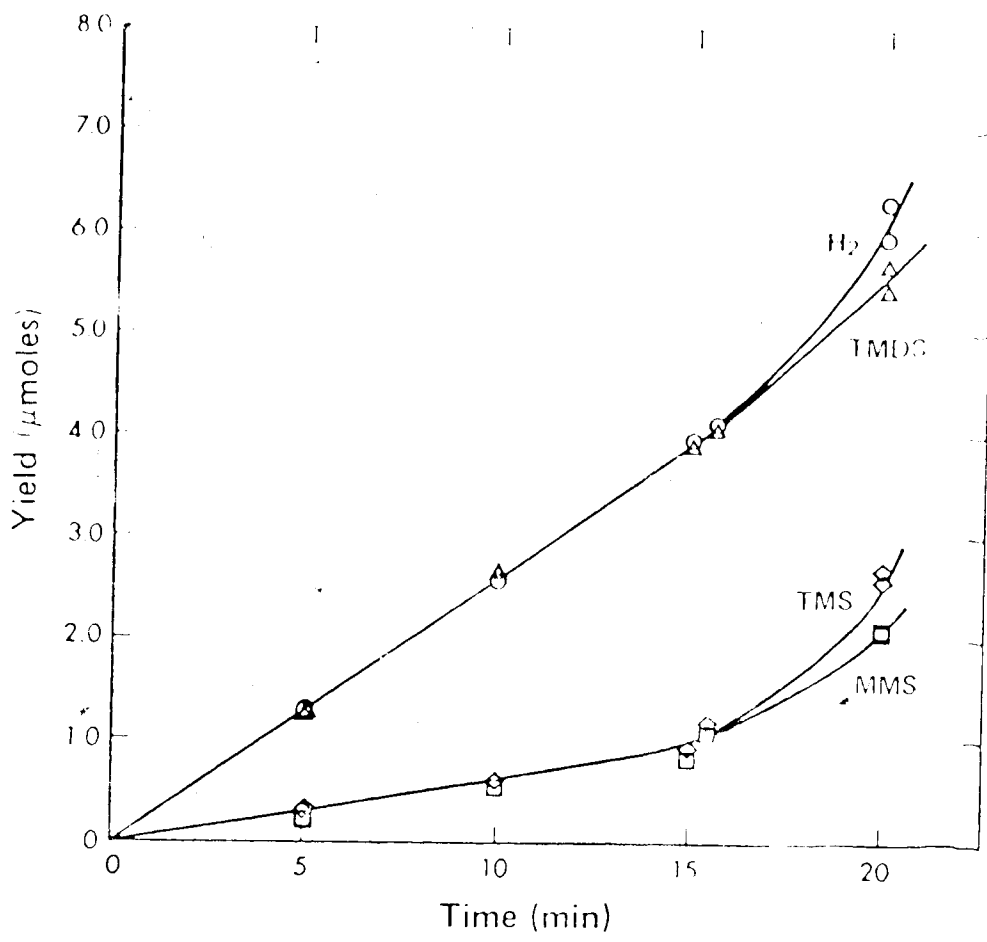


Figure IV-1 Product Yields as a Function of Time
the Pyrolysis of ≈ 125 torr Me_2SiH_2
at 1050°C .

Thus, it was observed that the rate of pyrolysis in a reaction vessel which had been heated and evacuated for several days (up to a week) was always high; after 2 or 3 experiments performed in rapid succession, however, the reaction rates decreased to reasonably reproducible values.

The effect of polymer deposition on the product yields is evident from the data in Table IV-2. The yields of TMS and MMS were profoundly influenced by the mode of pretreatment of the vessel, which suggests that these two products might be of heterogeneous origin. In contrast, those of H_2 and TMDS were virtually unaffected.

4. Determination of the Reaction Orders, and the Effect of Ethylene on the Reaction Rate

The rates of product formation as a function of DMS pressure (in the range 41 - 395 torr) have been measured between 440 and 500°C, and the results are listed in Tables IV-3 - IV-5; the conversions did not exceed 0.6 and were generally in the range of 0.1 - 0.3%. The effect of added ethylene is also shown in these Tables where it is seen that the yields of H_2 and TMDS are unaffected by the presence of a radical scavenger but those of TMS and particularly MMS are greatly reduced. Some new products were formed, the most predominant of which was tentatively identified as dimethylethylsilane from its mass spectrum

TABLE IV-2
 The Effect of Polymer Deposition on the Product Yields
 in the Pyrolysis of Me_2SiH_2 at 490°C ^a

Run No.	P(DMS), torr	Yields, moles		
		H ₂	TMDS	CH ₄
1 b	125.7	3.40	3.34	3.65
2 c	127.2	2.69	2.71	1.11
3 c	126.3	2.56	2.59	0.651

- a Reaction time 10.00 min; cell volume 206.6 cc; $\text{SiV} = 1.0 \text{ cm}^{-1}$.
 b The cell was heated at 510°C and evacuated for 1 month.
 c The cell was heated at 510°C and evacuated for 16 hours.

TABLE IV-3
 Product Yields and Rates of Formation as a Function of Dimethylsilane
 Pressure at 500°C and 480°C; Effect of Added Ethylene^a

P(DMS), torr	Time, s	[DMS], M x 10 ³	C ₂ H ₄ %	Yields, μ moles		Rate, M s ⁻¹ x 10 ⁹					
				H ₂	TMS	H ₂	TMS				
T=500°C											
212.8	240	4.400	-	3.06	3.04	0.77	0.72	61.7	61.3	15.5	15.7
149.8	240	3.096	-	2.10	2.09	0.42	0.41	42.35	42.2	6.47	6.27
105.9	240	2.196	-	1.44	1.444	0.172	0.168	29.0	29.1	3.47	3.29
41.4	300	0.858	9.14	0.695	0.684	0.022	0.021	11.2	11.0	3.35	3.34
T=480°C											
296.2	300	6.302	-	1.82	1.77	1.34	1.32	29.4	28.6	21.6	21.25
98.6	600	2.099	-	1.057	1.03	0.182	0.156	8.53	8.31	1.41	1.26
53.6	900	1.139	-	0.809	0.82	0.127	0.117	4.35	4.41	0.63	0.63

^a Cell volume 206.6 cc, S/V = 1.0 cm⁻¹. The cell, freshly coated by polymer, was heated at 510°C and evacuated for ~ 16 hours.

TABLE IV-4
Product Yields and Rates of Formation as a Function of Dimethyl Silane
Pressure at 490°C; Effect of Added Ethylene^a

P(DMS), torr	Time, s	[DMS], M x 10 ³	C ₂ H ₄ %	Yields, μ moles		Rate, M s ⁻¹ x 10 ⁹		
				H ₂	TMS	H ₂	TMS	
214.0	300	4.494	-	2.47	2.44	1.77	39.85* 29.6*	26.5*
156.6	300	3.288	-	1.57	1.53	0.455	25.3	7.34
127.1	300	2.668	-	1.28	1.24	0.273	20.65	4.40
125.6	300	2.637	-	1.27	1.23	0.274	20.5	4.42
125.5	300	2.636	0.89	1.25	1.20	0.263	20.2	4.24
109.8	420	2.305	-	1.51	1.47	0.297	17.4	3.32
78.8	600	1.654	-	1.52	1.485	0.220	12.3	1.78
75.1	306	1.576	-	0.725	0.724	0.076	11.5	1.20

^a Cell Volume 206.6 cc, S/V = 1.0 cm⁻¹. The cell, freshly coated by polymer, was heated at 510°C and evacuated for ~ 16 hours before each run, unless stated otherwise.
* This experiment was performed in a surface-active cell and the resulting high rates are not included in the order plots.

TABLE IV-5
Product Yields and Rates of Formation as a Function of Dimethylsilane Pressure at 460 and 440°C; Effect of Added Ethylene^a

P(DMS), torr	Time, s	[DMS], M x 10 ³	C ₂ H ₄ %	Yields, μ moles			Rate, M s ⁻¹ x 10 ⁹				
				H ₂	TMDS	TMS	MMS	H ₂	TMDS	TMS	MMS
T=460°C											
282.5	720	6.172	-	1.26	1.28	1.39	1.35	8.47	8.61	9.34	9.08
242.7	960	5.306	9.14	1.44	1.38	0.261	0.120	7.26	6.96	1.32	0.61
143.1	1800	3.060	-	1.43	1.42	1.17	1.16	3.85	3.82	3.15	3.12
119.0	1920	2.602	9.14	1.245	1.22	0.159	0.095	3.14	3.08	0.40	0.24
58.0	4200	1.268	9.14	1.27	1.25	0.123	0.059	1.46	1.44	0.14	0.07
47.4	4800	1.036	-	1.19	1.20	0.307	0.285	1.20	1.21	0.31	0.29
T=440°C											
394.6	1800	8.872	-	2.17	2.06	7.41	7.29	5.83*	5.54*	19.9*	19.6*
340.2	2850	7.644	9.14	2.025	1.86	0.601	0.122	3.44	3.16	1.02	0.21
197.9	2700	4.448	-	0.954	0.921	1.15	1.14	1.71	1.65	2.06	2.04
169.1	3000	3.801	9.14	0.908	0.855	0.197	0.087	1.465	1.38	0.32	0.14
82.4	9000	1.851	9.14	1.21	1.14	0.236	0.075	0.651	0.613	0.127	0.040
68.5	15600	1.540	-	1.67	1.68	1.06	1.00	0.519	0.521	0.338	0.30*

^a Cell volume 206.6 cc, S/V = 1.0 cm⁻¹. The cell freshly coated by polymer was heated at 500°C and evacuated for ~ 16 hours before each run, unless stated otherwise.

* This experiment was performed in a surface-active cell and the resulting high rates are not included in the order plots.

(cf. Appendix 11). Since ethylene begins to decompose around 500°C ⁷⁶, experiments performed in the presence of ethylene were carried out at lower temperatures (440 and 460°C), and at relatively low concentrations of ethylene.

The rate data for H_2 and TMDS from Tables IV-3 to IV-5 in the presence and absence of ethylene are plotted in Figure IV-2 in logarithmic form. The plots were linear at all temperatures and the orders of H_2 and TMDS formation, determined by standard least mean square analyses of the slopes, are listed in Table IV-6.

The rate data for TMS and MMS formation in the absence of ethylene, Tables IV-3 to IV-5, are plotted logarithmically in Figures IV-3 and IV-4, and the orders, determined by standard least square analyses, and listed in Table IV-6, are approximately 2.0.

B. Discussion

Comparison of the Pyrolysis of DMS and MMS:

Similarities and Differences

When comparing the overall thermal behavior of dimethylsilane with that of monomethylsilane (MMS) one can notice several striking similarities are apparent. In both cases the major products were hydrogen and substituted disilane (TMDS, DMDS) were formed. The minor products were

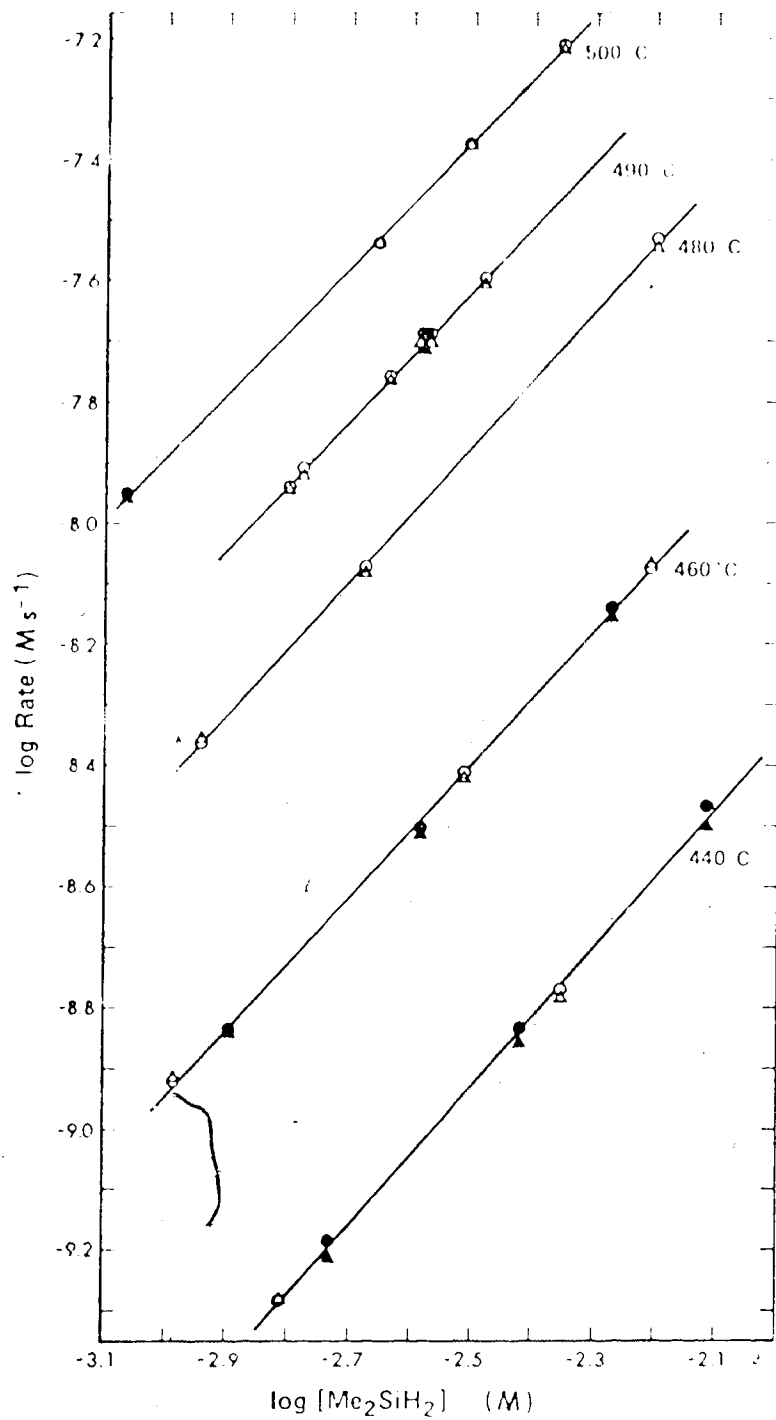


Figure IV-2. Order Plots for H_2 and TMDS Formation in the Pyrolysis of Me_2SiH_2 at Different Temperatures.
 ○ - H_2 , △ -TMDS in the Absence of Ethylene;
 ● - H_2 , ▲ -TMDS in the Presence of Ethylene.

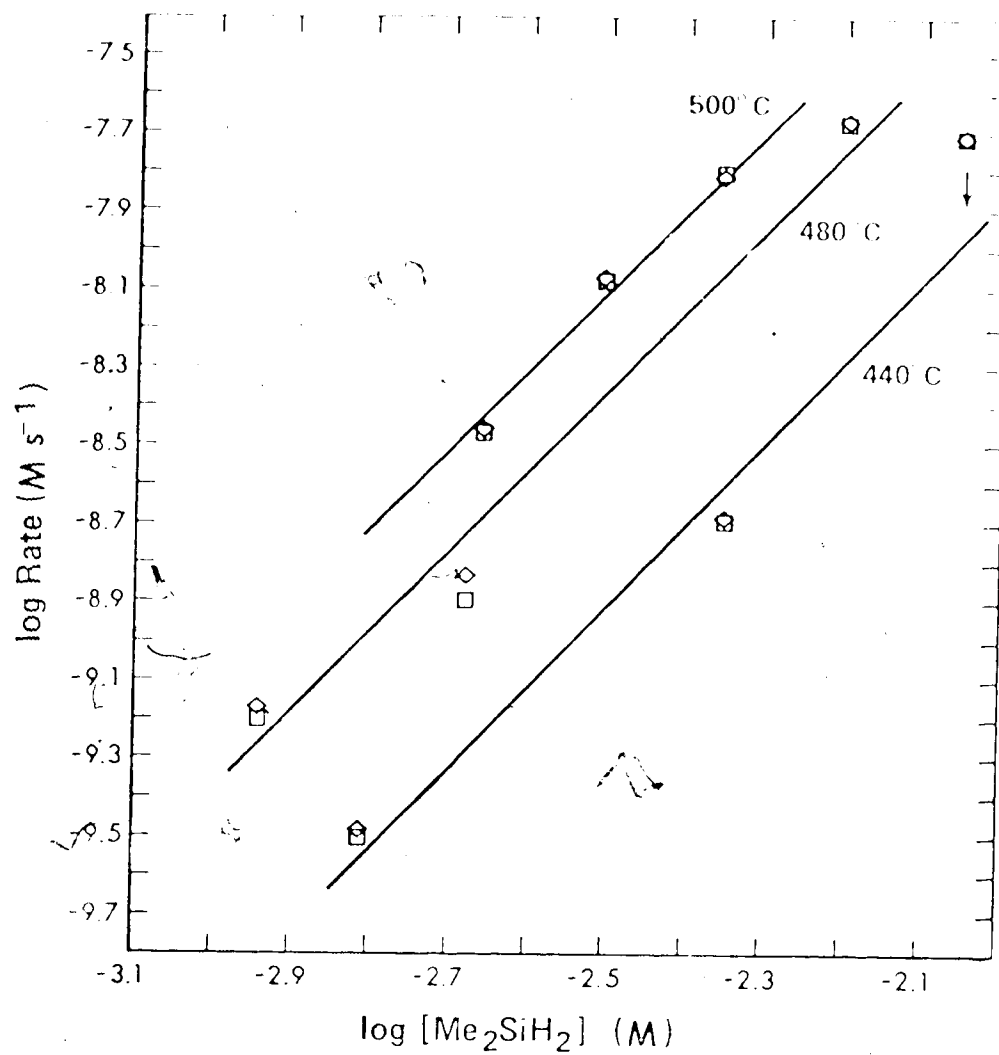


Figure IV-3. Order Plots for TMS and MMS Formation in the Pyrolysis of Me_2SiH_2 in the Absence of Ethylene at 440, 480 and 500°C.

◇ - TMS, □ - MMS.

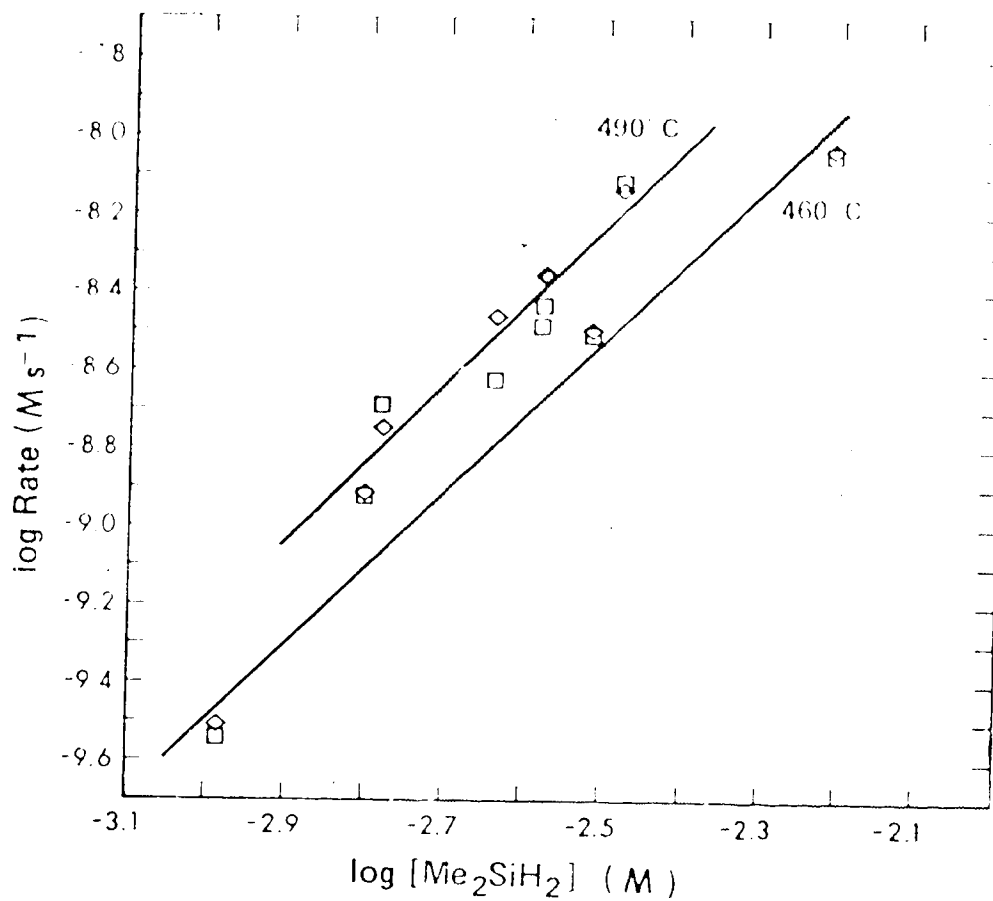


Figure IV-4. Order Plots for TMS and MMS Formation in the Pyrolysis of Me_2SiH_2 in the Absence of Ethylene at 460 and 490°C.

◇ - TMS, □ - MMS.

TABLE IV-5
 Reaction Orders for Product Formation in the Pyrolysis of
 Dimethylsilane at Different Temperatures

Temperature, °C	Order ^a		
	H ₂ ^b	TMDS ^b	TMS ^c
500.0	1.04±0.01 (4)	1.05±0.01 (4)	2.15±0.25 (3)
490.0	1.08±0.02 (7)	1.05±0.01 (7)	2.27±0.16 (6)
480.0	1.12±0.01 (3)	1.10±0.02 (3)	2.07±0.31 (3)
460.0	1.11±0.01 (6)	1.10±0.02 (6)	1.94±0.16 (3)
440.0	1.16±0.02 (5)	1.13±0.02 (5)	1.73 (2)

^a The number of experimental points is given in parentheses.

^b Based on experimental data (in Table IV-3 to IV-5) both in the presence and absence of ethylene.

^c Using the experiments in the absence of ethylene only.

two silanes which differed by one methyl group from the substrate molecules, i.e. Me_3SiH and Me_2SiH_2 from Me_3SiH_3 and Me_2SiH_2 and SiH_4 from MeSiH_3 . Methane was a negligible reaction product in both cases, which indicated that the splitting of the Si-C bond was not an important primary step.

In the pyrolyses of MMS and DMS, the reaction rates, particularly those of the minor products, were affected by the nature of the surface, especially by the extent of polymer deposition. Finally, in both cases, the minor products were strongly affected by the addition of ethylene and this suggests that silyl radicals are present in the DMS system as well, and participate in the formation of the minor products. It would appear therefore that the thermal decompositions of MMS and DMS proceed by similar reaction mechanisms.

Some important differences in the pyrolysis of DMS however, should be noted:

(i) Different Thermal Stability

At 440°C , the rate of decomposition was slower by more than two orders of magnitude than in the pyrolysis of MMS. Thus, assuming that the reaction mechanism is similar to that of MMS, one or more of the rate determining steps in the pyrolysis of DMS must have either

a higher activation energy or lower A factor (or both) than the corresponding reactions in the pyrolysis of MMS.

(ii) Effect of Added Ethylene

Whereas C_2H_4 affected the rates of formation of all the products formed in the pyrolysis of MMS (cf. Figure III-9 and Table III-15), it does not seem to have any significant effect on the rates of H_2 and TMS formation in the pyrolysis of DMS (cf. Figure IV-2).

Assuming that the reaction mechanisms for the pyrolyses of DMS and MMS are formally similar, these results seem to indicate that:

- (a) in the pyrolysis of DMS the contribution of the radical process to the yields of the major products is less important than it was in the case of MMS, i.e., the length of the radical chain by which these products might be formed must be much shorter.
- (b) at the highest ethylene concentrations used, 9%, some TMS and MMS are still formed whereas in the case of MMS, under the same conditions, the minor product DMS is completely suppressed. Assuming that TMS and MMS are also formed by silyl radical precursors, ethylene must scavenge dimethylsilyl radicals much less efficiently than methylsilyl radicals. In fact, the rate of addition

of α -ethyl radicals to ethylene has been reported to decrease with increasing methylation of the radical center.¹² The higher reaction temperatures used in the MM_2 pyrolysis may have also decreased the concentration of ethylene.

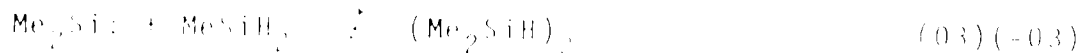
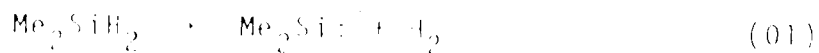
(iii) The Reaction Orders

The reaction orders for the radical yields in the pyrolysis of MM_2 were between 1.5 and 1.9 and it was concluded that both linear and quadratic termination of the chain was occurring. In the case of IM_2 , however, the orders for the apparent radical products, IMS and MMS , are ~ 2.0 indicating that only a linear chain termination may be operative.

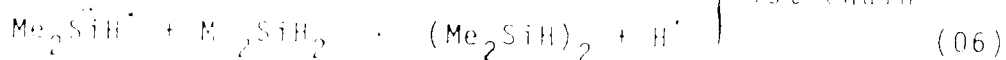
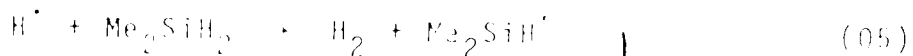
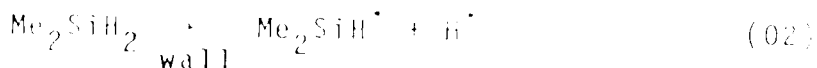
Since the orders of H_2 and IMS in the pyrolysis of IMS were slightly higher than unity (see Table IV-6), some contribution from the radical process to the yields of these major products has to be considered, in spite of the fact that there was no apparent suppression of the yields in the presence of ethylene. The following reaction scheme can now be suggested for the pyrolysis of IMS .

2. Reaction Scheme for the Pyrolysis of Dimethylsilane

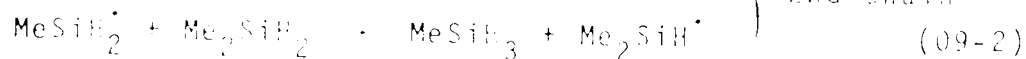
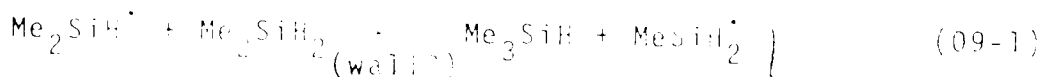
Molecular:



Radical:



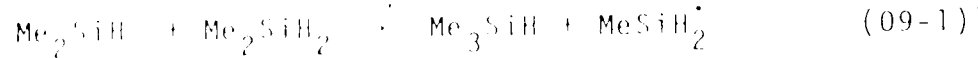
} 1st chain



} 2nd chain

This reaction scheme is formally similar to that of MMS, except that only linear heterogeneous termination of the chain and two types of propagation chains are assumed to take place. The first is propagated by reactions (05) and (06) and leads to the formation of H_2 and TMS, and the second chain, propagated by (09-1) and (09-2) is responsible for the formation of the minor products, TMS and MS. Although there is some evidence

that the metathetical reaction step,



is heterogeneous, further studies would be required to define the nature of this reaction.

3. Determination of the Rate Constants for the Molecular and Radical Processes in the Pyrolysis of DMS

Steady-state treatment of the reaction sequence (01)-(09) yields the following rate expressions:

$$R(\text{H}_2) = (k_{01} + k_{02})[\text{DMS}] + k_{06} \frac{2k_{02}}{k_{08}} [\text{DMS}]^2 \quad (10)$$

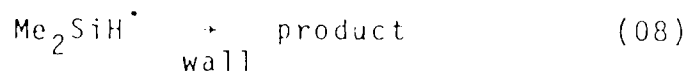
$$R(\text{TMDS}) = k_{01}[\text{DMS}] + k_{06} \frac{2k_{02}}{k_{08}} [\text{DMS}]^2 - R(\text{Polymer}) \quad (11)$$

$$R(\text{TMS}) = k_{09-1} \frac{2k_{02}}{k_{08}} [\text{DMS}]^2 \quad (12)$$

$$R(\text{MMS}) = k_{09-1} \frac{2k_{02}}{k_{08}} [\text{DMS}]^2 \quad (13)$$

Normally, these rate expressions resemble those for H_2 and DMDS in the pyrolysis of MMS for the case of linear termination of the chain. The rate expression for eq. (11), is similar to that for H_2 ; eq. (10), but contains one additional term, $R(\text{Polymer})$. However, since the rates of formation of H_2 and of TMDS were essentially the same (cf. Tables IV-3 to IV-5 and Figure IV-2), the

formation of polymer in the pyrolysis of DMS at low conversions must be very minor and this term can therefore be neglected. The coefficient of the first order term in eq. (11) contains only the rate constant k_{01} . This is a consequence of the fact that the chain termination step, reaction (08)



was assumed not to produce any significant TMDS.

The reaction orders for H_2 and TMDS formation were very close to unity (cf. Table IV-6), and thus the relative contribution of the first order terms in rate expressions (10) and (11) must be considerably more important than that of the second order terms.

The reaction scheme predicts that the rates of TMS and MMS formation should be the same, and be second order with respect to the substrate. Experimentally, the reaction orders for both products were ≈ 2.0 but the yields of MMS were always somewhat lower than those of TMS. However, thermal decomposition of MMS is certain to take place at the temperatures used in this study and this could explain the smaller yields. Hence the data on TMS will be used for the following kinetic treatments.

Since $R(\text{polymer})$ in eq. (11) can be neglected, equations (10)-(12) can be rearranged to give:

$$\frac{R(H_2)}{[DMS]} = (k_{01} + k_{02}) + k_{06} \frac{2k_{02}}{k_{08}} [DMS] \quad (14)$$

$$\frac{R(TMDS)}{[DMS]} = k_{01} + k_{06} \frac{2k_{02}}{k_{08}} [DMS] \quad (15)$$

$$\frac{R(TMS)}{[DMS]} = k_{09} + k_{08} \frac{2k_{02}}{k_{08}} [DMS] \quad (16)$$

The kinetic plots of equations (14) and (15), using the rate data for H_2 and TMDS both in the presence and absence of ethylene given in Tables IV-3 to IV-5 (excluding those denoted by asterisks) are shown in Figure IV-5.

The plots are linear and the first and second order coefficients at different temperatures, determined from the intercepts and slopes, respectively, are listed in Tables IV-7 and IV-8. From Table IV-7, $k_{01} + k_{02} \approx k_{01}$ and therefore the radical contribution to the H_2 and TMDS yields must be very small. k_{02} will henceforth be neglected in the first order coefficient term.

There is an alternative and probably more accurate method for evaluating these rate constant ratios.

It will be recalled (cf. Section III.B.4.iv) that in the pyrolysis of MMS, there is a good correlation between the rates of formation of the products formed in the radical process, i.e. DMS , $H_{2, Rad}$ and $DMDS_{Rad}$ and that this correlation is actually predicted by the reaction mechanism. A similar correlation between the minor

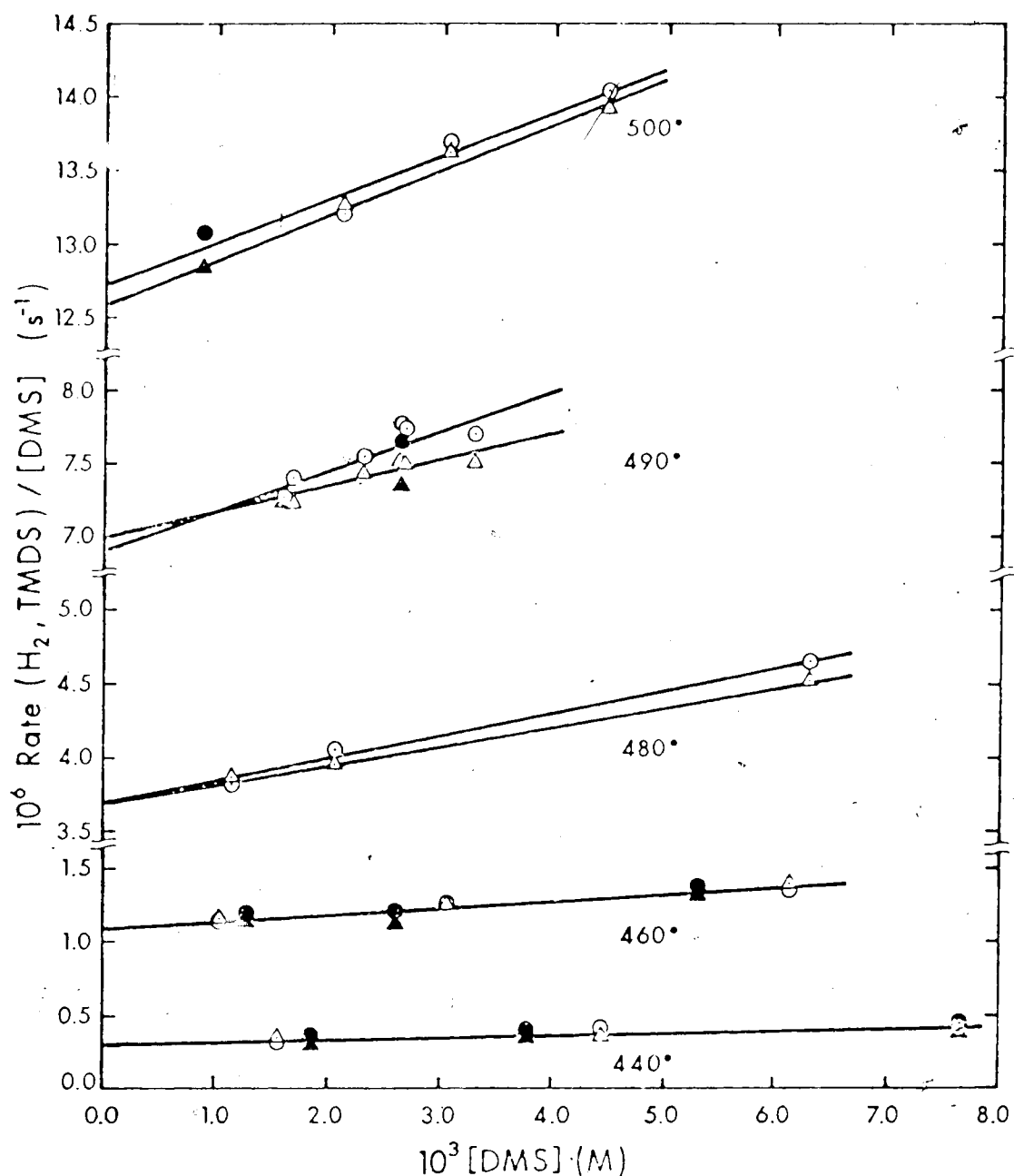


Figure IV-5. Plots of Equations (14) and (15) at Different Temperatures.

○, ● -Rate (H₂)/[DMS] versus [DMS];

△, ▲ -Rate (TMDS)/[DMS] versus [DMS].

The Closed Symbols (●, ▲) Refer to Experiments in the Presence of Ethylene.

TABLE IV-7
 First Order Rate Constants ^a for H₂ and TMDS Formation
 in the Pyrolysis of DMS

Temp., °C	First Order Rate Coefficients, s ⁻¹			
	(k ₀₁ +k ₀₂) H ₂ ^b	(k ₀₁) TMDS ^c	(k ₀₁) H ₂ ^d	(k ₀₁) TMDS ^e
500	1.3x10 ⁻⁵	1.3x10 ⁻⁵	1.3x10 ⁻⁵	1.3x10 ⁻⁵
490	7.0x10 ⁻⁶	7.0x10 ⁻⁶	7.2x10 ⁻⁶	7.0x10 ⁻⁶
480	3.7x10 ⁻⁶	3.7x10 ⁻⁶	3.8x10 ⁻⁶	3.8x10 ⁻⁶
460	1.1x10 ⁻⁶	1.1x10 ⁻⁶	1.1x10 ⁻⁶	1.1x10 ⁻⁶
440	3.1x10 ⁻⁷	3.1x10 ⁻⁷	3.1x10 ⁻⁷	3.1x10 ⁻⁷

^a Since few points were available, error limits are not quoted.

^b From equation (14), Figure IV-5.

^c From equation (15), Figure IV-5.

^d From equation (17), Figure IV-6.

^e From equation (18), Figure IV-6.

TABLE IV-8
 Rate Constant Ratios $k_{06}^{2k_{02}}/k_{08}$, for H_2 and TMDS
 Formation by the Radical Process in the Pyrolysis
 of DMS at Different Temperatures ^a

Temperature, °C	$k_{06} \frac{2k_{02}}{k_{08}}, M^{-1}s^{-1}$	
	H_2 ^b	TMDS ^c
500.0	2.9×10^{-4}	3.1×10^{-4}
490.0	2.7×10^{-4}	1.6×10^{-4}
480.0	1.6×10^{-4}	1.8×10^{-4}
460.0	4.7×10^{-5}	4.5×10^{-5}
440.0	1.8×10^{-5}	1.3×10^{-5}

^a Error limits are not quoted since few points were available.

^b Slope of the plot of eq (14).

^c Slope of the plot of eq (15).

products TMS and MMS and $H_{2, \text{Rad}}$ and TMDS_{Rad} are also predicted by the proposed mechanism for the pyrolysis of DMS. Thus substitution of eq. (16) into (14) and (15) yields

$$\frac{R(H_2)}{[DMS]} = k_{01} + \frac{k_{06}}{k_{09-1}} \frac{R(TMS)}{[DMS]} \quad (17)$$

$$\frac{R(TMDS)}{[DMS]} = k_{01} + \frac{k_{06}}{k_{09-1}} \frac{R(TMS)}{[DMS]} \quad (18)$$

The plots of equations (17) and (18), using the data in Tables IV-3 to IV-5 (in the absence of ethylene) are illustrated in Figure IV-6; significantly, even the abnormally high rate data denoted by an asterisk in Tables IV-3 and IV-5 could be included in these plots. The rate data derived from the slopes and intercepts are listed in Table IV-7 and IV-9, respectively. The results are in good agreement with those derived from the slopes and intercepts of equations (14) and (15) and thus support the proposed mechanism.

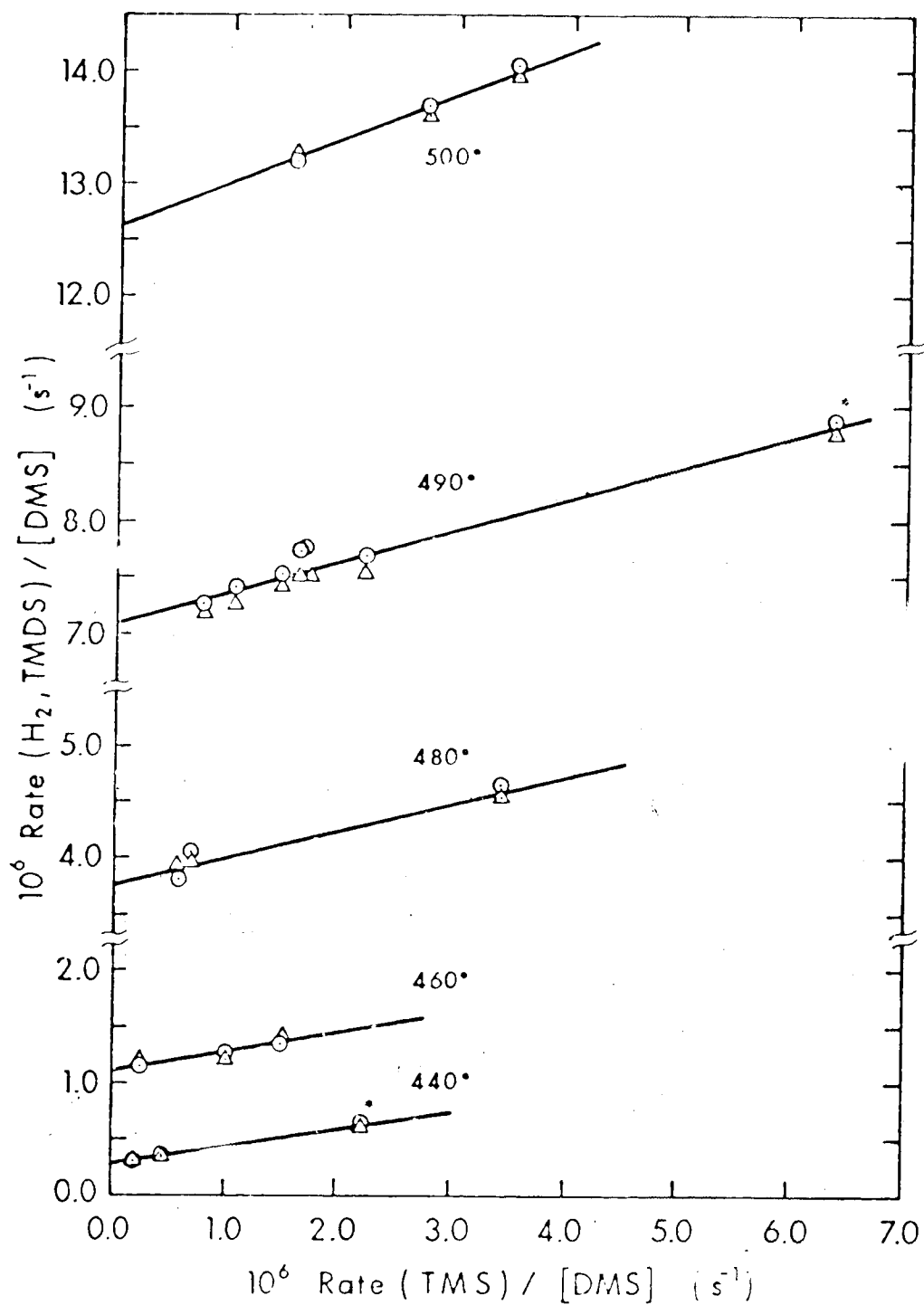


Figure IV-6. Plots of Equations (17) and (18) at Different Temperatures.
 ○ -Rate (H₂)/[DMS] versus Rate(TMS)/[DMS]
 △ -Rate (TMDS)/[DMS] versus Rate(TMS)/[DMS]
 * -Experiments in the "surface-active" cell (cf. Tables IV-4 and IV-5).

TABLE IV-9
 Rate Constant Ratios ^a k_{06}/k_{09-1} for H₂ and TMDS Formation
 by the Radical Process in the Pyrolysis of DMS
 at Different Temperatures

Temperature, °C	Rate Constant Ratio k_{06}/k_{09-1}	
	H ₂ ^b	TMDS ^c
500	0.42	0.34
490	0.27	0.27
480	0.26	0.22
460	0.17	0.18
440	0.16	0.14

^a Error limits are not quoted since few points were available.

^b Slope of the plot of eq. (17).

^c Slope of the plot of eq. (18).

4. Arrhenius Parameters for the Molecular and Radical Processes in the Pyrolysis of Dimethylsilane

(i) Molecular Process

The first order rate constant k_{01} has been derived from four kinetic plots using two slightly different methods of treating the experimental data. All four values, listed in Table IV-7, are in excellent agreement at all temperatures and are plotted in the Arrhenius form in Figure IV-7. From the intercept and slope,

$$\log k_{01} \text{ (s}^{-1}\text{)} = 14.3 - (68,000)/2.3 RT$$

with estimated errors of

$$\Delta \log k_{01} \text{ (s}^{-1}\text{)} = \pm 0.3 \pm (1,000)/2.3 RT$$

The activation energy and the A-factor for reaction (01) are higher and lower, respectively, than the corresponding values in the pyrolysis of MMS, 63.2 kcal/mol and $10^{15.0} \text{ s}^{-1}$, which is in agreement with the higher thermal stability of DMS (vide supra).

(ii) Radical Process

The rate constant ratios k_{06}/k_{09-1} and k_{06} ($2k_{02}/k_{08}$) obtained by different kinetic treatments are

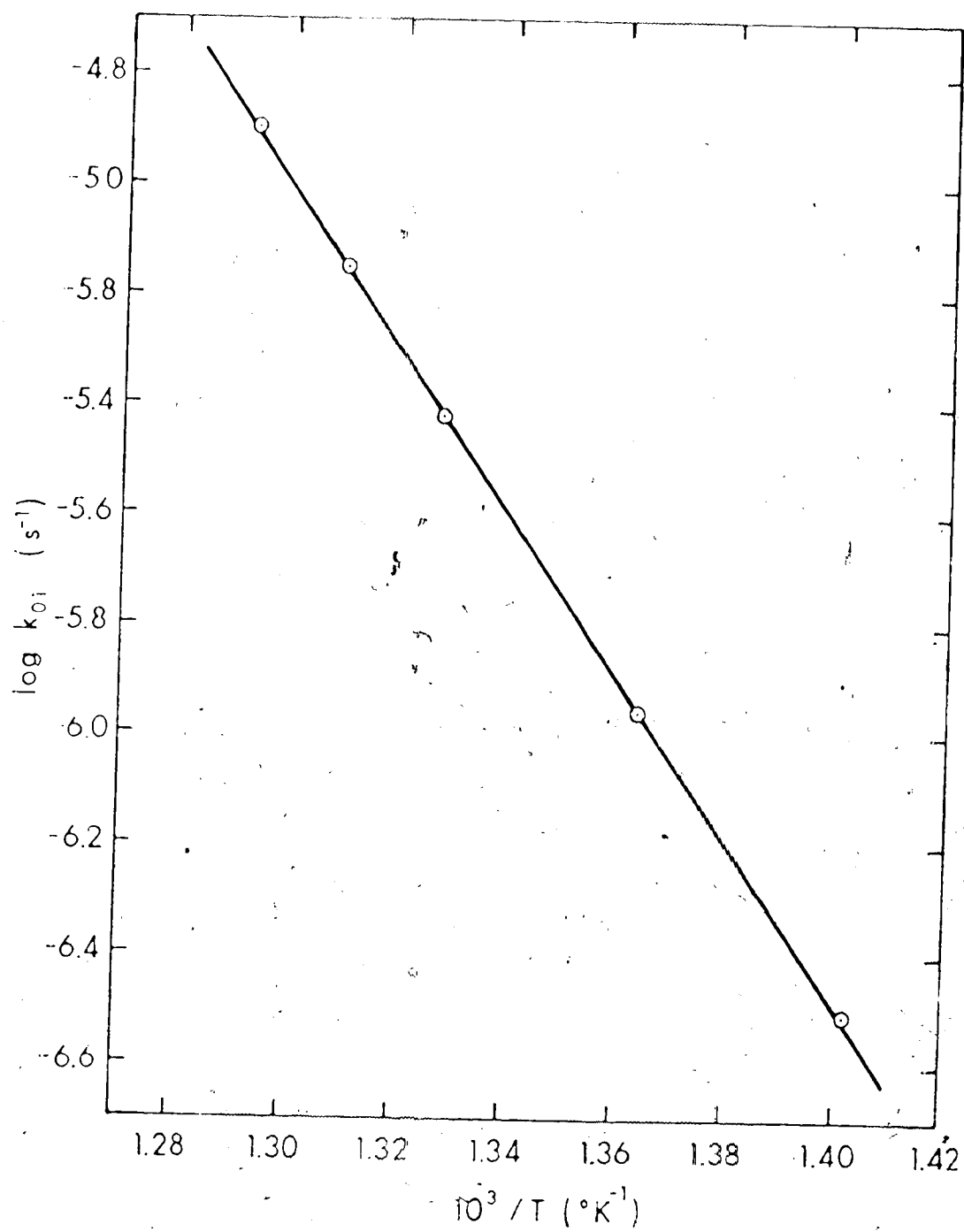
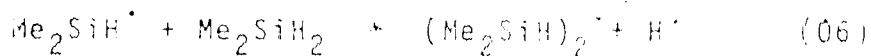


Figure IV-7. Arrhenius Plot for the First Order Rate Constant k_{01} .

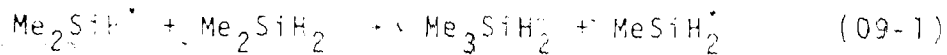
given in Tables IV-8 and IV-9, and the corresponding Arrhenius plots are shown in Figures IV-8 and IV-9. The plots are reasonably linear but there is considerable scatter which, however, is not surprising in view of the fact that the radical process is largely heterogeneous and relatively few experimental points could be used.

The apparent Arrhenius parameters for the radical process are given in Table IV-10.

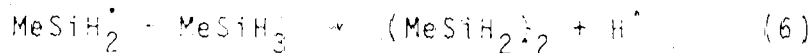
Thus $E_{06} - E_{09-1} = 16 \pm 2$ kcal/mol which indicates that the reaction



requires a considerably high activation energy in comparison with that of reaction (09-1)



It may be noted that E_a for the analogous reaction involving methylsilyl radicals



has been estimated to be 13-15 kcal/mol (cf. Section III.B.3.ii.b). If abstraction of a methyl group by

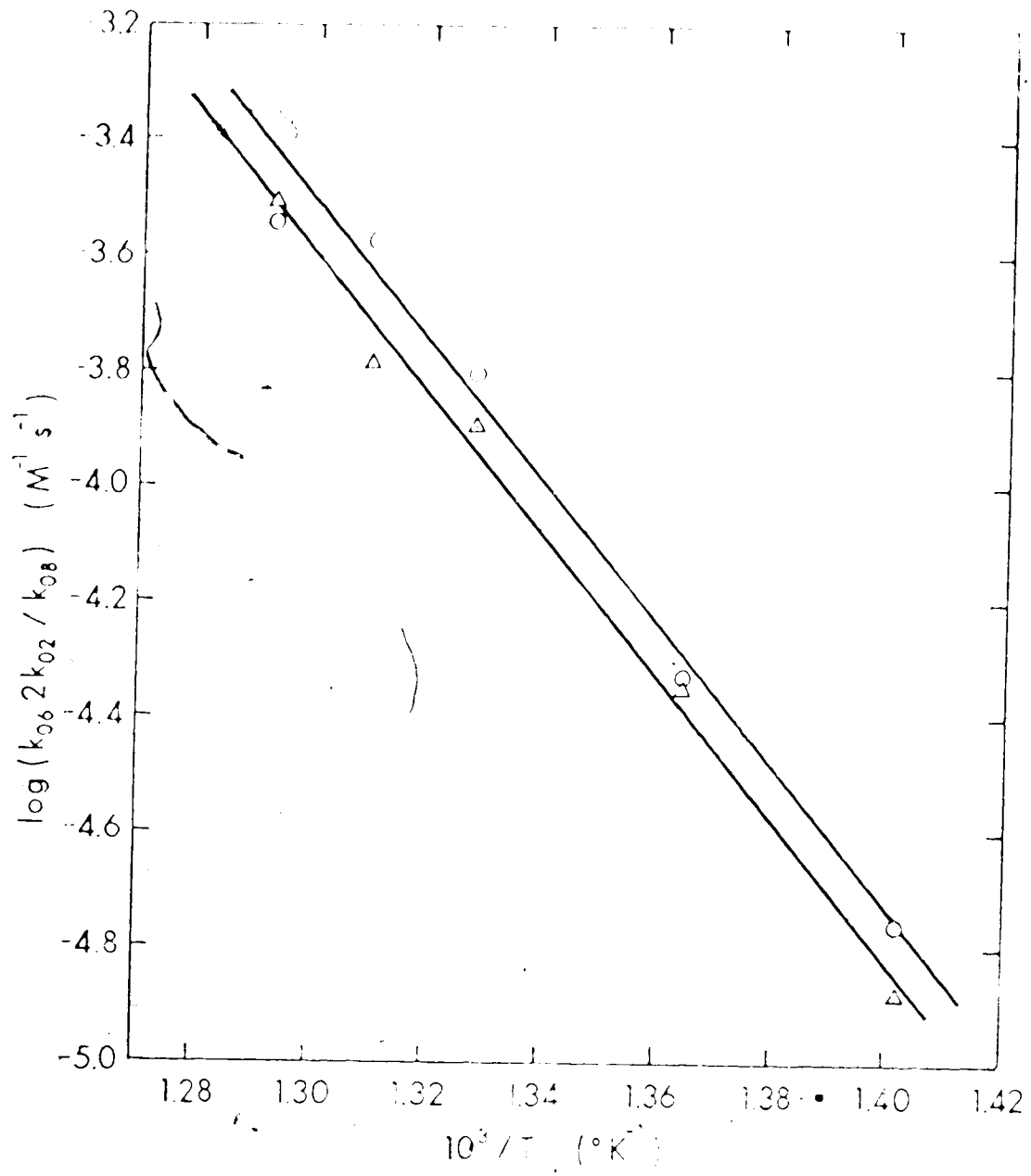


Figure IV-8. Arrhenius Plots for the Ratio Constant Ratio $k_{06}/2k_{02}/k_{08}$ based on H₂ (O), and TMDS, (Δ) Formations in the Analysis of DMS.

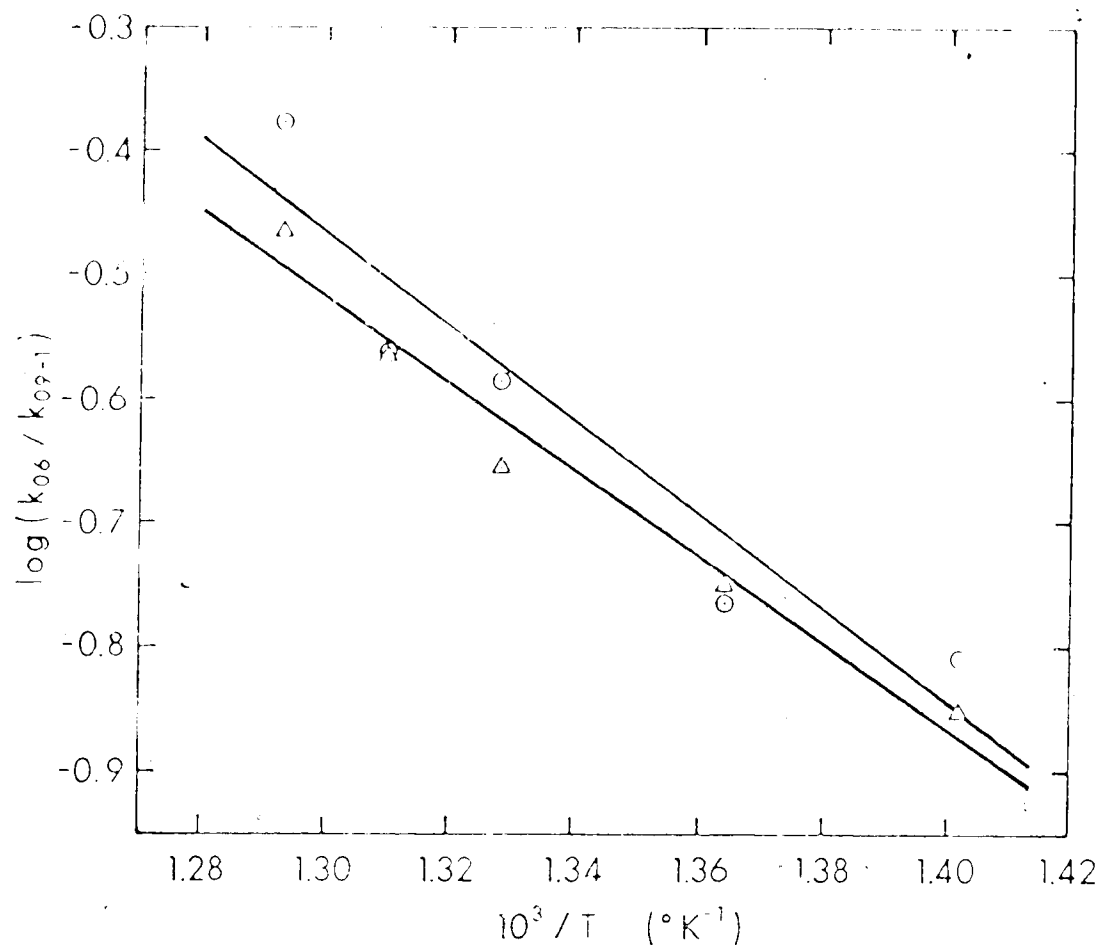


Figure IV-9. Arrhenius Plots for the Rate Constant Ratio k_{06}/k_{09-1} based on H_2 , (\odot), and TMS, (\triangle) Formation in the Pyrolysis of DMS.

TABLE IV-10
Arrhenius Parameters for the Rate Constant
Ratios of the Radical Process in the
Pyrolysis of DMS

Rate Constant Ratio	log A	E_a , kcal/mol
$(k_{06}/k_{09-1})_{H_2}$ ^a	4.4±1.1	17.0±3.5
$(k_{06}/k_{09-1})_{TMDS}$ ^b	3.9±0.5	15.6±1.7
$(k_{06}(2k_{02}/k_{08}))_{H_2}$ ^c	12.0±1.2 ^e	54.6±4.2
$(k_{06}(2k_{02}/k_{08}))_{TMDS}$ ^d	12.4±0.8 ^e	56.2±2.8

- ^a Slope of the plot of eq. (17).
^b Slope of the plot of eq. (18).
^c Slope of the plot of eq. (14).
^d Slope of the plot of eq. (15).
^e A is in units of $M^{-1}s^{-1}$.

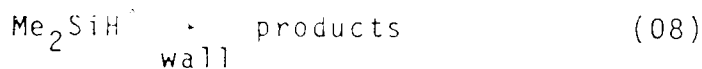
a dimethylsilyl radical is heterogeneous then E_{09} might indeed be very small. In any case E_{06} will be at least 16-20 kcal/mol, and could in fact be much higher.

Since E_{06} is relatively high and since reaction (06) is a chain propagating step, it follows that the chain length must be shorter than that in the case of MMS and consequently $R(H_2)_{Rad}$ and $R(TMDS)_{Rad}$ will not contribute very much to the overall rates. This may explain, at least partly, why ethylene has no observable effect on the H_2 and TMDS yields.

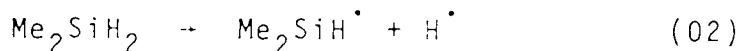
From the data in Table IV-10,

$$E_{06} + E_{02} - E_{08} \approx 55 \text{ kcal/mol}$$

Since $E_{06} \geq 16$ kcal/mol and the activation energy E_{08} for the heterogeneous chain termination reaction



is probably very small and can be neglected in comparison with E_{02} and E_{06} , the activation energy E_{02} for the chain initiation step



can be estimated to be

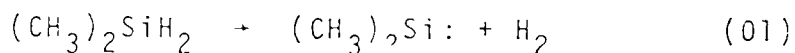
$$E_{02} \leq 39 \text{ kcal/mol}$$

Since the first bond dissociation energy in dimethylsilane, $D(\text{Me}_2\text{SiH-H})$, is very close or equal to that of $D(\text{MeSiH}_2\text{-H}) = 90 \text{ kcal/mol}$ (cf. Section III.B.5.i) it must be concluded that the primary reaction step (02) is heterogeneous, just as in the pyrolysis of MMS.

It is significant that the data from experiments performed in a highly surface active vessel could be incorporated in the linear plots of eqs (17) and (18), Figure IV-6. It would appear therefore that wall effects are compensated for in this particular kinetic treatment. Further, more detailed experiments should be very instructive in the elucidation of the nature of these radical processes

5. Some thermochemical Implications of the Arrhenius Parameters for the Molecular Process

It has been shown that $k_{01} \gg k_{02}$ and therefore the Arrhenius coefficients $E_a = 68.0 \text{ kcal/mol}$ and $\log A(\text{s}^{-1}) = 14.3$, refer to the primary molecular step,



(i) Activation Energy

Assuming that the activation energy for the reverse reaction (-01) is approximately 8 kcal/mol (i.e. the same as that estimated for the analogous reaction $\text{CH}_3\text{SiH}_3 + \text{H}_2$, see Section III.B.5.i), the enthalpy change for reaction (01), ΔH_{01}^0 , will be:

$$\Delta H_{01}^0 = E_{01} - E_{-01} = 68 - 8 = 60 \text{ kcal/mol}$$

Since

$$\Delta H_{01}^0 = \Delta H_f^0(\text{Me}_2\text{Si:}) - \Delta H_f^0(\text{Me}_2\text{SiH}_2) + \Delta H_f^0(\text{H}_2)$$

and $\Delta H_f^0(\text{Me}_2\text{SiH}_2)$ is approximately -16 ± 1 kcal/mol^{13,14},

$$\Delta H_f^0(\text{Me}_2\text{Si:}) = 44 \text{ kcal/mol} ;$$

this value is considerably higher than earlier estimates, e.g. 33¹⁷, 29¹¹², and 16 kcal/mol²⁷. Even though the estimated activation energy E_{-01} used in the calculation of the reaction enthalpy ΔH_{01}^0 may be somewhat higher than 8 kcal/mol, it is unlikely to be as high as 36 kcal/mol, implied in the low value of 16 kcal/mol for $\Delta H_f^0(\text{Me}_2\text{Si:})$.

ΔH_{01}^0 is related to the bond dissociation energies by

$$\Delta H_{01}^0 = D(\text{Me}_2\text{SiH-H}) + D(\text{Me}_2\text{Si-H}) - D(\text{H-H})$$

and since $D(\text{H-H}) = 104 \text{ kcal/mol}$ ¹⁰⁸ and $D(\text{Me}_2\text{SiH-H}) = 90 \text{ kcal/mol}$, the second bond dissociation energy $D(\text{Me}_2\text{Si-H})$ is $D(\text{Me}_2\text{Si-H}) = 104 + 60 - 90 = 74 \text{ kcal/mol}$. This is lower by approximately 16 kcal/mol than the first BDE, and is about 5 kcal/mol higher than the corresponding second BDE in MMS ($D(\text{MeSiH-H}) \sim 69 \text{ kcal/mol}$, cf. Section III.B.5.i).

Since the first BDEs in MMS and DMS are identical, it would therefore appear that the differences in the activation energies of the molecular processes occurring in the pyrolyses of DMS and MMS, 68 and 63 kcal/mol, respectively, reflect the differences in the second (Si-H) BDEs.

It should be noted, however, that the activation energies for insertion of $\text{Me}_2\text{Si:}$ and MeSiH: into H_2 were assumed to be the same and this might not be the case. Thus if it is assumed, for example, that $E_{-01} \sim 13 \text{ kcal/mol}$, which is quite plausible, then the second BDEs (Si-H) in both compounds become identical and the observed differences in the activation energies E_{01} and E_1 would simply reflect the differences in E_{-01} and E_{-1} .

(ii) The Preexponential Factor

The A factor for reaction (01), $A_{01} = 10^{14.3} \text{ s}^{-1}$, can be used to calculate the entropy of activation, ΔS_{01}^\ddagger from the relation

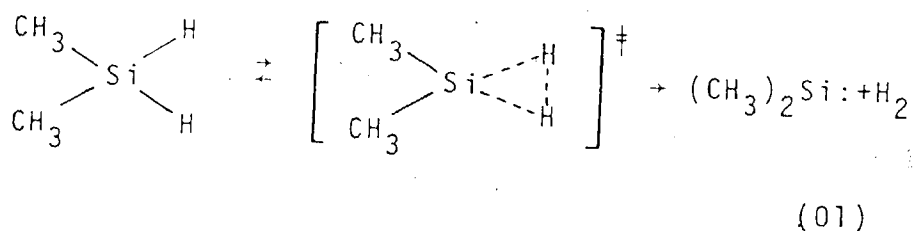
$$A_{01} \approx \left(\frac{ekT}{h}\right) e^{\Delta S_{01}^\ddagger / R} \quad (19)$$

Thus, at the mean reaction temperature, 460°C ,

$$\Delta S_{01}^\ddagger = 3.15 \text{ e.u.}$$

indicating a somewhat more rigid transition state than in the case of MMS.

By analogy with the primary molecular reaction (1) in the pyrolysis of MMS, reaction (01) is assumed to proceed via a three-centered cyclic transition state,



and the activation entropy ΔS_{01}^\ddagger can be calculated in the same manner as before for MMS (cf. Section III.B.5.ii).

Again, since $\Delta S_{\text{tran}}^\ddagger$ and $\Delta S_{\text{elec}}^\ddagger$ are zero and $\Delta S_{\text{rot}}^\ddagger = 0$ (no change in symmetry numbers), the only significant contribution to ΔS_{01}^\ddagger is expected to arise from $\Delta S_{\text{vib}}^\ddagger$, in particular from the changed stretching and bending frequencies of the Si-H bonds.

The calculation of $\Delta S_{\text{vibs}}^\ddagger$ is shown in Table IV-11; the Si-H bond frequencies in DMS were taken from the literature¹¹³. The new frequencies for the transition state were estimated as

$$\omega_{\text{Si-H},\ddagger} \approx 2/3 \omega_{\text{Si-H,DMS}}$$

and the corresponding absolute vibrational entropies, S_{DMS}^0 , S_{\ddagger}^0 , were calculated from Benson's tabulated data¹¹¹.

From Table IV-11 is seen that the calculated activation entropy,

$$\Delta S_{01,\text{calc}}^\ddagger \approx \Delta S_{\text{vib}}^\ddagger = 3.1 \text{ e.u.}$$

is in excellent agreement with the experimental value of 3.15 e.u.

TABLE IV-11
 Estimated Contribution of the Si-H Vibrational Modes in Me_2SiH_2 to the
 Entropy of Activation at 730°K

Mode Description	Frequency, cm^{-1}		Vib. Entropy ^c , e.u.		$\Delta S_{\text{vib}}^\ddagger$ e.u.
	DMS ^a	(DMS) [†] b	S_{DMS}^0	$S_{\text{†}}^0$	
SiH_2 sym.str.	2150	→ R.C. d	0.2	→ 0	-0.2
SiH_2 bend	950	→ 630	1.0	→ 1.7	+0.7
SiH_2 twist	600	→ 400	1.8	→ 2.6	+0.8
SiH_2 wag	900	→ 600	1.1	→ 1.8	+0.7
SiH_2 antisym.str.	2150	→ 1430	0.2	→ 0.5	+0.3
SiH_2 rock	470	→ 313	2.2	→ 3.0	+0.8
			Total	→ 3.1	

^a Taken from reference 113.

^b Estimated, $\omega_{\text{†}} \approx \frac{2}{3}\omega_{\text{DMS}}$.

^c Estimated from the tabulated data of Benson¹¹¹.

^d Reaction coordinate.

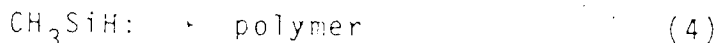
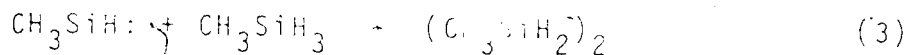
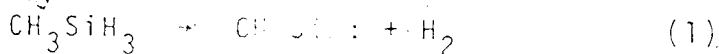
It seems therefore very likely that the transition state leading to elimination of molecular hydrogen in the pyrolysis of DMS and MMS is a three-centered cyclic complex. This may also apply to the unimolecular decomposition of other silicon hydrides.

CHAPTER V

SUMMARY AND CONCLUSIONS

Between 340 and 440°C monomethylsilane pyrolyzes to form hydrogen and dimethyldisilane as major products and dimethylsilane and polymer as minor products. The orders of formation of H₂ and DMDS vary between 1.1 at 441°C and 1.6 at 340°C. The rate of decomposition is strongly affected by the nature of the surface but relatively little by the surface to volume ratio of the reaction vessel.

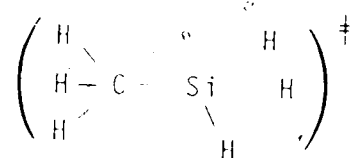
In the presence of 10% added ethylene the formation of hydrogen and dimethyldisilane is strongly suppressed and that of dimethylsilane is completely inhibited. The orders of formation of H₂ and DMDS were both 1.0 at all temperatures. It is proposed that the H₂ and DMDS yields formed under these conditions arise solely from a molecular process:



The kinetic data for H₂ and DMDS yielded identical Arrhenius parameters, within experimental error:

$$\log k_1^{\text{molec}} (\text{s}^{-1}) = (14.95 \pm 0.11) - (63200 \pm 330) / (2.3RT)$$

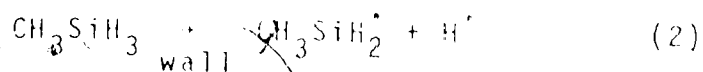
The second bond dissociation energy in monomethylsilane is calculated to be 69 kcal/mol and $\Delta H_f^0(\text{CH}_3\text{SiH}_2) = 53$ kcal/mol. The entropy of activation is $\Delta S_1^\ddagger = 6.3$ e.u.. Assuming a three-centered activated complex,



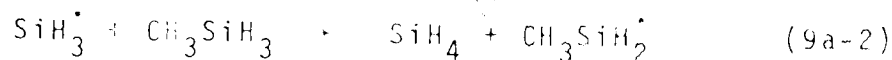
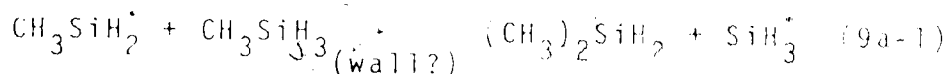
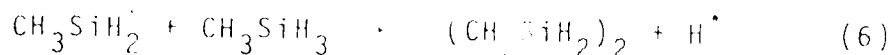
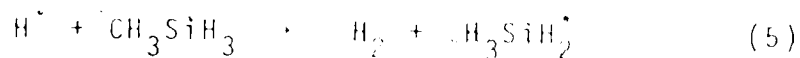
the individual contributions to ΔS_1^\ddagger were estimated using established procedures and the close agreement between the calculated value, 6.1 e.u., and the experimental one supports the suggested structure.

The molecular product yields calculated from k_1^{molec} were then subtracted from the total yields (in the absence of ethylene) to obtain the following reaction orders for the products formed in the radical process at 415°C: 1.6 (H_2); 1.5 (DMDS) and 1.5 (DMS). These values are indicative of a radical chain mechanism which is proposed to consist of

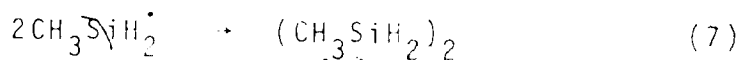
initiation



propagation



termination



The reaction sequence (1)-(9) cannot be solved since two types of chain termination steps are possible. Kinetic treatments performed for the two extreme cases of quadratic termination, i.e. reaction (7) and linear termination (8) led to the following relations for $R(\text{H}_2)$:

$$\frac{R(\text{H}_2)_{\text{quad}}}{[\text{MMS}]^{1/2}} = (k_1 + k_2)^{\text{quad}} + \left\{ k_6 \left(\frac{k_2}{k_7} \right)^2 \right\}^{\text{quad}} [\text{MMS}]^{1/2} \quad (I)$$

$$\frac{R(\text{H}_2)_{\text{Total}}}{[\text{MMS}]} = (k_1 + k_2)^{\text{lin}} + \left\{ k_6 \cdot \frac{2k_2}{k_8} \right\}^{\text{lin}} [\text{MMS}] \quad (II)$$

The experimental data obey the predicted linearity of these plots, from which it is concluded that $(k_1 + k_2)^{\text{lin}} \gg (k_1 + k_2)^{\text{quad}} \gg k_1^{\text{molec}}$. Thus $k_1 \gg k_2$ and the second

terms in eqs (I) and (II) correspond solely to H_2 formation by the radical process.

From the Arrhenius parameters of the second term coefficients for the radical process obtained from the slopes of the plots of eqs (I) and (II) the following rate parameters can be estimated for the initiation reaction (2) for the two cases of quadratic and linear termination:

$$\log k_2^{\text{quad}} (s^{-1}) \approx 8 - (57,000)/(2.3RT)$$

$$\log k_2^{\text{lin}} (s^{-1}) \approx (2.8) - (28,000)/(2.3RT)$$

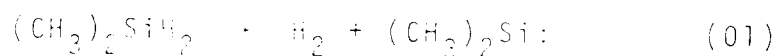
Since the activation energy for each of these cases is much less than $D(\text{CH}_3\text{SiH}_2\text{-H})$ and the preexponential factors are several orders of magnitude less than the value $10^{15 \pm 1} s^{-1}$ normally associated with a unimolecular homogeneous decomposition, it is concluded that the radical initiation step (2) is heterogeneous.

The chain length of the radical process is estimated to be $\sim 10^6$ and the chain termination step (8) is probably heterogeneous. Most of the products arising from radical precursors are formed in the chain propagation reactions.

The results obtained from the pyrolysis of dimethylsilane are not as extensive but still allow meaningful conclusions. Dimethylsilane pyrolyses between

440 and 600 °C to yield hydrogen and 1,1,2,2-tetramethyldi-silane (TMS) as major products and trimethylsilane (TMS), monomethylsilane (MMS) and polymer as minor products.

As in the case of monomethylsilane the rate of decomposition depends on the nature of the surface, but to a lesser degree. The orders of formation are 1.1 (H₂), 1.1 (TMS), 2.0 (TMS) and 2.0 (TMS). Ethylene has no apparent effect on the H₂ and TMS yields but those of the minor products TMS and MMS are strongly suppressed. A mechanism formally similar to that in the pyrolysis of monomethylsilane is proposed, consisting of two parallel molecular and radical processes. From the data on H₂ and TMS the following rate parameters were measured for the molecular primary step:



$$\log k_1 (\text{s}^{-1}) = 14.3 - (68,000)/(2.3RT)$$

The second bond dissociation energy in dimethylsilane, 74 kcal/mol, is again considerably lower than the first and the calculated entropy of activation, 3.1 e.u., is in agreement with the experimentally observed value 3.2 e.u. when a three-centered transition state is assumed. $\Delta H_f^0((\text{CH}_3)_2\text{Si}\cdot)$ is estimated to be 44 kcal/mol. The radical component of the overall rate was estimated in a manner similar to the

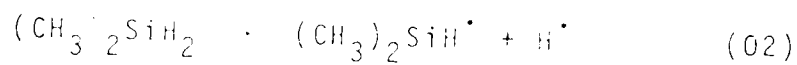
case of monomethylsilane. Since only linear termination of the chain is assumed to take place, kinetic treatment is simplified and leads to the relations

$$\frac{R(H_2)}{[DMS]} = (k_{01} + k_{02}) + k_{06} \frac{2k_{02}}{k_{08}} [DMS] \quad (III)$$

$$\frac{R(TMDS)}{[DMS]} = k_{01} + k_{06} \frac{2k_{02}}{k_{08}} [DMS] \quad (IV)$$

$$\frac{R(TMS)}{[DMS]} = \frac{R(MMS)}{[DMS]} = k_{09-1} \frac{2k_{02}}{k_{08}} [DMS] \quad (V)$$

where k_{02} refers to the radical initiation step



and the higher order rate constant terms refer to the chain propagation and termination steps. From the temperature dependence of these ratios it is concluded that $E_{02} = 39$ kcal/mol and therefore reaction (02) is heterogeneous. Similarly to the case of monomethylsilane,

$$k_{01} \gg k_{02}$$

The radical chain length is several orders of magnitude less than that in the pyrolysis of monomethylsilane because one of the chain propagating steps features a relatively high activation energy.


These results are in excellent agreement with other prediction that molecular decomposition of

silicon compounds becomes increasingly important as the energy available decreases. The use of ethylene as a silyl radical scavenger in thermal systems has demonstrated how the radical and molecular processes can be elucidated and how the notorious surface effects can be minimized. Caution must be exercised however since the yields of the major products from the pyrolysis of dimethylsilane were not suppressed by ethylene. Either ethylene cannot scavenge dimethylsilyl radicals, or, because of the shorter chain length, the radical yields of H_2 and TMS are very small. Further work is obviously necessary.

By analogy, it is highly probable therefore that monosilane, SiH_4 , also decomposes by two independent molecular and radical processes and the present controversy in fact revolves around their relative importance. If the radical chain length is long, then the results often quoted (cf. Section I.A.6.ii) in support of radical initiation may be misleading since they tend to point to a highly overestimated importance for this reaction. The use of ethylene as a radical scavenger in this system should unambiguously resolve this problem.

Finally, it has been shown that heterogeneous reactions play a very important role in the pyrolysis of monomethyl- and dimethylsilane. In both cases the initial


Si-H cleavage is definitely heterogeneous and there is strong evidence that one or more of the chain terminating steps are heterogeneous as well. These reactions are responsible for the formation of the minor products which, in future work, might be suitable as monitors for heterogeneous processes.



BIBLIOGRAPHY

1. (a) L. Glasgow, C. Olbrich and P. Potzinger, Chem. Phys. Lett., 14, 466 (1972);
 (b) L. Burger, Angew. Chem. Intern. Ed. Eng., 12, 474 (1973);
 (c) C. E. Moore, Atomic Energy Levels, Natl. Bur. Std. U.S. Circ., 467, Vol. 1(1948), Vol. 2(1952), Vol. 3(1958).
2. E. A. V. Ebsworth, in: "Organometallic Compounds of the group IV Elements", A. G. MacDiarmid, ed., Vol. 1, Marcel Dekker, Inc., New York, 1968, p. 1.
3. C. F. Shaw III and A. L. Allred, Organometal. Chem. Rev. A, 5, 95 (1970); J. Attridge, *ibid.*, 323 (1970); A. N. Egorochkin, N. S. Vyazankin, N. S. Ostasheva, O. V. Kuz'min, N. S. Nametkin, I. F. Kovalev and M. G. Voronkov, J. Organometal. Chem., 59, 1117 (1973); B. G. Ramsey, "Electronic Transitions in Organometal-oids", Academic Press, Inc., New York (1969); J. Nagy and J. Reffy, J. Organometal Chem., 22, 565 (1970).
4. D. N. Roark and G. J. D. Peddle, J. Am. Chem. Soc., 94, 5837 (1972):
5. L. E. Gusel'nikov, N. S. Nametkin and V. M. Vdovin, Russian Chem. Rev., 43, 620 (1974); T. J. Barton and J. A. Kilgour, J. Am. Chem. Soc., 96, 2278 (1974); C. M. Golino, R. D. Bush and L. H. Sommer, *ibid.*, 97, 7371 (1975).
6. C. M. Golino, R. D. Bush and L. H. Sommer, J. Am. Chem. Soc., 96, 614 (1974); D. R. Parker and L. H. Sommer, *ibid.*, 98, 618 (1976).
7. L. H. Sommer and J. MeLick, J. Organometal. Chem., 101, 171 (1975).
8. O. L. Chapman, C.-C. Chang, J. Kolc, M. L. Jung, J. A. Lowe, F. J. Barton and M. L. Tumej, J. Am. Chem. Soc., 98, 7844 (1976); M. R. Chedekel, M. Skoglund, R. L. Kreger and H. Schechter, *ibid.*, 7846 (1976).
9. H. Sakurai, Y. Kamiyama and Y. Nakadaira, J. Am. Chem. Soc., 98, 7453 (1976).

10. M. D. Curtis, *J. Organometal. Chem.*, 60, 63 (1973);
R. Damrauer and D. R. Williams, *ibid.*, 66, 241 (1974).
11. P. Potzinger and F. W. Lampe, *J. Phys. Chem.*, 74,
719 (1970).
12. S. H. Hajiev and M. J. Agarunov, *J. Organometal. Chem.*,
22, 305 (1970).
13. P. Potzinger, A. Ritter and J. Krause, *Z. Naturforsch.*,
30a, 347 (1975).
14. Q. Quanne, *J. Phys. Chem.*, 75, 2480 (1971).
15. R. Walsh and J. M. Wells, *J. Chem. Soc., Faraday I*,
72, 100 (1976); *J. Chem. Soc., Chem. Comm.*, 513 (1973).
16. I. M. T. Davidson and A. V. Howard, *J. Chem. Soc.*,
Chem. Comm., 323 (1973).
17. I. M. T. Davidson and A. V. Howard, *J. Chem. Soc.*,
Faraday I, 71, 69 (1975).
18. W. C. Steele, L. D. Nichols and F. G. A. Stone, *J.*
Am. Chem. Soc., 84, 441 (1962).
19. R. Walsh and J. M. Wells, *J. Chem. Soc., Faraday I*,
72, 1212 (1976).
20. O. P. Strausz, E. Jakubowski, H. S. Sandhu and
H. E. Gunning, *J. Chem. Phys.*, 51, 559 (1969).
21. W. C. Steele and F. G. A. Stone, *J. Am. Chem. Soc.*,
84, 3599 (1962).
22. G. G. Hess, F. W. Lampe and L. H. Sommer, *J. Am. Chem.*
Soc., 86, 3174 (1964).
23. G. G. Hess, F. W. Lampe and L. H. Sommer, *J. Am. Chem.*
Soc., 87, 5327 (1965).
24. J. A. Kerr, A. Stephens and J. C. Young, *Int. J. Chem.*
Kinetics, 1, 339 (1969).
25. I. M. T. Davidson, C. Eaborn and J. M. Simmie, *J.*
Chem. Soc., Faraday I, 70, 249 (1974).
26. J. A. Kerr, *Chem. Revs.*, 66, 465 (1966).

27. I. M. T. Davidson and J. I. Matthews, *J. Chem. Soc., Faraday I*, 72, 1403 (1976).
 28. L. Kaplan, in: "Free Radicals", J. K. Kochi, ed., Vol. 2, Wiley-Intersci., New York, 1973, p. 361.
 29. L. Morchouse, J. J. Christiansen and W. Gordy, *J. Chem. Phys.*, 45, 1751 (1966); J. H. Sharp and M. C. R. Symons, *J. Chem. Soc. (A)*, 3089 (1970).
 30. M. F. Lappert and P. W. Lednor, *Advances in Organometal. Chem.*, 14, 345 (1976); H. Sakurai, in: "Free Radicals", J. K. Kochi, ed., Vol. 2, Wiley-Intersci., New York, 1973, p. 741.
 31. M. A. Nay, G. N. Woodall, O. P. Strausz and H. E. Gunning, *J. Am. Chem. Soc.*, 87, 179 (1965).
 32. T. L. Pollock, H. S. Sandhu, A. Jodhan and O. P. Strausz, *J. Am. Chem. Soc.*, 95, 1017 (1973).
 33. L. Gammie, Ph.D. Thesis, University of Alberta, 1976; L. Gammie, I. Safarik and O. P. Strausz, unpublished results.
 34. R. Hiatt and S. W. Benson, *Int. J. Chem. Kinetics*, V, 385 (1973).
 35. E. R. Austin and F. W. Lampe, *J. Phys. Chem.*, 80, 2811 (1976).
 36. P. Cadman, G. M. Tilley and A. F. Trotter-Dickenson, *Chem. Comm.*, 1721 (1970); *J. Chem. Soc., Faraday I*, 68, 1849 (1972).
 37. P. P. Gaspar, A. D. Haizlip and K. Y. Chao, *J. Am. Chem. Soc.*, 94, 9032 (1972).
 38. J. H. Purnell and R. Walsh, *Proc. Roy. Soc., Ser. A*, 293, 543 (1966).
 39. M. A. Ring, M. J. Puentes and H. E. O'Neal, *J. Am. Chem. Soc.*, 92, 4845 (1970).
 40. K. Y. Chao and P. P. Gaspar, *J. Am. Chem. Soc.*, 96, 1284 (1974).
 41. L. Endrenyi and D. J. LeRoy, *J. Phys. Chem.*, 71, 1334 (1967).
- 

42. F. W. Lampe and F. H. Field, *Can. J. Chem.*, 37, 995 (1959).
43. D. C. White and E. G. Rochow, *J. Am. Chem. Soc.*, 96, 3897 (1954).
44. H. Niki and G. J. Mains, *J. Phys. Chem.*, 68, 304 (1964).
45. O. P. Strausz, K. Obi and W. K. Duholke, *J. Am. Chem. Soc.*, 90, 1359 (1968).
46. K. Obi, A. Clement, H. E. Gunning and O. P. Strausz, *J. Am. Chem. Soc.*, 91, 1622 (1969).
47. A. G. Alexander, Ph.D. Thesis, University of Alberta, 1972.
48. E. Kamaratos and F. W. Lampe, *J. Phys. Chem.*, 74, 2267 (1970).
49. P. P. Gaspar, S. A. Böck and W. E. Eckelman, *J. Am. Chem. Soc.*, 90, 6914 (1968); P. P. Gaspar, P. Markusch, J. D. Holten III and J. J. Frost, *J. Phys. Chem.*, 76, 1352 (1972).
50. J. F. Schmidt and F. W. Lampe, *J. Phys. Chem.*, 73, 2707 (1969).
51. I. M. T. Davidson, in: "Reaction Kinetics", Vol. 1, Specialist Periodic Report, The Chemical Society London, 1975, p. 212.
52. I. M. T. Davidson, *Quart. Revs.*, 25, 111 (1971).
53. R. A. Jackson, *Adv. Free Radical Chem.*, 3, 231 (1969).
54. W. Kirmse, "Carbene Chemistry", Academic Press, New York, 1971; H. Bürger, *Angew. Chem., Inter. Ed., Eng.*, 12, 474 (1973).
55. O. F. Zeck, G. P. Gennaro and Y. N. Tang, *J. Am. Chem. Soc.*, 96, 5967 (1974); I. Dubois, G. Herzberg and R. D. Verma, *J. Chem. Phys.*, 47, 4262 (1967).
56. I. M. T. Davidson, *J. Organometal Chem.*, 24, 97 (1970).
57. M. Bowrey and J. H. Purnell, *Proc. Roy. Soc., Ser. A.*, 321, 341 (1971); *J. Am. Chem. Soc.*, 92, 2594 (1970).

58. R. B. Baird, M. D. Sefcik and M. A. Ring, *Inorg. Chem.*, 10, 883 (1971).
59. W. A. Attwell and D. R. Weyenberg, *Angew. Chem., Intern. Ed., Eng.*, 8, 469 (1969).
60. R. E. Berkley, I. Safarik, O. P. Strausz and H. E. Gunning, *J. Phys. Chem.*, 77, 1741 (1973).
61. R. E. Berkley, I. Safarik, H. E. Gunning and O. P. Strausz, *J. Phys. Chem.*, 77, 1434 (1973).
62. O. M. Nefedev and M. N. Manakov, *Angew. Chem., Intern. Ed., Eng.*, 5, 1021 (1966).
63. R. T. Conlin and P. P. Gaspar, *J. Am. Chem. Soc.*, 98, 868 (1976).
64. P. S. Skell and E. J. Goldstein, *J. Am. Chem. Soc.*, 86, 1442 (1964) (two papers).
65. M. D. Sefcik and M. A. Ring, *J. Am. Chem. Soc.*, 95, 5168 (1973).
66. P. John and J. H. Purnell, *J. Chem. Soc., Faraday I*, 69, 1455 (1973).
67. M. D. Sefcik and M. A. Ring, *J. Organometal. Chem.*, 59, 167 (1973).
68. B. Cox and J. H. Purnell, *J. Chem. Soc., Faraday I*, 71, 859 (1975).
69. M. Ishikawa and M. Kumada, *J. Organometal. Chem.*, 81, C3 (1974).
70. D. Seyferth and D. C. Annarelli, *J. Am. Chem. Soc.*, 97, 7162 (1975); *J. Organometal. Chem.*, 117, C51 (1976).
71. R. L. Jenkins, R. A. Kedrowski, L. E. Elliot, D. C. Tappen, D. J. Schlyer and M. A. Ring, *J. Organometal. Chem.*, 86, 347 (1975).
72. H. J. Emeleus and K. Stewart, *Trans. Faraday Soc.*, 32, 1577 (1936).
73. A. G. Aléxander, O. P. Strausz, R. Pottier and G. P. Semeluk, *Chem. Phys. Lett.*, 13, 608 (1972).

74. W. L. Hase, C. J. Mazac and J. W. Simons, *J. Am. Chem. Soc.*, 95, 3454 (1973).
75. J. A. Cowfer, K. P. Lynch and J. V. Michael, *J. Phys. Chem.*, 79, 1139 (1975).
76. K. J. Laidler and L. F. Loucks, in: "Comprehensive Chemical Kinetics", C. H. Bamford and C. F. Tipper, eds., Vol. 5, Elsevier, New York, 1972, p. 36.
77. A. J. Vanderwielen, M. A. Ring and H. E. O'Neal, *J. Am. Chem. Soc.*, 97, 993 (1975).
78. J. I. Matthews, Ph.D. Thesis, University of Leicester, 1975.
79. E. M. Tebben and M. A. Ring, *Inorg. Chem.*, 8, 1787 (1969).
80. P. Estacio, M. D. Sefcik, E. K. Chan and M. A. Ring, *Inorg. Chem.*, 9, 1068 (1970).
81. G. Fritz, J. Grobe and D. Kummer, *Advan. Inorg. Chem.*, 7, 349 (1965); G. Fritz, *Angew. Chem., Intern. Ed., Eng.*, 6, 677 (1967).
82. R. P. Clifford, B. G. Gowenlock, C. A. F. Johnson and J. Stevenson, *J. Organometal. Chem.*, 34, 53 (1972).
83. I. M. T. Davidson and C. A. Lambert, *J. Chem. Soc. (A)*, 882 (1971); *Chem. Comm.*, 1276 (1969).
84. D. P. Paquin, R. J. O'Connor and M. A. Ring, *J. Organometal. Chem.*, 80, 341 (1974).
85. J. J. Kohanek, P. Estacio and M. A. Ring, *Inorg. Chem.*, 8, 2516 (1969).
86. P. P. Gaspar and B. J. Herold, in: "Carbene Chemistry", W. Kirmse, ed., Academic Press, New York, 1971, p. 536.
87. P. John and J. H. Purnell, *J. Organometal. Chem.*, 29, 233 (1971).
88. C. H. Haas and M. A. Ring, *Inorg. Chem.*, 14, 2253 (1975).

89. G. B. Watts and K. U. Ingold, *J. Am. Chem. Soc.*, 94, 491 (1972).
90. P. T. Frangopol and K. U. Ingold, *J. Organometal Chem.*, 25, C9 (1970).
91. F. A. Lindemann, *Trans. Faraday Soc.*, 17, 598 (1922).
92. C. N. Hinshelwood, *Proc. Roy. Soc., Ser. A.*, 113, 230 (1927).
93. O. K. Rice and H. C. Ramsperger, *J. Am. Chem. Soc.*, 49, 1617 (1927).
94. L. S. Shiner, *J. Phys. Chem.*, 32, 225, 1065 (1928).
95. R. A. Marcus and O. K. Rice, *J. Phys. and Colloid Chem.*, 54, 104 (1951); R. A. Marcus, *J. Chem. Phys.*, 20, 359 (1952).
96. P. Vitins, Ph.D. Thesis, University of Alberta, 1973, p. 45.
97. P. J. Robinson and K. A. Holbrook, "Unimolecular Reactions", Wiley-Interscience, London, 1972.
98. N. M. Emanuel and D. G. Knorre, "Chemical Kinetics-Homogeneous Reactions", J. Wiley & Sons, New York, 1973, p. 302.
99. I. Safarik and O. P. Strausz, Unpublished results.
100. J. Hong, Ph.D. Thesis, University of Detroit, 1972.
101. K. Obi, H. S. Sandhu, H. E. Gunning and O. P. Strausz, *J. Phys. Chem.*, 76, 3911 (1972).
102. K. R. Jennings and R. J. Cvetanovic, *J. Chem. Phys.*, 35, 1233 (1961); W. Braun and M. Lenzi, *Disc. Faraday Soc.*, 44, 252 (1967); J. A. Eyre, T. Hikida and L. M. Dorfman, *J. Chem. Phys.*, 53, 1281 (1970); N. J. Kurylo, N. C. Peterson and W. Braun, *J. Chem. Phys.*, 53, 2776 (1970); J. A. Cowfer, D. G. Keil, J. V. Michael and C. Yeh, *J. Phys. Chem.*, 75, 1584 (1971).
103. A. F. Dodonov, C. K. Lavrovskaya and V. L. Tal'roze, *Kinet. Katal.*, 10, 22 (1969); R. D. Penzharn and B. de B. Darwent, *J. Chem. Phys.*, 55, 1508 (1971).

104. T. Yokota, Ph.D. Thesis, Catholic University, Washington, D.C., 1968, p. 67.
105. W. L. Jones, S. D. Macknight and L. Teng, Chem. Revs., 73, 415 (1973).
106. I. M. T. Davidson and I. L. Stephenson, J. Chem. Soc. (A), 282 (1968).
107. S. W. Benson, "Thermochemical Kinetics", J. Wiley & Sons, New York, 1968, p. 67.
108. "Handbook of Chemistry and Physics", R. C. Weast, ed., 50-th Ed., Chemical Rubber Co., 1969.
109. Reference 107, page 85.
110. D. F. Ball, T. Carter, D. C. McKean and L. A. Woodward, Spectrochimica Acta, 20, 1721 (1964).
111. Reference 107, page 200.
112. J. I. Matthews, Ph.D. Thesis, University of Leicester, 1975.
113. K. Ohno, M. Hayashi and H. Murata, J. Hiroshima Univ., Ser. A., 36, 121 (1971).

APPENDIX I
 MASS SPECTRUM OF METHYLETHYLSILANE

m/e	Relative Intensity ^a	Postulated Ion
74	18	MeEtSiH ₂ ⁺
73	45	MeEtSiH ⁺
72	54	MeEtSi ⁺
59	23	EtSiH ₂ ⁺ , Me ₂ SiH ⁺
58	14	EtSiH ⁺ , Me ₂ Si ⁺
57	8	EtSi ⁺
55	7	
53	8	
46	12	MeSiH ₃ ⁺
45	<u>100</u>	MeSiH ₂ ⁺
44	76	MeSiH ⁺
43	42	MeSi ⁺
42	16	
41	5	
31	17	SiH ₃ ⁺
29	16	
28	16	
27	13	
15	5	

^a Ionization voltage of ca 70 volts; the peaks with a relative intensity of less than 5% of the base peak (100) were omitted.

APPENDIX II

MASS SPECTRUM OF DIMETHYLETHYLSILANE

m/e	Relative Intensity ^a	Postulated Ion
88	4	Me ₂ EtSiH ⁺
87	15	Me ₂ EtSi ⁺
73	26	MeEtSiH ⁺
72	7	MeEtSi ⁺
60	11	Me ₂ SiH ₂ ⁺
59	100	Me ₂ SiH ⁺ , EtSiH ₂ ⁺
58	35	Me ₂ Si ⁺ , EtSiH ⁺
54	9	
45	42	MeSiH ₂
44	6	MeSiH ⁺
43	24	MeSi ⁺
42	7	
31	10	SiH ₃ ⁺
29	8	
28	5	

^a Ionization voltage of ca 70 volts; the peaks with a relative intensity of less than 5% of the base peak (100) were omitted.

APPENDIX III

CORRECTION PROCEDURE FOR DECOMPOSITION OF POLYMER

The polymer formed in the pyrolysis of monomethylsilane is thermally unstable and decomposes slowly to yield hydrogen and methane as major products. The rate of decomposition increases with the extent of polymer deposition and the observed hydrogen yields from the pyrolysis of monomethylsilane must therefore be corrected for degassing of the polymer. The correction procedure is illustrated in Figure AIII-1.

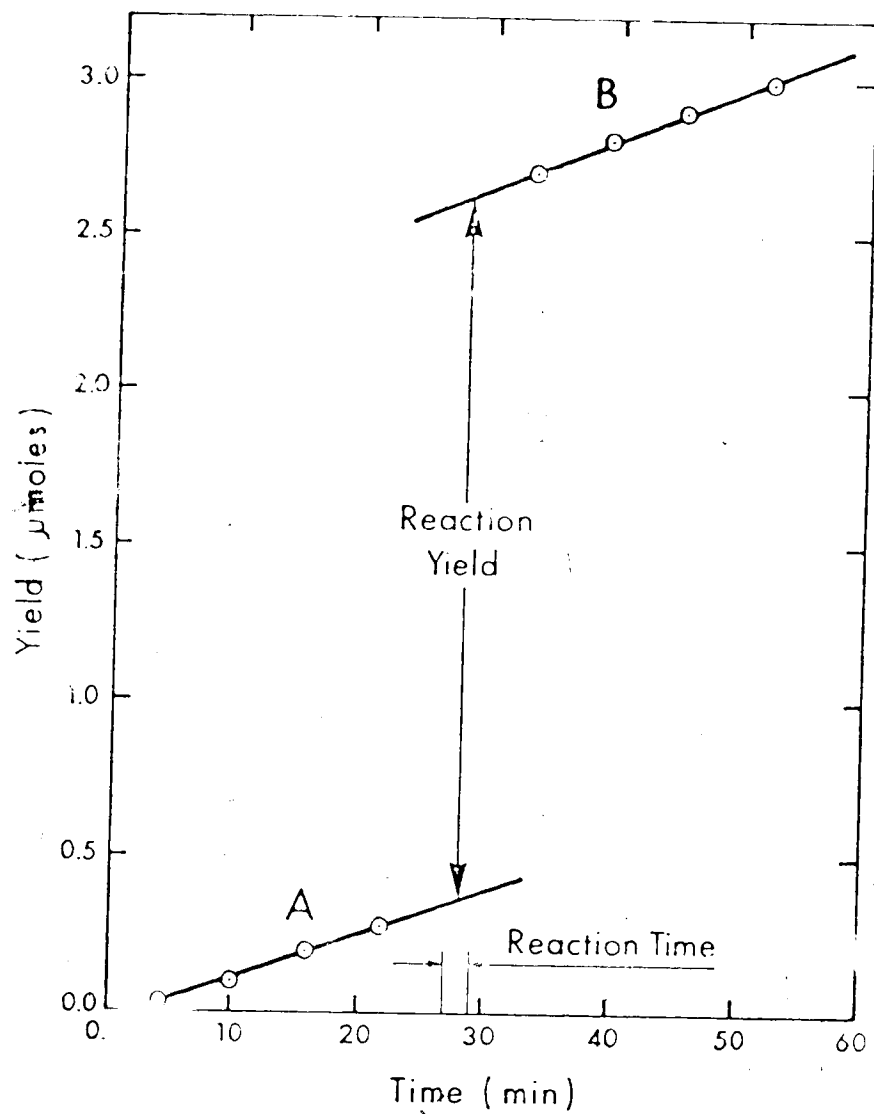


Figure AIII-1. Correction of the Observed H_2 Yields for Decomposition of the Polymer.
 A-degassing before the experiment,
 B-after the experiment.
 The difference between A and B at the midpoint of the reaction time corresponds to the actual yield.